

Vectorial aspects of iron transfer in human term placenta.

A study involving polarly cultured trophoblast cells and vesicles isolated from microvillous and basal syncytiotrophoblast membranes.

Vectoriële aspecten van ijzer transport in de humane terme placenta

Een studie met polair gekweekte trofoblast cellen en vesicles geïsoleerd van microvillieuze en basale syncytiotrofoblast membranen.

Proefschrift

Ter verkrijging van de graad van doctor aan de
Erasmus Universiteit Rotterdam op gezag van Rector Magnificus
Prof. Dr. P.W.C. Akkermans M.A.
en volgens het besluit van het College voor Promoties

De openbare verdediging zal plaatsvinden op
woensdag 28 oktober 1998 om 15.45 uur

door

Christina Elisabeth Huberta Verrijt
geboren te Someren

Promotie-commissie.

Promotor: Prof. Dr. H.G. van Eijk

Co-promotor: Dr. J.P. van Dijk

Overige leden: Prof. Dr. J.F. Koster
Prof. J.H.P. Wilson
Prof. Dr. S.L.S. Drop

Het onderzoek beschreven in dit proefschrift werd verricht bij de Vakgroep Biochemie, afdeling Chemische Pathologie van de Erasmus Universiteit te Rotterdam.

Contents

Abbreviations

vii

Chapter 1	Introduction	1
1.1	General introduction	3
1.2	Transferrin, an iron-transport protein	3
1.3	Cellular iron uptake	4
1.3.1	Tf-dependent iron uptake	4
1.3.2	Tf-independent iron uptake	7
1.4	Intracellular iron pool	8
1.5	Regulation of intracellular iron homeostasis	9
1.6	Human term placenta	9
1.7	Placental transport mechanisms	12
1.8	Placental iron transfer	13
1.9	Aim of the thesis	14
	References	16

⊗

Chapter 2	Materials and Methods	27
2.1	Materials	29
2.1.1	Chemicals	29
2.1.2	Tissue source	30
2.2	Isolation and culture of human term trophoblast cells	30
2.3	Isolation and characterization of membrane vesicles	31
2.3.1	Isolation of membrane vesicles	31
2.3.2	Marker enzymes	32
2.3.3	Orientation of membrane vesicles	33
2.3.4	Gel electrophoresis of membrane vesicles	34
2.3.5	Determination of membrane cholesterol and phospholipid content	34
2.3.6	Fatty acid analysis in phospholipids	35
2.4	Protein determination	35
2.5	Isolation of transferrin variants	36
2.6	Labelling of transferrin with ^{59}Fe and ^{125}I	36
2.6.1	Loading of apoTf with ^{59}Fe	36
2.6.2	Labelling of diferric Tf with ^{125}I	36
2.7	Transferrin binding to placental membrane vesicles	36
2.7.1	Estimation of endogenous transferrin	36
2.7.2	Transferrin binding assay	37
2.8	Uptake of diferric Tf by cultured trophoblast cells	37
2.8.1	Uptake of ^{125}I - $^{59}\text{Fe}_2\text{Tf}$ by trophoblast cells cultured on plastic dishes	37
2.8.2	Uptake of ^{125}I - $^{59}\text{Fe}_2\text{Tf}$ by trophoblast cells cultured on a permeable filter	38
2.9	Uptake of gold-labelled diferric Tf (Au-Tf) by cultured trophoblast cells	38
2.9.1	Coupling of 6 nm gold to Tf	38
2.9.2	Incubation of membrane-grown trophoblast cells with Au-Tf	39

2.10	Immunolocalization of TfRs	39
2.11	Electron microscopy	40
2.12	Transferrin synthesis by cultured trophoblast cells	40
2.12.1	Identification of transferrin mRNA by RT-PCR	40
2.12.2	De novo synthesis of transferrin	41
2.12.3	Estimation of transferrin content	42
2.12.4	Heterogeneity of trophoblast transferrin	42
2.13	Uptake of non-Tf iron by trophoblast cells	42
2.13.1	Stock-solutions of $^{59}\text{Fe(III)}$ nitrilotriacetate and ^{59}Fe -ascorbate	42
2.13.2	Non-Tf iron uptake by cultured trophoblast cells	43
2.14	Ferrireductase assays	43
	References	44

Chapter 3	Two models for placental transport studies: purified membrane vesicles and trophoblast cells in culture	47
3.1	General introduction	49
3.2	Isolation and characterization of microvillous and basal membrane vesicles	49
3.2.1	Introduction	49
3.2.2	Materials and Methods	49
3.2.3	Results	52
3.2.4	Discussion	57
3.3	Description of trophoblast cells in culture	59
3.3.1	Introduction	59
3.3.2	Isolation and purification of trophoblast cells	59
3.3.3	Differentiation of cultured trophoblast cells	60
	References	67

Chapter 4	Binding of human isotransferrin variants to microvillous and basal membrane vesicles from human term placenta	73
4.1	Introduction	75
4.2	Materials and Methods	75
4.3	Results	77
4.4	Discussion	81
	References	84

Chapter 5	Accumulation and release of iron in polarly cultured trophoblast cells	87
5.1	Introduction	89
5.2	Materials and Methods	89
5.3	Results	91
5.4	Discussion	98
5.5	Appendix	100
	References	102

Chapter 6	Transferrin in cultured human term trophoblast cells.	
	Synthesis and heterogeneity	105
6.1	Introduction	107
6.2	Materials and Methods	107
6.3	Results	108
6.4	Discussion	114
	References	116
Chapter 7	Non-transferrin iron uptake by trophoblast cells in culture.	
	Significance of a NADH-dependent ferrireductase	119
7.1	Introduction	121
7.2	Materials and Methods	121
7.3	Results	123
7.4	Discussion	129
	References	132
Chapter 8	General discussion	135
	References	140
	Summary/Samenvatting	143
	Publications	148
	Dankwoord	150
	Curriculum Vitae	151

Abbreviations

Au-Tf	: gold-labelled diferric transferrin
BMV	: basal membrane vesicles
BPS	: bathophenanthroline disulphonic acid
BSA	: bovine serum albumin
DMEM	: Dulbecco's modification of Eagle's medium
DFO	: desferrioxamine (desferal)
EBSS	: Earle's Balanced Salts
EGF	: epidermal growth factor
FCS	: fetal calf serum
Fe(III)CN	: ferricyanide
FZ	: ferrozine
h	: hour(s)
hCG	: human chorionic gonadotropin
HEPES	: 2-[4-(2-hydroxyethyl)-1-piperazinyl]-ethansulphonic acid
hPL	: human placental lactogen
H ₀	: tissue homogenate
K _a	: affinity constant
K _d	: dissociation constant
kD	: kiloDalton
LIP	: labile iron pool
LMW	: low molecular weight
MEM	: Modified Eagle's medium
min	: minute(s)
MMV	: microvillous membrane vesicles
NTA	: nitrilotriacetate
PAGE	: polyacrylamide gelelectrophoresis
PCR	: polymerase chain reaction
PMSF	: phenylmethylsulphonyl fluoride
PBS	: phosphate buffered saline
RT	: reverse transcription
SDS	: sodium dodecyl sulphate
SP	: schwangerschaftsprotein
TCA	: trichloroacetic acid
Tf	: transferrin
bb Tf	: bi-bi-antennary tetra-sialo transferrin
bt Tf	: bi-tri-antennary penta-sialo transferrin
tt Tf	: tri-tri-antennary hexa-sialo transferrin
TfR	: transferrin receptor
Tris	: tris(hydroxymethyl)aminomethane
V-ATPase	: vacuolar ATPase

1

Introduction

1.1 General introduction

Iron is an essential element for all living cells, with the exception of certain members of the *Lactobacillus* and *Bacillus* bacteria (1). It plays an important role in growth and development because of its presence in the active centres of enzymes that catalyze key reactions involved in energy metabolism (e.g. cytochromes of the electron transport chain, mitochondrial aconitase), respiration (e.g. hemoglobin, myoglobin) and DNA synthesis (e.g. ribonucleotide reductase) (2,3).

The main oxidation states of iron are the ferric [Fe(III)] and ferrous [Fe(II)] states. Under most physiological conditions, iron exists in the oxidized ferric state. At neutral pH, ferric salts are hydrolyzed to the nearly insoluble ferric hydroxide (solubility product of $\text{Fe}(\text{OH})_3$ is 4×10^{-38}) (3,4). Moreover, free iron can be very toxic by catalyzing the formation of hydroxyl radicals in the presence of molecular oxygen (5). These hydroxyl radicals are extremely strong oxidizing agents and can lead to damage to DNA, proteins and lipids. Thus, on the one hand iron is essential for living organisms, but on the other hand free iron can be very toxic. In order to maintain low concentrations of free iron, iron is usually bound to chelator molecules, like transferrin. Furthermore, cells contain sophisticated mechanisms for the regulation of iron uptake, utilization and storage.

1.2 Transferrin, an iron-transport protein

Transferrin (Tf) has two major functions: it serves as transport protein for iron in serum and it minimizes the amount of free iron in plasma. Human serum Tf is a glycoprotein with a molecular mass of 80 kD (for reviews: 6,7). It consists of two homologous domains (the N-terminal and C-terminal domain), which both are capable of binding one ferric atom. Binding of iron to Tf is pH dependent and requires the binding of a synergistic anion (e.g. carbonate or bicarbonate) for stabilization (8). The affinity constants for Fe(III) binding to the N- and C- terminal domains at pH 7.4 are respectively 1×10^{22} and 6×10^{22} /M (9).

The C-terminal domain of Tf contains two N-linked complex type oligosaccharide chains: the glycan chains (Figure 1.1). These glycan chains show variety in their degree of branching, differing from bi-antennary to tetra-antennary structures (10). Both the degree of branching of the N-linked glycan chains and the varying amount of sialic acids at their terminal residues are responsible for the microheterogeneity of Tf. Differences in sialic acid content result in different pI-values, which can be shown by isoelectric focusing (11).

During pregnancy, the complexity of the carbohydrate chains increases in maternal and fetal guinea-pig serum (12) as well as in maternal human serum (11), whereas the complexity of Tf is reduced in term human fetal serum.

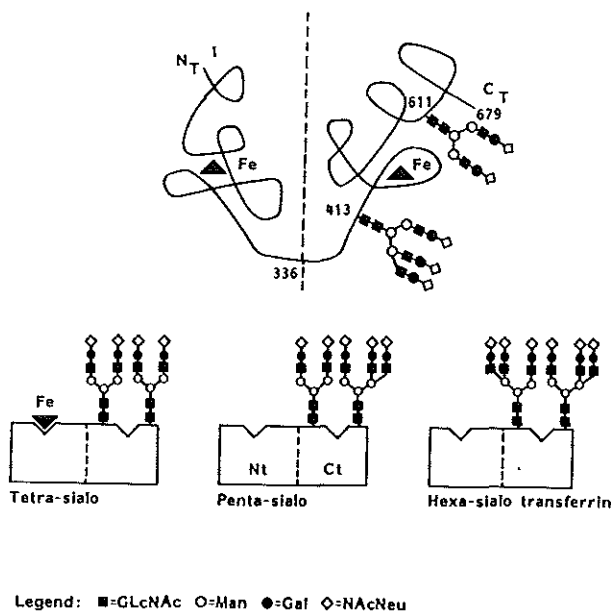


Figure 1.1

Schematic representation of a diferric Tf molecule, containing two N-linked glycan chains in the C-terminal domain. Both the C- and the N-terminal domain contain a ferric atom. Three isoTf variants are shown at the bottom of the picture: bi-bi-antennary tetra-sialo Tf, bi-tri-antennary penta-sialo Tf and tri-tri-antennary hexa-sialo Tf. Reprinted from (7).

The major site of Tf synthesis is the liver, although Tf synthesis (in limited amounts) has also been shown in the brain, Sertoli cells and fetal membranes (13-16). Recently, Tf mRNA has been demonstrated in rat and mouse placental extracts (14,17). Furthermore, rat placental cells in culture secrete Tf (18), suggesting Tf synthesis in placenta.

1.3 Cellular iron uptake

1.3.1 Tf-dependent iron uptake

Several mechanisms have been described for cellular iron uptake from Tf. The first step involves binding of two ferric atoms to Tf. Next, either of the following mechanisms can take place:

1) Tf-receptor mediated endocytosis.

The major route of cellular iron uptake from Tf is receptor-mediated endocytosis (7,19-21). At physiological pH, diferric Tf binds to a specific transferrin receptor (TfR) at the cell surface. The TfR (Figure 1.2) is a disulphide-linked dimer of two identical transmembrane subunits, which both are able to bind one diferric Tf (22). The TfR has a higher affinity for diferric Tf ($K_a = 1.1 \times 10^8 /M$) than for apoTf ($K_a = 4.6 \times 10^6 /M$) at pH 7.4. ApoTf will therefore not compete with diferric Tf in binding to the TfR under physiological conditions (23). The diferric Tf-TfR complexes are clustered and localized in clathrin-coated pits before internalization into the cytoplasm in endocytic vesicles, called endosomes. These primary endosomes lose their clathrin coat and the intravesicular pH is lowered to pH 5-6 by means of a vacuolar type H^+ ATPase (V-ATPase) (24). At this reduced pH, the affinity of iron for Tf is lowered, resulting in iron release from the Tf-TfR complex.

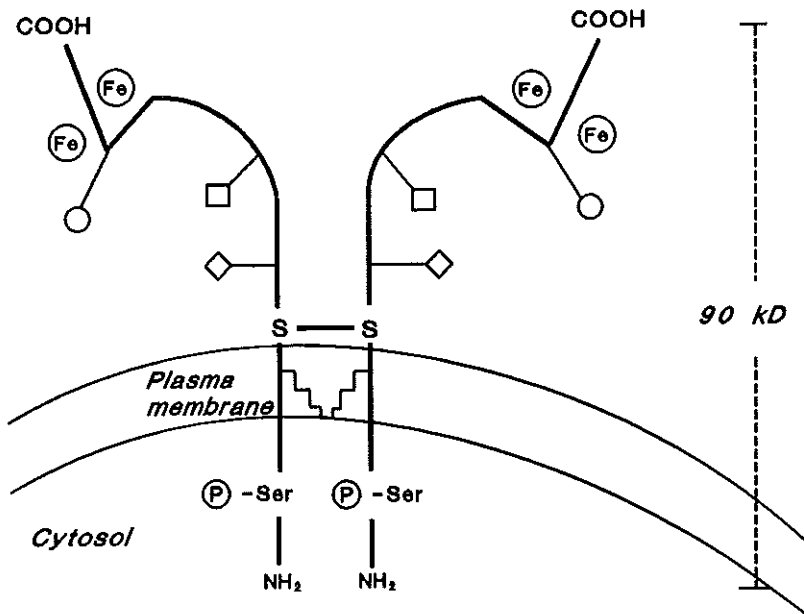


Figure 1.2

Schematic representation of the transferrin receptor. The TfR is a dimer consisting of two identical 95 kD polypeptide structures, linked by disulphide bonds. The N-terminal domains are found in the cytoplasm and contain phosphorylation sites. The extracellular C-terminal domains contain a number of oligosaccharides (\diamond , \square , \circ). Each monomer can bind one Tf molecule (which may contain two ferric atoms).

Complete release of iron from the Tf-TfR complex would take hours at the pH of the endosome (25), whereas the entire endocytosis takes only 2 to 3 minutes in most cell types (20). Additional mechanisms have therefore been proposed, such as: (i) a change in conformation of the TfR at pH 5.6, which will accelerate the release of iron from Tf (20,26); (ii) NADH-dependent reduction of iron, which has been suggested to play a role in endosomal iron release and subsequent translocation (27,28); after reduction, ferrous iron is transferred across the membrane into the cytoplasm, presumably through a channel formed by the 17 kD proton channel subunit of the V-ATPase (28,29).

The affinity of the TfR for apoTf at pH 5.5 ($K_a = 7.7 \times 10^7$ /M) (19) is high enough to keep Tf bound to the TfR after iron is released in the acidic endosome. In this way Tf escapes traffic towards the lysosomes with successive digestion. The iron-depleted endosome returns to the cell membrane, with which it fuses. Since the apoTf-TfR complex is then exposed to the extracellular pH of 7.4, the apoTf will dissociate from the TfR and can be used for a new cycle of iron uptake and delivery.

II) Reduction of diferric Tf.

Another, probably less important, mechanism of iron uptake from Tf involves a transmembrane reductase (19,30,31). This model also starts with the binding of diferric Tf to the TfR at the cell surface. However, before endocytosis of the Tf-TfR complex, Tf-bound iron is reduced. In the reductive model diferric Tf is suggested to bind to TfR in close proximity to a plasma transmembrane NADH:ferricyanide oxidoreductase. Such a reductase has been shown in hepatocytes and reticulocytes (32-34). Intracellular oxidation of NADH followed by cooperative proton and electron fluxes will destabilize the Tf-iron bond and reduce iron, which becomes bound to a plasma membrane binder specific for ferrous iron (19,21,35). Iron is then transported across the plasma membrane to the cytosolic compartment by hitherto unidentified channels. The iron-depleted Tf is finally released from the TfR.

III) Low affinity adsorptive endocytosis.

A third method for iron uptake from Tf is independent of the TfR. Hepatocytes have been shown to possess a mechanism for non-specific and non-saturable iron uptake in parallel with TfR-mediated iron uptake (36). Diferric Tf is non-specifically and with low affinity bound to the cell membrane followed by endocytic internalization. As with TfR-mediated endocytosis, the release of iron from Tf is both pH- and energy-dependent (37). After iron is transferred into the cytosol, it is predominantly incorporated into ferritin for storage. This mechanism has been described to play a physiological role in iron uptake by hepatocytes. However, thus far it has not been described for other cell types.

IV) Fluid phase endocytosis.

A minor pathway for iron uptake is fluid phase endocytosis. Binding of Tf to the plasma membrane is not required. Extracellular fluid is endocytosed together with the particles that are present in the fluid. Uptake of particles in this way is also called pinocytosis.

1.3.2 Tf-independent iron uptake

Recent studies show that some cells are able to take up iron independent of Tf (recent review: 5). The Tf-independent iron transport system may play a role in some pathological conditions with iron overload, where the iron-binding capacity of Tf is exceeded.

The essential first step in Tf-independent iron uptake in all eukaryotes requires the activity of a ferrireductase. A Tf-independent iron uptake mechanism, involving reduction of ferric iron, has been described in *Saccharomyces cerevisiae* (recent review: 38). Iron uptake in these simple eukaryotes starts with the reduction of Fe(III) to Fe(II) by externally directed reductases Fre1p and Fre2p. The external reduction is mediated by the oxidation of intracellular compounds followed by electron transport across the membrane. The uptake of ferrous iron requires the activity of Fet3p, a copper-containing oxidase. Uptake of copper, which occurs via the plasma membrane copper transport protein Ctr1p, is necessary for the function of Fet3p. The FET3 gene is homologous to the multi-copper oxidase family that includes ceruloplasmin (39). Part of this mechanism for iron uptake in yeast may be conserved in higher eukaryotes.

Surface ferrireductases have been demonstrated in hepatocytes (32,33), reticulocytes (33), liver plasma membranes (40), mouse duodenum (41,42), human duodenum (43), human placental trophoblast membranes (44), human erythroleukemia K562 cells (45,46), HeLa cells (47) and Caco-2 cells (48). Several investigators have shown the coupling of iron reduction and uptake in cultured cells (46,47,49). The exact mechanism of iron translocation after reduction is not clear yet. However, more than one Tf-independent iron transport system seem to exist. Some characteristics of Tf-independent iron transport systems are described below:

I) Neither endocytosis nor acidic endosomes are required for the Tf-independent pathway (5).

II) Either "high"- and "low"-affinity transport systems have been described. Fibroblasts, HeLa cells (50,51), and HepG2 cells (49) show low affinity (K_M : 5-30 μ M), while hepatocytes (52), reticulocytes (53,54) and K562 cells (55) show high affinity (K_M : 0.3-1.5 μ M) Tf-independent iron transport systems.

III) Both calcium-dependent (HeLa cells, 50; human skin fibroblasts, 51) and calcium-independent (K562 cells, 55) mechanisms have been shown.

IV) The Tf-independent uptake system can be inhibited by other transition metals. The ability of the metal to inhibit iron transport is a function of the cell type, its physiological state, and the media in which the studies are carried out (5).

1.4 Intracellular iron pool

After iron is released from Tf in the endosome and transferred into the cytosol, it will incorporate into an intermediate labile iron pool (LIP) before it is used for heme synthesis or stored into ferritin (56-58). In studies with cultured rat hepatocytes, the LIP has been shown to be a desferrioxamine (DFO)-chelatable pool, which is rapidly in transit through the cell (59). With permeable and non-permeable Fe(II) and Fe(III) chelators it has been demonstrated that the LIP in K562 cells mainly consists of Fe(II), indicating the presence of intracellular reductive mechanisms (60). Pollack, Campana & Weaver (61) suggested that the low molecular weight iron in guinea pig reticulocytes is in the ferrous oxidation state.

With intracellular fluorescence analysis in intact cells, using the iron-sensitive probe calcein, it has been shown that the LIP concentrations in resting erythroid and myeloid cells are in the range of 0.2-1.5 μ M, varying with cell iron loads and iron chelator treatment (62).

The LIP is probably composed of low molecular weight ligands. Some low molecular weight ligands that have been described are sugars, amino acids, peptides, citrate, ATP or other nucleotides (56,58,61,63,64). Recently, mobilferrin, a soluble 56 kD protein, has been identified as a low molecular weight iron binding protein (65) and suggested to play a role in intracellular iron transport (66,67).

When the amount of iron exceeds the amount that is required for metabolic processes, iron is stored in ferritin, the main iron storage protein (68,69 for reviews). Ferritin is composed of 24 polypeptide subunits from which two distinct isoforms exist: a 21 kD H(heavy)- and a 19 kD L(light)-isoform. Ferritin shows variable combinations of these subunits, allowing heterogeneity of the protein. The subunit composition of ferritin seems to be tissue specific. For example the placenta and the heart contain H-rich ferritin, whereas L-rich ferritin predominates in liver and spleen. Ferritin can contain up to 4500 ferric atoms, however, in vivo ferritin is normally 20 % saturated. Iron enters ferritin mainly in its ferrous form, is then oxidized by a ferroxidase located on the H-subunits, and stored in the ferric state as ferric-oxyhydroxide phosphate $(\text{FeOOH})_x(\text{FeO-OPO}_3\text{H}_2)$ (70). The L-subunit has a nucleation site that is involved in the formation of the Fe core. Differences in the proportion of H- and L-subunits result in differences in function of the ferritin. A high amount of the L-subunit is associated with Fe storage, whereas a higher amount of the H-

subunit is responsible for easier uptake of free iron and may therefore play a role in cell protection (68,71).

1.5 Regulation of intracellular iron homeostasis

Since iron is an essential element for living cells, but also can be very toxic when it is present in excess, a sensitive regulation mechanism is very important. Intracellular iron homeostasis is maintained by the co-ordinated regulation of the expression of the TfR and ferritin. Ferritin and TfR contain specific sequences, iron responsive elements (IRE), within their mRNA. These IREs are located in the 5'- and 3'- untranslated region of respectively ferritin and TfR mRNAs. A cytoplasmic protein, the IRE-binding protein (IRE-BP), can bind to these IREs. Binding of IRE-BP to the IRE at the 5'-end of ferritin mRNA inhibits its translation, therefore decreasing the amount of ferritin protein. Binding of IRE-BP to the IRE at the 3'- end of TfR mRNA protects the mRNA from degradation, resulting in higher amounts of TfR. IRE-BP to IRE binding is mediated by intracellular free iron. The IRE-BP is an iron-sulphur protein and can show aconitase activity. When the concentration of intracellular free iron is high, the IRE-BP is in its [4Fe-4S] state, resulting in high aconitase activity and low affinity for IREs. On the other hand, when intracellular free iron concentration is low, the IRE-BP is in its [3Fe-4S] state, corresponding with low aconitase activity and high affinity for IREs. Thus, low iron concentrations result in an increase in the concentration of the TfR and a decrease in the concentration of ferritin, whereas high iron concentrations show the opposite. (See 72-74 for reviews).

1.6 Human term placenta

The placenta is an organ that separates the maternal from the fetal blood circulation. It displays several unique functions: it plays a role in the exchange of compounds between mother and developing fetus, mediating the transport of nutrients from mother to fetus and the reverse transport of waste products from fetus to the mother; it serves as an endocrine organ, secreting steroid and protein hormones; and it is involved in the immunologic barrier against rejection of the fetus by the maternal immune system.

The human placenta is of the haemomonochorial type, which means that maternal blood directly contacts the trophoblast (haemochorial) and only one (mono) layer of trophoblast divides the maternal blood from the fetal endothelium (75,76). At the end of the fourth month the human placenta is fully formed and weighs about 100 g. The term placenta is discoid, with a diameter of approximately 20 cm and weighs about 500 g (77).

Figure 1.3 shows a diagrammatic presentation of the human term placenta. Maternal blood enters the placenta by the spiral arteries and is carried away by uterine veins. Entering of maternal blood into the intervillous space by means of the spiral arteries occurs probably not before 28-30 days post-ovulation (78). The fetal arterial blood is supplied from two arteries within the umbilical cord and returns to the fetus via a single cord vein.

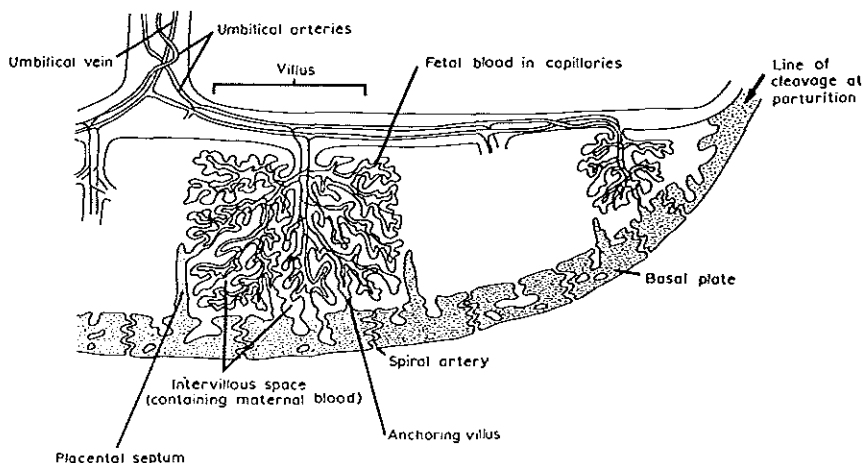


Figure 1.3

Schematic representation of the structure of human term placenta. From (79).

The most important placental structures are the highly branched villi, which are fully surrounded by maternal blood (77,79). A villous consists of villous stroma, containing the fetal vessels, and a trophoblast layer, consisting of syncytiotrophoblast overlying a layer of cytotrophoblast which rests on a basement membrane (Figure 1.4). The syncytiotrophoblast is formed by differentiation and fusion of cytotrophoblast cells (80,81). The maternal-facing plasma membrane of the syncytiotrophoblast is in immediate contact with maternal blood and contains microvilli, enlarging the surface with a factor of 9.4 between 25 and 36 weeks and a factor of 7.7 at 40 weeks of gestation. The total microvillous exchange surface is estimated at 94 m² at 36 weeks, decreasing to 67 m² at the end of gestation (82). Early in pregnancy the microvilli are relatively long, whereas they become shorter and more branched as pregnancy progresses (82,83). The basal surface of the syncytiotrophoblast,

directed to the fetal side, lacks microvilli. During pregnancy part of the cytotrophoblast layer disappears, thus decreasing the distance between fetal and maternal circulation (77).

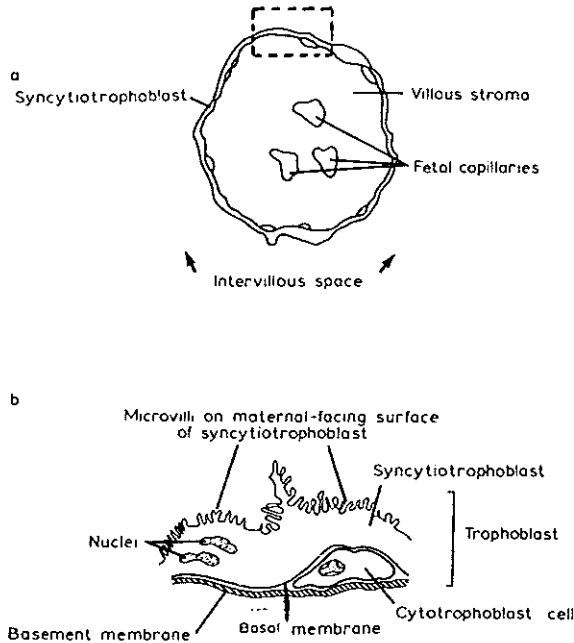


Figure 1.4

Figure 1.4a shows a schematic representation of a cross-section through a villous, which is surrounded by maternal blood in the intervillous space (see also Figure 1.3). A magnification of the trophoblast layer (bordered in Figure 1.4a) is represented in Figure 1.4b. In the trophoblast layer, cytotrophoblast cells are covered with syncytiotrophoblast, which is formed by fusion and differentiation of cytotrophoblast cells. The microvillous surface of the syncytiotrophoblast faces the maternal blood, whereas the basal surface is directed to the fetal side. From (79).

The syncytiotrophoblast is the major site for placental transport. As mentioned before, the syncytiotrophoblast is formed by differentiation and fusion of cytotrophoblast cells. There are some major differences between cytotrophoblast and syncytiotrophoblast. The cytotrophoblast is undifferentiated and contains relatively few mitochondria, vesicles, lysosomes and endoplasmic reticulum (77). Furthermore, it produces human chorionic gonadotropin (hCG)-releasing hormone and inhibine (84,85). Whereas the cytotrophoblast is quite undifferentiated, the syncytiotrophoblast is a metabolically active epithelium and contains a high concentration of organelles like mitochondria, lysosomes, vesicles and both rough and smooth endoplasmic reticulum (77). The syncytiotrophoblast produces specific

hormones like hCG, human placental lactogen (hPL), progesterone, human pregnancy-specific β_1 -glycoprotein and so called schwangerschaftsproteins (SP's) (86-88).

1.7 Placental transport mechanisms

One of the more important functions of the placenta is the transfer of all kind of nutrients from mother to fetus. The rate of placental transfer depends upon a number of physical factors such as the surface area of the exchange membrane, the thickness of the endothelio-syncytial membrane, the maternal and fetal blood flow, hydrostatic pressure in the intervillous chamber, blood pressure in fetal capillaries, and the difference between maternal and fetal osmotic pressures (89). Several mechanisms can be distinguished in transplacental exchanges (89-92).

I) Passive diffusion.

Most compounds cross the human placenta by passive diffusion. This process is energy-independent. Compounds are transferred down a concentration gradient. Water, electrolytes, respiratory gases, as well as most lipid soluble drugs cross placental membranes by passive diffusion (91).

II) Facilitated diffusion.

With facilitated diffusion, substances also are transferred from a region with a higher to a region with a lower concentration. However, a specific carrier is required. Facilitated diffusion is an energy-independent, saturable process that can be competitively inhibited. Glucose and other carbohydrates are transferred by this mechanism (93,94).

III) Active transport.

Active transport occurs against an electrochemical or concentration gradient and requires energy. Transport is carrier-mediated, saturable and competition between related compounds is possible. Energy, needed for this uphill transport, can be supplied directly by ATP-hydrolysis or through coupling to the flux of another compound down its electrochemical gradient in the same (cotransport or symport) or in the opposite (exchange or antiport) direction of substrate movement. Nearly all amino acids (95) and several cations like Na^+ , H^+ , Ca^{2+} and Mg^{2+} are transported in this manner (96-99).

IV) Endocytosis.

Principally three ways of endocytosis can be distinguished: 1) receptor mediated endocytosis, 2) fluid phase endocytosis (also called pinocytosis) and 3) phagocytosis.

Phagocytosis refers to a ligand-induced process responsible for the uptake of large particles. For fluid phase endocytosis specific binding of the substrate to the membrane is not necessary. Vesicles are formed at the plasma membrane and the substrate enters the cytoplasm together with the fluid in these vesicles. With receptor mediated endocytosis the ligand molecule must first interact with a specific receptor at the cell surface. The ligand-receptor complexes are clustered in coated pits, which are invaginated and pinched off to form coated vesicles in the cytoplasm. Clustering of the receptor proteins within coated pits is the initial and essential step of receptor-mediated endocytosis. This process may be either spontaneous or triggered by the ligand (100). Receptors such as those for LDL, Tf, α 2-macroglobuline, mannose-6-phosphate and asialoglycoproteins are clustered in coated pits independent of prior ligand binding. Receptors for EGF, PDGF and insulin for example require ligand binding as a trigger for internalization. Metabolic energy is needed for all these processes. An example of receptor mediated endocytosis in the placenta is transport of IgG (101). The trophoblast also expresses several members of the LDL-receptor family, with one of its functions the uptake of lipids (102). Iron can be taken up by means of receptor mediated endocytosis of diferric Tf (103,104).

1.8 Placental iron transfer

Iron is an important element for growth and development. During pregnancy, the demand for iron is increased. Together with the increasing demand, there is an increase in the amount of iron that is transferred across the placenta. In humans about 5 mg iron per day is transferred at term (105). The total amount of iron transferred during pregnancy is 250-300 mg (106), corresponding to 23 % of maternal stores (107). Maternal serum Tf is the major source of iron in men (107). Placental iron transfer is unidirectional from mother to fetus. In the last trimester iron transfer is directed against a concentration gradient: both the concentration and the iron-saturation of Tf are higher in fetal plasma compared to maternal plasma (107,108).

Human trophoblast cells in culture express TfRs during differentiation towards syncytiotrophoblast (109). Both the maternal-facing microvillous (110,111) and the fetal-facing basal plasma membrane (112) of placental syncytiotrophoblast contain TfRs. It has been shown that iron but not maternal Tf is transferred to the fetus, and that iron passes a placental LIP prior to transport across the basal membrane (113,114). Using cultured cytotrophoblast cells as a model for the in situ syncytiotrophoblast, it has been shown that the syncytiotrophoblast takes up iron by means of receptor-mediated endocytosis of maternal diferric Tf. After endocytosis and release of iron, apoTf returns to the maternal surface (103). Syncytiotrophoblast cells in culture regulate their iron uptake by variation of the number of TfRs and the rate of receptor-mediated endocytosis and exocytosis (104).

Besides Tf-mediated iron uptake, iron in the form of ferric ammonium citrate is also taken up by cultured cytotrophoblasts (115). The mechanism for this iron uptake has not been described.

BeWo cells, derived from a human choriocarcinoma cell line that displays many biochemical and morphological properties common to placental trophoblast, have been shown to take up iron from Tf by receptor-mediated endocytosis just like normal trophoblast cells in culture (116). Polarized BeWo cells, cultured on permeable filters, are shown to contain TfRs at the microvillous and the basal surface and to take up diferric Tf from both sides (117). The recycling of Tf and its receptor occurs through relatively separate endosomes (117).

In the cytosol iron is released from the endosomes into the LIP, probably as ferrous iron (118), where it becomes chelated to a heterogeneous family of low molecular weight components. The LIP is in dynamic equilibrium with other compartments among which ferritin (103,113,115). From the LIP iron is available to meet the fetal needs. How and in which form iron is transferred across the basal syncytiotrophoblast plasma membrane is unknown. The most likely hypothesis is that iron is transported as low molecular weight chelates. For example, lactate has been described as a binding molecule for low molecular weight iron (119). However, in humans lactate is mainly transported from the fetus to the mother (120). Other candidates are ATP, citrate and peptides. Also cytoferrin, another low molecular weight iron binding compound that has been found in human placenta, has been suggested to play a role in maternofetal iron transport (121).

Another hypothesis has been suggested by Harris (122). In this model a special role is contributed to the TfRs at the basal plasma membrane. It suggests that iron enters the placenta by receptor-mediated endocytosis at the maternal side, binds to ferritin (which is probably in dynamic equilibrium with LIP) in the cell and from there it becomes assimilated into fetal apoTf. This hypothesis seems not likely, since at physiological pH basal TfRs have a much higher affinity for diferric Tf than for apoTf (112). Therefore, fetal apoTf will hardly enter the placenta. Moreover, fetal Tf is not in direct contact with the placental basal membrane.

1.9 Aim of the thesis

Although placental iron transfer has extensively been studied for many years, the exact mechanisms have not been cleared up yet.

The main mechanism for placental iron uptake is receptor-mediated endocytosis of maternal diferric Tf. The placental trophoblast expresses TfRs not only on the maternal-facing microvillous surface, but also on the fetal-facing basal surface. No convincing

functional explanation for the presence of basal TfRs has been given so far. During pregnancy the isoTf pattern in maternal serum changes to Tfs with more complex carbohydrate chains. Human fetal serum Tf shows a distribution to less complicated Tfs. These changes might be functional with respect to the regulation of placental iron transfer. We therefore investigated the binding of some isoTf variants to microvillous and basal plasma membrane vesicles, isolated from the same human term placenta (Chapter 4). The observation that Tf binds to basal membranes, as studied with membrane vesicles, is not sufficient to conclude that these receptors are effectively involved in Tf uptake. With polar cultured trophoblast cells we investigated the binding and endocytosis of Tf at the microvillous and basal side of the syncytiotrophoblast (Chapter 5). We also determined uptake of diferric Tf by trophoblast cells cultured on plastic dishes and compared the initial rate of endocytosis of diferric Tf with the steady state rate of iron uptake (Chapter 5).

Tf is mainly synthesized in the liver. Other organs have been shown to synthesize Tf, although in a smaller amount. Tf mRNA was detected previously in rat and mouse placental extracts. The exact origin of this Tf remained unclear. Using a highly purified trophoblast cell population, we were able to show that the human syncytiotrophoblast synthesizes Tf. The heterogeneity of this Tf was determined and appeared to be different from both maternal and fetal serum Tf (Chapter 6).

Although receptor-mediated endocytosis of diferric Tf is the major pathway for iron uptake in eukaryotic cells, Tf-independent iron transport mechanisms have been described for several cell types. With membrane vesicles we were able to characterize a NADH-dependent ferrireductase. We provided evidence that this reductase is involved in uptake of non-Tf iron in cultured human term trophoblast cells. We suggested a role for this mechanism in transfer of iron across the basal membrane to the fetal side (Chapter 7). Finally, we propose a model for iron transfer in human term placenta (Chapter 8).

References

1. Beard JL, Dawson H & Piñero DJ (1996) Iron metabolism: a comprehensive review. *Nutrition Reviews*, 54:295-317.
2. Crichton RR & Ward RJ (1992) Iron metabolism- new perspectives in view. *Biochemistry*, 31:11257-11264.
3. Richardson DR & Ponka P (1997) The molecular mechanisms of the metabolism and transport of iron in normal and neoplastic cells. *Biochimica et Biophysica Acta*, 1331:1-40.
4. Testa U (1985) Transferrin receptors: structure and function. *Current Topics in Hematology*, 5:127-161.
5. De Silva DM, Askwith CC & Kaplan J (1996) Molecular mechanisms of iron uptake in eukaryotes. *Physiological Reviews*, 76:31-47.
6. Aisen P (1980) The transferrins. In: *Iron in Biochemistry and Medicine*, II. Jacobs, A & Worwood, M, eds. London, Academic Press, 87-123.
7. De Jong G, van Dijk JP & van Eijk HG (1990) The biology of transferrin. *Clinica Chimica Acta*, 190:1-46.
8. Aisen P, Aasa R, Malmstrom BG & Vanngard T (1967) Bicarbonate and the binding of iron to transferrin. *Journal of Biological Chemistry*, 242:2484-2490.
9. Evans RW & Williams J (1978) Studies of the binding of different iron donors to human serum transferrin and isolation of iron binding fragments from the N- and C-terminal regions of the protein. *Biochemical Journal*, 173:543-552.
10. Spik G, Bayard B, Fournet B, Strecker G, Bouqueler S & Montreuil J (1975) Studies on glucoconjugates LXIV. Complete structure of the carbohydrate units of human serotransferrin. *FEBS Letters*, 50:296-299.
11. De Jong G & van Eijk HG (1988) Microheterogeneity of human serum transferrin: a biological phenomenon studied by isoelectric focusing in immobilized pH gradients. *Electrophoresis*, 9:589-598.
12. Bierings MB, Heeren JWA, van Noort WL, van Dijk JP & van Eijk HG (1987) Pregnancy and guinea-pig isotransferrins - isolation and characterization of both isotransferrins. *Clinica Chimica Acta*, 165:205-211.

13. Levin MJ, Tuil D, Uzan G, Dreyfus J-C & Kahn A (1984) Expression of the transferrin gene during development of non-hepatic tissues: high level of transferrin mRNA in fetal muscles and adult brain. *Biochemical and Biophysical Research Communications*, 122:212-217.
14. Aldred AR, Dickson PW, Marley PD & Schreiber G (1987) Distribution of transferrin synthesis in brain and other tissues in the rat. *Journal of Biological Chemistry*, 262:5293-5297.
15. Bloch B, Popovici T, Choucham S, Levin MJ, Tuil D & Kahn A (1987) Transferrin gene expression in choroid plexus of the adult rat brain. *Brain Research Bulletin*, 18:573-576.
16. Schreiber G (1987) Synthesis, processing, and secretion of plasma proteins by the liver and other organs and their regulation. In: Putnam FW, *Plasma proteins*. Academic Press, Florida, USA, V:293-363.
17. Yang F, Friedrichs WE, Buchanan JM, Herbert DC, Weaker FJ, Brock JH & Bowman BH (1990) Tissue specific expression of mouse transferrin during development and aging. *Mechanisms of Ageing and Development* 56:187-197.
18. Boockfor FR, Harris SE, Barto JM & Bonner JM (1994) Placental cell release of transferrin: analysis by reverse haemolytic plaque assay. *Placenta*, 15:501-509.
19. Thorstensen K & Romslo I (1990) Review article. The role of transferrin in the mechanism of cellular iron uptake. *Biochemical Journal*, 271:1-10.
20. Aisen P (1992) Entry of iron into cells: a new role for the transferrin receptor in modulating iron release from transferrin. *Annals of Neurology*, 32:S62-S68.
21. Qian ZM & Tang PL (1995) Mechanisms of iron uptake by mammalian cells. *Biochimica et Biophysica Acta*, 1269:205-214.
22. Kühn LC (1989) The transferrin receptor: a key function in iron metabolism. *Schweizerische Medizinische Wochenschrift*, 119:1319-1326.
23. Young SP, Bomford A & Williams R (1984) The effect of the iron saturation of transferrin on its binding and uptake by rabbit reticulocytes. *Biochemical Journal*, 219:505-510.
24. Forgac M (1989) Structure and function of vacuolar class of ATP-driven proton pumps. *Physiological Reviews*, 69:765-796.
25. Foley AA & Bates GW (1989) The influence of inorganic anions on the formation and stability of Fe^{3+} -transferrin-anion complexes. *Biochimica et Biophysica Acta*, 956:154-162.

26. Baker EN & Lindley PF (1992) New perspectives on the structure and function of transferrins. *Journal of Inorganic Biochemistry*, 47:147-160.
27. Núñez MT, Gaete V, Watkins JA & Glass J (1990) Mobilization of iron from endocytic vesicles. The effects of acidification and reduction. *Journal of Biological Chemistry*, 265:6688-6692.
28. Watkins JA, Altazan JD, Elder P, Li C-Y, Nunez M-T, Cui X-X & Glass J (1992) Kinetic characterization of reductant dependent processes of iron mobilization from endocytic vesicles. *Biochemistry*, 31:5820-5830.
29. Li C-Y, Watkins JA & Glass J (1994) The H⁺-ATPase from reticulocyte endosomes reconstituted into liposomes acts as an iron transporter. *Journal of Biological Chemistry*, 269:10242-10246.
30. Crane FL, Sun IL, Clark MG, Grebing C & Löw H (1985) Transplasma-membrane redox systems in growth and development. *Biochimica et Biophysica Acta*, 811:233-264.
31. Morley CGD & Bezkorovainy A (1985) Review. Cellular iron uptake from transferrin: is endocytosis the only mechanism? *International Journal of Biochemistry*, 17:553-564.
32. Clark MG, Patrick EJ, Patten GS, Crane FL, Löw H & Grebing C (1981) Evidence for extracellular reduction of ferricyanide by rat liver. A trans-plasma membrane redox system. *Biochemical Journal*, 200:565-572.
33. Thorstensen K (1988) Hepatocytes and reticulocytes have different mechanisms for the uptake of iron from transferrin. *Journal of Biological Chemistry*, 263:16837-16841.
34. Thorstensen K & Romslo I (1988) Uptake of iron from transferrin by isolated rat hepatocytes. A redox-mediated plasma membrane process. *Journal of Biological Chemistry*, 263:8844-8850.
35. Jefferies WA, Gabathuler R, Rothenberger S, Food M & Kennard ML (1996) Pumping iron in the '90s. *Trends in Cell Biology*, 6:223-228.
36. Page MA, Baker E & Morgan EH (1984) Transferrin and iron uptake by rat hepatocytes in culture. *American Journal of Physiology*, 246:G26-G33.
37. Trinder D, Zak O & Aisen P (1996) Transferrin receptor-independent uptake of diferric transferrin by human hepatoma cells with antisense inhibition of receptor expression. *Hepatology*, 23:1512-1520.
38. Klausner RD & Dancis A (1994) A genetic approach to elucidating eukaryotic iron metabolism. *FEBS Letters*, 355:109-113.

39. Askwith CC, Eide D, Van Ho A, Bernard PS, Li L, Davis-Kaplan S, Sipe DM & Kaplan J (1994) The *FET3* gene of *S. cerevisiae* encodes a multi copper oxidase required for ferrous iron uptake. *Cell*, 76:403-410.
40. Sun IL, Navas P, Crane FL, Morr  DJ & L w H (1987) NADH diferric transferrin reductase in liver plasma membrane. *Journal of Biological Chemistry*, 262:15915-15921.
41. Raja KB, Simpson RJ & Peters TJ (1992) Investigation of a role for reduction in ferric iron uptake by mouse duodenum. *Biochimica et Biophysica Acta*, 1135:141-146.
42. Pountney DJ, Raja KB, Bottwood MJ, Wrigglesworth JM & Simpson RJ (1996) Mucosal surface ferricyanide reductase activity in mouse duodenum. *BioMetals*, 9:15-20.
43. Riedel H-D, Remus AJ, Fitscher BA & Stremmel W (1995) Characterization and partial purification of a ferrireductase from human duodenal microvillus membranes. *Biochemical Journal*, 309:745-748.
44. B rczi A & Faulk WP (1992) Iron-reducing activity of plasma membranes. *Biochemistry International*, 28:577-584.
45. B rczi A, Sizendky JA, Crane FL & Faulk WP (1991) Diferric transferrin reduction by K562 cells. A critical study. *Biochimica et Biophysica Acta*, 1073:562-570.
46. Inman RS, Coughlan MM & Wessling-Resnick M (1994) Extracellular ferrireductase activity of K562 cells is coupled to transferrin-independent iron transport. *Biochemistry*, 33:11850-11857.
47. Jordan I & Kaplan J (1994) The mammalian transferrin-independent iron transport system may involve a surface ferrireductase activity. *Biochemical Journal*, 302:875-879.
48. Han O, Failla ML, Hill AD, Morris ER & Smith JC (1995) Reduction of Fe(III) is required for uptake of nonheme iron by Caco-2 cells. *Journal of Nutrition*, 125:1291-1299.
49. Randell EW, Parkes JG, Olivieri NF & Templeton DM (1994) Uptake of non-transferrin-bound iron by both reductive and nonreductive processes is modulated by intracellular iron. *Journal of Biological Chemistry*, 269:16046-16053.
50. Sturrock A, Alexander J, Lamb J, Craven CM & Kaplan J (1990) Characterization of a transferrin-independent uptake system for iron in HeLa cells. *Journal of Biological Chemistry*, 265:3139-3145.
51. Kaplan J, Jordan I & Sturrock A (1991) Regulation of the transferrin-independent iron transport system in cultured cells. *Journal of Biological Chemistry*, 266:2997-3004.
52. Barisani D, Berg CL, Wessling-Resnick M & Gollan JL (1995) Evidence for a low K_M transporter for non-transferrin-bound iron in isolated rat hepatocytes. *American Journal of Physiology*, 269:G570-G576.

53. Morgan EH (1988) Membrane transport of non-transferrin-bound iron by reticulocytes. *Biochimica et Biophysica Acta*, 943:428-439.
54. Qian ZM & Morgan EH (1991) Effect of metabolic inhibitors on uptake of non-transferrin-bound iron by reticulocytes. *Biochimica et Biophysica Acta*, 1073:456-462.
55. Inman RS & Wessling-Resnick M (1993) Characterization of transferrin-independent iron transport in K562 cells. *Journal Biological Chemistry*, 268:8521-8528.
56. Jacobs A (1977) Low molecular weight intracellular iron transport compounds. *Blood*, 50:433-439.
57. Crichton RR (1991) *Inorganic Biochemistry of Iron Metabolism*. Ellis Horwood Ltd., London.
58. Pollack S (1992) Receptor-mediated iron uptake and intracellular iron transport. *American Journal of Hematology*, 39:113-118.
59. Rothman RJ, Serroni A & Farber JL (1992) Cellular pool of transient ferric iron, chelatable by deferoxamine and distinct from ferritin, that is involved in oxidative cell injury. *Molecular Pharmacology*, 42:703-710.
60. Breuer W, Epsztejn S & Cabantchik ZI (1995) Iron acquired from transferrin by K562 cells is delivered into a cytoplasmic pool of chelatable iron(II). *Journal of Biological Chemistry*, 270:24209-24215.
61. Pollack S, Campana T & Weaver J (1985) Low molecular weight iron in guinea pig reticulocytes. *American Journal of Hematology*, 19: 75-84.
62. Epsztejn S, Kakhlon O, Glickstein H, Breuer W & Cabantchik ZI (1997) Fluorescence analysis of the labile iron pool of mammalian cells. *Analytical Biochemistry*, 248:31-40.
63. Weaver J & Pollack S (1989) Low-M_r iron isolated from guinea pig reticulocytes as AMP-Fe and ATP-Fe complexes. *Biochemical Journal*, 261:787-792.
64. Deighton N & Hider RC (1989) Intracellular low molecular weight iron. *Biochemical Society Transactions*, 17:490.
65. Conrad ME, Umbreit JN, Moore EG, Peterson RDA & Jones MB (1990) A newly identified iron binding protein in duodenal mucosa of rats. Purification and characterization of mobilferrin. *Journal of Biological Chemistry*, 265:5273-5279.
66. Conrad ME & Umbreit JN (1993) A concise review: iron absorption - the mucin-mobilferrin-integrin pathway. A competitive pathway for metal absorption. *American Journal of Hematology*, 42:67-73.

67. Conrad ME, Umbreit JN, Moore EG & Heiman D (1996) Mobilferritin is an intermediate in iron transport between transferrin and hemoglobin in K562 cells. *Journal of Clinical Investigation*, 98:1449-1454.
68. Arosio P, Cairo C & Levi S (1989) *Iron in Immunity, Cancer and Inflammation*. John Wiley & Sons Ltd: 55-79.
69. Worwood M (1990) Ferritin. *Blood Reviews*, 4:259-269.
70. Harrison PM, Glegg GA & May K (1980) Ferritin structure and function. In: *Iron in biochemistry and medicine II*. Jacobs A & Worwood M Academic Press, London/New York:131-171.
71. Arosio P, Levi S, Santambrogio P, Cozzi A, Luzzago A, Cesareni G & Albertini A (1991) Structural and functional studies of human ferritin H and L chains. *Current Study in Hematology & Blood Transfusion*, 58: 127-131.
72. Leibold EA & Guo B (1992) Iron-dependent regulation of ferritin and transferrin receptor expression by the iron-responsive element binding protein. *Annual Reviews of Nutrition*, 12:345-368.
73. Kühn LC & Hentze MW (1992) Coordination of cellular iron metabolism by post-transcriptional gene regulation. *Journal of Inorganic Biochemistry*, 47:183-195.
74. Klausner RD, Rouault TA & Harford JB (1993) Regulating the fate of mRNA: the control of cellular iron metabolism. *Cell*, 72:19-28.
75. Grosser O (1909) *Vergleichende Anatomie und Entwicklungsgeschichte der Eihäute und der Placenta*. Braumüller W., Vienna.
76. Grosser O (1927) *Frühentwicklung, Eihautbildung und Placentation des Menschen und der Säugetiere*. Bergmann, J.F., München.
77. Page KR (1993) *The physiology of the human placenta*. Kings Lynn & Guilford, Biddles Ltd., England: 16-25.
78. Carter AM (1997) When is the maternal placental circulation established in man? *Placenta*, 18:83-87.
79. Truman P & Ford HC (1984) The brush border of the human term placenta. *Biochimica et Biophysica Acta*, 779:139-160.
80. Enders AC (1965) Formation of syncytium from cytotrophoblast in the human placenta. *Obstetrics and Gynaecology*, 25:378-386.

81. Simpson RA, Mayham TM & Barnes PR (1992) From 13 weeks to term, the trophoblast of human placenta grows by the continuous recruitment of new proliferative units: a study of nuclear number using the disector. *Placenta*, 13:501-512.
82. Teasdale F & Jean-Jacques G (1985) Morphometric evaluation of the microvillous surface enlargement factor in the human placenta from mid-gestation to term. *Placenta*, 6:375-381.
83. Fox H (1997) Aging of the placenta. *Archives of Disease in Childhood*, 77: F165-F170.
84. Khodr GS & Siler-Khodr TM (1980) Placental luteinizing hormone-releasing factor and its synthesis. *Science*, 207:315-318.
85. Petraglia F, Sawchenko P, Lim ATW, Rivier J & Vale W (1987) Localization, secretion and action of inhibin in human placenta. *Science*, 237:187-189.
86. Horne CH, Towler CM, Pugh-Humphreys RG, Thomson AW & Bohn H (1976) Pregnancy-specific β_1 glycoprotein – a product of the syncytiotrophoblast. *Experientia*, 32:1197-1199.
87. Dreskin RB, Spicer SS & Green WB (1970) Ultrastructural localization of chorionic gonadotropin in human term placenta. *Journal of Histochemistry and Cytochemistry*, 18:862-874.
88. Watkins WB (1978) Use of immuno-cytochemical techniques for the localization of human placental lactogen. *Journal of Histochemistry and Cytochemistry*, 26:288-292.
89. Bourget P, Roulot C & Fernandez H (1995) Models for placental transfer studies of drugs. *Clinical Pharmacokinetic Concepts*, 28:161-180.
90. Van Kreel BK (1981) A mathematical approach to mechanisms of placental transfer. *Placenta* (supplement 1): 81-100.
91. Soma H. (1984) Placental morphological structures and their significance to pharmacokinetics and pharmacodynamics. *Clinical Pharmacology in Pregnancy*. Kuemmerle, HP & Brendel, K, Eds. Thieme-Stratton Inc., New York: 23-27.
92. Pacifici GM & Nottoli R (1995) Placental transfer of drugs administered to the mother. *Clinical Pharmacokinetic Concepts*, 28:235-269.
93. Johnson LW & Smith CH (1980) Monosaccharide transport across microvillous membrane of human placenta. *American Journal of Physiology*, 238:C160-C168.
94. Johnson LW & Smith CH (1985) Glucose transport across the basal plasma membrane of human placental syncytiotrophoblast. *Biochimica et Biophysica Acta*, 815:44-50.

95. Yudilevich DL & Sweiry JH (1985) Transport of amino acids in the placenta. *Biochimica et Biophysica Acta*, 822:169-201.
96. Balkovetz DF, Leibach FH, Mahesh VB, Devoe LD, Cragoe JrJ & Ganapathy V (1986) Na⁺/H⁺-exchanger of human placental brush-border membrane: identification and characterization. *American Journal of Physiology*, 251:C852-C860.
97. Van Dijk JP (1981) Active transfer of plasma bound compounds calcium and iron across the placenta. *Placenta (Supplement 1)*:139-164.
98. Fisher GJ, Kelley LK & Smith SH (1987) ATP-dependent calcium transport across basal plasma membranes of human placental trophoblast. *American Journal of Physiology*, 252:C38-C46.
99. Brunette MG & Leclerc M (1991) Ca²⁺ transport through the brush border membrane of human placenta syncytiotrophoblasts. *Canadian Journal of Physiology and Pharmacology*, 70:835-842.
100. Bu G & Schwartz AL (1994) Receptor-mediated endocytosis. *The Liver: Biology and Pathobiology*, third edition. Arias, IM, Boyer, JL, Fausto, N, Jakoby, WB, Schachter, DA & Scharfetz, DA (eds.). Raven Press Ltd., New York pp. 259-275.
101. Sooranna SR & Contractor SF (1990) Binding and internalization of immunoglobulin G by cultured human trophoblast. *Journal of Developmental Physiology*, 13:333-338.
102. Coukos G, Gåfvels ME, Wittmaack F, Matsuo H, Strickland DK, Coutifaris C & Straus III JF (1994) Potential roles for the low density lipoprotein receptor family of proteins in implantation and placentation. *Annals of the New York Academy of Sciences*, 734:91-102.
103. Douglas GC & King BF (1990) Uptake and processing of ¹²⁵I-labelled transferrin and ⁵⁹Fe-labelled transferrin by isolated human trophoblast cells. *Placenta*, 11:41-57.
104. Starreveld JS, van Denderen J, Kroos MJ, van Eijk HG & van Dijk JP (1996) Effects of iron supplementation on iron uptake by differentiation cytotrophoblasts. *Reproduction, Fertility & Development*, 8:417-422.
105. Fletcher J & Suter PEN (1969) The transport of iron by the human placenta. *Clinical Science*, 36:209-220.
106. Burman D (1974) Iron metabolism in infancy and childhood. In: *Iron in Biochemistry and Medicine*. Jacobs, A & Worwood, M, Eds. Academic Press, London/New York: 543-562.
107. Van Dijk JP (1988) Review Article: regulatory aspects of placental iron transfer - a comparative study. *Placenta*, 9:215-226.

108. Van Dijk JP (1977) Iron metabolism and placental transfer of iron in the term rhesus monkey (*Macaca mulatta*): a compartmental analysis. *European Journal of Obstetrics, Gynecology and Reproductive Biology*, 7:127-139.
109. Bierings MB, Adriaansen HJ & van Dijk JP (1988) The appearance of transferrin receptors on cultured human cytotrophoblast and in vitro-formed syncytiotrophoblast. *Placenta*, 9:387-396.
110. Wada HG, Hass PE & Sussman HH (1979) Transferrin receptor in human placental brush border membranes. Studies on the binding of transferrin to placental membrane vesicles and the identification of a placental brush border glycoprotein with high affinity for transferrin. *Journal of Biological Chemistry*, 254:12629-12635.
111. Loh TT, Higuchi DA, van Bockxmeer FM, Smith CH & Brown EB (1980) Transferrin receptors on the human placental microvillous membrane. *Journal of Clinical Investigation*, 65:1182-1191.
112. Vanderpuye OA, Kelley LK & Smith CH (1986) Transferrin receptors in the basal plasma membrane of the human placental syncytiotrophoblast. *Placenta*, 7:391-403.
113. Van Dijk JP, van Kreel BK & Heeren JWA (1985) Studies on the mechanisms involved in iron transfer across the isolated guinea pig placenta by means of bolus experiments. *Journal of Developmental Physiology*, 7:1-16.
114. Contractor SF & Eaton BM (1986) Role of transferrin in iron transport between maternal and fetal circulations of perfused lobule of human placenta. *Cell Biochemistry and Function*, 4:69-74.
115. Starreveld JS, Kroos MJ, van Suijlen JDE, Verrijt CEH, van Eijk HG & van Dijk JP (1995) Ferritin in cultured human cytotrophoblasts: synthesis and subunit distribution. *Placenta*, 16:383-395.
116. Van der Ende A, du Maine A, Simmons CF, Schwartz AL & Strous GJ (1987) Iron metabolism in BeWo chorion carcinoma cells. Transferrin-mediated uptake and release of iron. *Journal of Biological Chemistry*, 262:8910-8916.
117. Cerneus DP & van der Ende A (1991) Apical and basolateral transferrin receptors in polarized BeWo cells recycle through separate endosomes. *Journal of Cell Biology*, 114:1149-1158.
118. Wong CT, McArdle HJ & Morgan EH (1987) Effect of iron chelators on placental uptake and transfer of iron in rat. *American Journal of Physiology*, 252:C477-C482.
119. Inoue T, Toh N & Kimoto E (1987) Studies on the major intermediate transit iron complex in human placenta. *Inorganica Chimica Acta*, 135:1279-1285.

120. Schaefer A, Piguard F, Dellenbach P & Haberey P (1993) Placental-fetal "alanine-lactate cycle" in the human during late gestation. *Trophoblast Research*, 7:103-114.
121. Knisely AS, Grady RW, Kramer EE & Jones RL (1989) Cytoferrin, maternofetal iron transport, and neonatal hemochromatosis. *American Journal of Clinical Pathology*, 92:755-759.
122. Harris ED (1992) New insights into placental iron transport. *Nutrition Reviews*, 50:329-337.

2

Materials and Methods

2.1 Materials

2.1.1 Chemicals

Human serum transferrin was purchased from Behringwerke (Marburg and Lahn, Germany). Calcium/magnesium free Earle's Balanced Salts (EBSS) and Modified Eagle's medium (MEM) without L-methionine and L-glutamine were from Gibco BRL, Life Technologies LTD (Scotland). Dulbecco's modification of Eagle's medium (DMEM) without L-glutamine with 4.5 g/l dextrose, fetal calf serum (FCS), Medium 199 (M199), penicillin, streptomycin and amphotericin were from ICN Biomedicals Inc. (Costa Mesa, CA). NADH, NADPH, DNase I, L-glutamine and Complete® protease inhibitor cocktail were from Boehringer Mannheim (FRG). Trypsin 1:250, aprotinin (protease inhibitor), bovine serum albumin (BSA), DL-propranolol, L-methionine and phenylmethylsulphonylfluoride (PMSF) were from Sigma Chemical Co. (St. Louis, MO). Percoll and Concanavalin A (Con A) Sepharose were from Pharmacia (Sweden). Phosphate buffered saline (PBS) tablets were from Oxoid Unipath LTD (Hampshire, UK). Reverse transcriptase was from Perkin Elmer Cetus (Norwalk, CT, USA). Restriction enzymes PstI and HindIII were respectively from Boehringer Mannheim (FRG) and Gibco BRL (Gaithersburg, USA). Goldstar DNA polymerase and PCR-buffer were from Eurogentec (Seraing, Belgium). All other chemicals and reagents were from Sigma, ICN or Boehringer Mannheim.

Isotopes

[³⁵S]-methionine was from ICN Biomedicals Inc. (Costa Mesa, CA). [³H]-dihydroalprenolol and Na¹²⁵I were from Amersham Life Science (Buckinghamshire, UK). ⁵⁹FeCl₃ in 0.5 M HCL was from DuPont, NEN Life Science Products (Boston, MA).

Antibodies

Mouse anti-vimentin and mouse anti-cytokeratin were from ICN Biomedicals Inc. (Costa Mesa, CA). Rabbit anti-human transferrin (titre = 2800 mg/l), mouse anti-human platelet p24, CD9 clone P1/33/2 and FITC-labelled rabbit anti-mouse IgG were from DAKO A/S (Denmark). Dynabeads® M-450 goat anti-mouse IgG was from Dynal A.S. (Oslo, Norway). Anti-transferrin receptor mouse monoclonal antibody clone B3/25 was from Boehringer Mannheim (FRG). AuroProbe™ EM 10 nm gold labelled goat anti-mouse IgG was from Amersham Life Science (Buckinghamshire, UK). Goat anti-rabbit IgG coupled to alkaline phosphatase was from BioRad (Richmond, USA). Rabbit polyclonal antibody to the 67 kD subunit of the *Neurospora* vacuolar ATPase (V-ATPase) (1) was kindly supplied by Dr. B.J. Bowman, University of California, Santa Cruz: Sinsheimer Laboratories).

2.1.2 Tissue source

Normal human term placentae were obtained from the department of Obstetrics and Gynaecology, University Hospital Rotterdam/Dijkzigt, within half an hour after spontaneous vaginal delivery.

2.2 Isolation and culture of human term trophoblast cells

The placentae were processed according to Kliman et al. (2) with slight modification (3). Approximately 50 g of villous tissue was cut into small pieces, washed with ice-cold 0.15 M NaCl and incubated in calcium/magnesium free EBSS pH 7.4, supplemented with 25 mM 2-[4-(2-hydroxyethyl)-1-piperazinyl]-ethansulphonic acid (HEPES), 0.04 mg/ml gentamicin, 0.8 mM MgSO₄, 1.0 mM CaCl₂, 0.1 mg/ml DNase I and 13.5 mg/ml trypsin 1:250 in a shaking water bath at 37°C. After the first incubation step of 10 min in 75 ml of this trypsin-DNase solution, the placental tissue was filtered through a nylon mesh (90 µm pore size). The filtrate was discarded and the remaining tissue was further digested three times for 30 min at 37°C in respectively 200, 125 and 100 ml trypsin-DNase solution. After each incubation, the cell suspension was filtered and centrifuged in the presence of FCS at 1,000 g for 5 min at 4°C. The pellets were resuspended in DMEM, pooled, centrifuged again at 1,000 g for 10 min and resuspended in 4 ml DMEM. A small trace of DNase was added to the cell suspension, followed by incubation for 5 min at 37°C. Subsequently the cell suspension was divided into two equal parts and each layered over a Percoll gradient. The gradient was made from 70 % to 5 % Percoll (v/v) in 5 % steps of 3 ml by dilutions of Percoll in EBSS. The osmolarity of the gradient was 300 mosmol. The gradient was centrifuged at 1,200 g for 20 min. Trophoblast cells were obtained from the middle of the Percoll gradient (density: 1.048–1.062 g/ml), washed with DMEM and finally resuspended in DMEM containing 10 % FCS. The isolated cell population was additionally purified by indirect immunopurification using mouse anti-human CD9 as primary (4) and goat anti-mouse IgG bound to Dynabeads as secondary antibody. For immunopurification cells were diluted to a concentration of 4×10^6 cells/ml DMEM with 10 % FCS and incubated with 1 µg anti-CD9/ 2×10^6 cells for 30 min at 4°C, centrifuged at 800 g for 6 min, washed twice and finally resuspended in 0.5 – 1 ml DMEM. Dynabeads (10^7 beads/ 20×10^6 cells) were added and cells were incubated for 20 min at 4°C. Cells coated with anti-CD9 became attached to the beads. The beads were removed from the cell suspension by a magnet. The remaining cell population consisted for over 96 % of cells from trophoblast origin. This was revealed by immunolabelling studies using mouse-anti-vimentin, mouse-anti-cytokeratin and FITC-labelled rabbit anti-mouse IgG. About 1.5×10^6 cells were cultured on 35 mm Falcon culture dishes (Greiner and Sohne, Germany) in 2.5 ml culture medium consisting of 80 vol. % Medium 199, 20 vol. % FCS, 4 mM L-glutamine, 0.3 mg/ml gentamicin, 50 IU/ml

penicillin, 50 µg/ml streptomycin and 2.5 µg/ml amphotericin. For some experiments 0.5×10^6 cells in 0.25 ml culture medium were cultured on 0.45 µm microporous membrane filters (Millicell HA culture plate inserts, Millipore). Cells were cultured at 37°C in humidified 5 % CO₂/95 % air. After 24 h, the cells were washed with phosphate buffered saline (PBS) and the medium was refreshed. After 48 h, the culture consisted of 17 % mononuclear cells, 21 % aggregates and 62 % syncytia (5).

2.3 Isolation and characterization of membrane vesicles

2.3.1 Isolation of membrane vesicles

Both microvillous and basal membrane vesicles were isolated from the same human term placenta. Microvillous membrane vesicles (MMV) were isolated according to the method of Booth, Olaniyan and Vanderpuye (6), modified by Dicke et al. (7). Basal membrane vesicles (BMV) were isolated according to a modification (7) of the method of Kelley, Smith and King (8).

All steps of the procedure were performed at 4°C, except where noted. After the decidua and the chorionic plate were removed, approximately 100 g of villous tissue was cut into small pieces and washed in 0.15 M NaCl to remove excess of blood. The villous tissue was homogenized, first using an electrical blender for 20 – 30 s and secondly using a motor-driven Potter homogenizer with ten strokes at 1700 rpm. This material was gently stirred in 150 ml phosphate-buffered saline (PBS, consisting of 136.9 mM NaCl, 2.7 mM KCl, 8.1 mM Na₂HPO₄ and 1.4 mM KH₂PO₄) at pH 7.4 for 1 h. The tissue was filtered through nylon mesh (90 µm pore size). The filtrate was used for further purification of MMV, whereas BMV were prepared from the remaining tissue.

Purification of BMV

After filtration, the remaining tissue was washed with 400 ml of 50 mM Tris-HCl buffer pH 7.4 and collected on nylon mesh (90 µm pore size). The tissue was sonicated in a total volume of 600 ml 50 mM Tris-HCl pH 7.4, using a Vibra-cell high intensity 250 Watt ultrasonic processor (Sonics & Materials Inc., Connecticut, USA) with a ¾" standard probe. The tissue was cooled in an ice-ethanol bath and sonicated at setting 10 (250 W) for 25 s. Sonicated tissue was collected on nylon mesh, washed three times with 5 mM Tris-HCl pH 7.4 (total volume of 400 ml) and then gently stirred for 30 min in 600 ml of the same buffer. To remove the basal cell membrane from the basement membrane, the tissue was incubated in 125 ml of 200 mM sucrose/50 mM Tris pH 7.4, containing 10 mM EDTA for 30 min at room temperature. This mixture was cooled with an ice-ethanol bath and sonicated at setting 10 for 25 s. Large pieces of remaining tissue were removed by filtration through nylon mesh (90 µm pore size) and the filtrate was centrifuged at 10,000 g for 20 min. The resulting supernatant was

centrifuged at 90,000 g for 30 min to yield a crude preparation of basal cell membrane. The pellet was resuspended in 15 ml of 250 mM sucrose/50 mM Tris pH 7.4 by passing it through syringe needles (23G and 25G) and centrifuged again at 90,000 g for 30 min. The final pellet was resuspended (23G and 25G syringe needles) in PBS pH 7.4 at a concentration between 6 and 10 mg/ml, frozen in liquid nitrogen and stored at -80°C .

Purification of MMV

The filtrate was stored overnight at 4°C . Next day, the filtrate was centrifuged at 800 g for 10 min, followed by subsequent centrifugation of the supernatant at 10,000 g for 10 min and re-centrifugation of the resulting supernatant at 90,000 g for 35 min. The pellet from the last centrifugation step was resuspended in 60 ml of 300 mM mannitol/10 mM Hepes/2 mM Tris pH 7.4 by passing it through a 23G and a 25G syringe needle. The suspension was stirred in the presence of 10 mM MgCl_2 for 10 min. Non-microvillous membranes were aggregated in the presence of Mg^{2+} and precipitated by centrifugation at 2,200 g for 12 min. The supernatant was re-centrifuged at 90,000 g for 35 min to yield the MMV. The final pellet was resuspended in PBS pH 7.4 (23G and 25G syringe needles) at a protein concentration between 6 and 10 mg/ml, frozen in liquid nitrogen and stored at -80°C .

Tissue homogenate (H_0)

H_0 was prepared by homogenizing 10 g of villous tissue in 50 ml of 250 mM sucrose/50 mM Tris/1 mM EDTA pH 7.4, first in an electrical blender for 1 min, followed by homogenizing with a motor-driven Potter for 10 strokes at 1700 rpm. The tissue was filtered through 6 layers of cotton gauze, the filtrate was frozen in liquid nitrogen and stored at -80°C .

2.3.2 Marker enzymes

Alkaline phosphatase

We measured the alkaline phosphatase activity according to Richterich, Colombo and Weber (9) as a marker for the microvillous membranes. Diluted vesicles (H_0 and BMV 10 times; MMV 50 times; 25 μl) were incubated in 1 ml reaction medium (1:1 of 100 mM Tris-maleate buffer pH 9 and a solution consisting of 10 mM MgCl_2 , 0.5 mM CaCl_2 and 0.4 mM ZnCl_2) containing the substrate p-nitrophenyl-phosphate (1.86 mg/ml) for 5 min at 37°C . The reaction was stopped by the addition of 3 ml ice-cold 1 M NaOH. The extinction was determined at 410 nm (Ultrospec III spectrophotometer, Pharmacia LKB). Para-nitrophenol at varying concentrations was used as standard.

Dihydroalprenolol binding

Dihydroalprenolol binding (8,10) was determined as a marker for basal membranes. We incubated 10 μl of vesicles in a total volume of 150 μl PBS pH 7.4 containing 10 nM [^3H]-dihydroalprenolol for 30 min at 30°C . The incubation was stopped by the addition of 2.5 ml ice-cold PBS pH 7.4. The vesicles were filtered through two glass-fibre filters GF/C (Whatman

International Ltd., UK) and washed four times with 2.5 ml ice-cold PBS pH 7.4. Filters were dried, universal liquid scintillation counting cocktail for aqueous and non-aqueous samples (Insta-gel plus, Packard, USA) was added and radioactivity was counted in a Packard liquid scintillation counter. Non-specific binding was determined in the presence of 30 μ M DL-propranolol.

Arylsulphatase

Arylsulphatase was measured as a marker for lysosomes (11). Reaction was started by the addition of 0.4 ml diluted reaction medium (0.02 M 4-nitrocatecholsulfate in 0.5 M NaAc-HAc buffer pH 5.5, diluted 1:1 with distilled water) to 20 μ l of undiluted samples, incubated for 15 min at 37°C and stopped by the addition of 1 ml ice-cold 1 M NaOH. Extinction was determined within 1 h at 515 nm. The extinction coefficient used was 11,200 l/mol/cm.

Succinate dehydrogenase

The activity of succinate dehydrogenase was determined as a marker for mitochondria (12). Undiluted samples (20 μ l) were shaken in 1 ml reaction medium (50 mM potassium phosphate buffer pH 7.4; 50 mM Na-succinate; 25 mM sucrose; 0.1 % 2-(p-iodophenyl)-3-(p-nitrophenyl)-5-(phenyltetrazolium) for 15 min at 37°C. After addition of 1 ml 10 % trichloroacetic acid (TCA), the formazan was extracted with 2 ml ethylacetate and its extinction measured at 490 nm. The activity was determined using an extinction coefficient of 20,100 l/mol/cm for formazan in ethylacetate.

NADPH-dependent cytochrome c reductase

NADPH-dependent cytochrome c reductase was measured as marker for the endoplasmic reticulum (13). Reduction of cytochrome c was determined by following the decrease in extinction at 550 nm in 3 ml reaction medium containing 0.1 mM NADPH, 0.33 mM KCN, 0.05 mM cytochrome c, and 0.05 M potassium phosphate buffer pH 7.5 for 5 min. We compared the reduction in the presence of 20 μ l undiluted samples to a control without the addition of vesicles. An extinction coefficient of 18,500 l/mol/cm for reduced minus oxidized cytochrome c was used.

All enzyme activities were determined relative to the protein concentration (see 2.4). We compared the enzyme activities of the vesicles to those of H_0 in order to determine the enrichments of membranes and organelles in our preparations.

2.3.3 Orientation of membrane vesicles

Orientation of MMV was determined by assaying the alkaline phosphatase activity as described, with and without previous treatment of the vesicles with 0.1 % saponin. Orientation of BMV was determined by assaying the Na^+K^+ -ATPase activity (14) after treatment of the vesicles with or without 0.1 % saponin or 40 nM valinomycin (15). ATPase activity of 20 μ l

five times diluted vesicles was determined in 0.2 ml medium, containing 100 mM NaCl, 10 mM KCl, 5 mM MgCl₂, 30 mM imidazole and 5 mM Na₂ATP at pH 7.4 and in the same medium without KCl, but with the addition of 0.1 mM ouabain. The samples were incubated for 30 min at 37°C, after which the reaction was stopped by the addition of 0.75 ml 8.6 % TCA. The amount of inorganic phosphate formed was determined by addition of 0.75 ml 0.66 M H₂SO₄, 1.15 % ammonium heptamolybdate, 9.6 % FeSO₄·6H₂O and determination of the extinction at 700 nm after 30 min at room temperature. As standards we used varying concentrations of K₂HPO₄. The Na⁺K⁺-ATPase activity could be determined as the difference in ATPase activity in these media.

2.3.4 Gel electrophoresis of membrane vesicles

Approximately 50 µg (5 µl) of BMV and MMV was diluted five times in sample buffer containing 10.0 ml distilled water, 2.5 ml 0.5 M Tris-HCl pH 6.8, 2.0 ml glycerol, 4.0 ml 10 % (w/v) SDS, 1.0 ml 0.8 M dithiothreitol (DTT) and 0.5 ml 1 % bromophenol blue. Samples were boiled for 5 min and put on 4–20 % Tris-HCl ready polyacrylamide gel (BioRad, Richmond, USA). Gels were run at 200 V for 45–60 min in Mini-PROTEAN II apparatus (BioRad) using runningbuffer, containing 0.3 % (w/v) Tris, 1.44 % (w/v) glycine and 0.1 % (w/v) SDS at pH 8.3. After electrophoresis, gels were dried and stained with Coomassie blue R-250 (BioRad). Kaleidoscope prestained standards (BioRad) and low molecular weight markers (Pharmacia, Sweden) were run together with the samples. In order to demonstrate the presence of V-ATPase, vesicles were subjected to SDS polyacrylamide gelelectrophoresis on a 10 % Tris-HCl gel (BioRad) under reducing conditions (1 h, 100 V). The gel was blotted on a 0.2 micron nitro-cellulose membrane (1 h, 100 V, 250 mA, 4°C, BioRad Trans-Blot Cell). V-ATPase was identified with an Immuno-lite[®] assay kit (BioRad) using a rabbit polyclonal antibody to the 67 kD subunit of *Neurospora* V-ATPase (1) as primary and goat anti-rabbit IgG coupled to alkaline phosphatase as secondary antibody. The blots were exposed to photosensitive film for 15 min and scanned with an Ultrosan XL Enhanced Laser Densitometer (Pharmacia LKB, Sweden). As a control the blot was incubated with pre-immune serum.

2.3.5 Determination of membrane cholesterol and phospholipid content

Lipid extraction

Lipids were extracted using the method of Bligh and Dyer (16). Approximately 1 mg membrane vesicles was diluted with distilled water until a volume of 0.4 ml. These dilutions were vortexed for 1 min in the presence of 0.5 ml chloroform and 1.0 ml methanol. Another 0.5 ml chloroform was added and samples were vortexed again for 1 min. Finally 0.5 ml distilled water was added, followed by 1 min of vortexing and centrifugation at 1,000 g for 15 min. The chloroform layer (bottom layer) contained the purified lipids. The extracted samples were saponified by incubation of the lipids in 3 ml of a mixture of 95 % ethanol/3.3 %

KOH for 30 min at 60°C (17). Samples were cooled to room temperature and hexane extracted twice (first with 3 ml, second with 2 ml hexane). Hexane was evaporated under nitrogen. Part of the evaporated lipid extract was directly used for a phosphorus assay, whereas another part was dissolved in isopropanol before determination of the cholesterol content.

Determination of cholesterol content

Total cholesterol content was measured with an enzymatic test from Boehringer according to the manufacturer's protocol (Boehringer Mannheim, FRG).

Total phosphorus analysis

Total phosphorus content was determined according to a modification (18) of the method of Fiske and Subbarow (19). Evaporated lipid extracts were destructured in 0.4 ml $\text{H}_2\text{SO}_4/\text{HClO}_4$ /distilled water (1.5:1.5:1.0) (v/v) at 210°C until solutions were colourless (about 4 h). Samples were slowly cooled, 3 ml distilled water, 200 μl 5 % ammoniummolybdate and 200 μl Fiske/Subbarow reagent (125 mg 1-amino-2-naphthol-4-sulphonic acid in 50 ml freshly prepared 15 % (w/v) $\text{Na}_2\text{S}_2\text{O}_5$ with the addition of 250 mg Na_2SO_3) were added and the solution was incubated for 10 min at 90°C. The extinction was measured at 830 nm and compared to standards up to 60 nmol inorganic phosphate.

2.3.6 Fatty acid analysis in phospholipids

Membrane lipids were extracted according to Bligh and Dyer (16) as described above. The lipids were separated by thin layer chromatography on Kieselgel 60 F254 plates (Merck, Darmstadt, Germany) activated at 110°C for 1 h. The solvent system contained n-hexane/diethylether/acetic acid (60:40:1) (v/v/v) with 0.02 % butylated hydroxytoluene. Cholesterol esters and phospholipids were identified by comparison with simultaneously run standards. Phospholipid spots were scraped off and fatty acids were transmethyalted with 14 % borontrifluoride in methanol for 10 min at 100°C, according to the method of Morrison and Smith (20). The fatty acid methyl esters were separated and quantified by capillary gas liquid chromatography on a CP-Sil88 column (WCOT, 50 m x 0.25 mm, 0.20 μm film; Chrompack, Bergen op Zoom, NL) in a Chrompack CP9000 capillary gas chromatograph. Identification of the fatty acid methyl esters was performed by comparison of the retention times to those of authentic standards (Alltech Ass., Deerfield, IL, USA).

2.4 Protein determination

Membrane vesicle protein was determined by a modification (21) of the Lowry method (22), using BSA as standard. In the case of cells, protein in the lysates was determined either by the method of Markwell (21) or using the Pierce Micro BCA Protein Assay Reagent, as indicated. In both cases BSA was used as standard.

2.5 Isolation of transferrin variants

Three isoTf variants bi-bi-antennary tetra-sialo Tf (bb Tf), bi-tri-antennary penta-sialo Tf (bt Tf) and tri-tri-antennary hexa-sialo Tf (tt Tf) were isolated from human serum Tf by Con A Sepharose chromatography and preparative isoelectric focusing (23). The subfractions were checked on sialic acid content by isoelectric focusing, using PhastGel IEF pH 4-6.5 (Pharmacia, Sweden) (24). Furthermore, carbohydrate analysis was performed on the isolated Tf variants (25). About 5–50 µg Tf was hydrolyzed in 2 M trifluoro acetic acid at pressures < 1 mm Hg for 16 h at 100°C. Approximately 5 nmol rhamnose was added as internal standard. The hydrolyzed samples were evaporated at room temperature and the residue was redissolved in 0.1–1 ml 90 % (v/v) ethanol. Carbohydrates were quantified by partition chromatography with 90 % ethanol as eluent and tetrazolium blue chloride as reagent, using an adapted amino acid analyzer (Alpha Plus, Pharmacia LKB, Cambridge, UK). The reaction product was measured at 570 nm.

2.6 Labelling of transferrin with ⁵⁹Fe and ¹²⁵I

2.6.1 Loading of apoTf with ⁵⁹Fe

ApoTf (in 0.1 M NaHCO₃ solution) was incubated with ⁵⁹FeCl₃ (specific activity ranging from 32 - 290 cpm/pmol Fe) in the presence of NTA (NTA:⁵⁹Fe = 2:1) for 30 min at room temperature. Excess of ⁵⁹Fe was removed by filtration on a disposable Sephadex PD-10 column (Pharmacia, Sweden). Diferric ⁵⁹Fe-Tf fractions were collected and further labelled with ¹²⁵I.

2.6.2 Labelling of diferric Tf with ¹²⁵I

About 300 µg of diferric Tf (either ⁵⁶Fe or ⁵⁹Fe) was reacted with 0.25 mCi Na¹²⁵I for 10 min at room temperature. The reaction was carried out in a glass vial containing 100 µg IodoGen. Excess of iodine was removed by filtration on a disposable Sephadex PD10 column, followed by extensive dialyses against PBS pH 8. The final specific activity ranged from 2.3x10⁴ - 6.1x10⁴ cpm ¹²⁵I/pmol Tf.

2.7 Transferrin binding to placental membrane vesicles

2.7.1 Estimation of endogenous transferrin

The amount of endogenous Tf in the membrane preparations was estimated using the Laurell-rocket immunoelectrophoresis (26). Electrophoresis was performed in 1% agarose

containing 1% Triton X-100 and 30 μ l of rabbit anti human Tf (antibody titre = 2800 mg/l) at 10 V/cm for 6 h. After drying the precipitates were stained with Coomassie Brilliant Blue R250. The amount of Tf in membrane vesicles was determined by comparing with Tf standards.

2.7.2 Transferrin binding assay

For each experiment, membrane vesicles (MMV and BMV) from the same human term placenta were used. Membrane vesicles were washed respectively with an acidic buffer (100 mM sodium citrate pH 5, containing 50 μ g/ml desferal) and an alkaline buffer (1 M sodium chloride in 10 mM Tris pH 8) to remove Tf bound to TfRs (27). After washing, 250 μ l of membrane vesicle suspension (75 μ g protein for MMV and 100 μ g protein for BMV) were incubated with 125 I-labelled isoTf variants, with final concentrations of 9.3×10^{-10} - 9.3×10^{-8} M for MMV and 4.6×10^{-10} - 7.0×10^{-8} M for BMV. After 1 h of incubation at 4°C (equilibrium was reached between 30 and 40 min), 0.2 ml of the vesicle suspension was centrifuged at 100,000 g for 20 min, washed with PBS without resuspending the pellet and centrifuged again (28). The final pellet was dissolved in 2 ml 1% sodium dodecyl sulphate (SDS) and radioactivity was measured. The data were evaluated by a non-linear curve-fit program, using the Langmuir equation for equilibrium binding ($B = [B_{\max} * x] / [x + K_d]$ + non-specific binding, where B is the fraction of Tf that is bound, B_{\max} is the saturation level for specific binding, x is the concentration of Tf in the incubation medium, K_d is the concentration of Tf at which half-maximal specific saturable binding is achieved, and the non-specific binding is a linear function of x). Non-specific binding was experimentally determined in the presence of a 100-fold molar excess of unlabelled human iso Tf variants. The limited amounts of especially bt and tt iso Tf made it impossible to routinely assess non-specific binding in this way. Since the experimentally determined specific binding corresponded with the specific binding calculated by the non-linear curve-fit program, we further used the latter method. Both the maximal binding and the affinity constant ($K_a = 1/K_d$) of the isoTf variants were determined.

2.8 Uptake of diferric Tf by cultured trophoblast cells

2.8.1 Uptake of 125 I- 59 Fe₂Tf by trophoblast cells cultured on plastic dishes

After 48 h of culture, cells were washed with PBS pH 7.4 and preincubated in DMEM containing 100 nM 125 I- 59 Fe₂Tf for 30 min at 4°C to saturate the surface TfRs. The medium was replaced by prewarmed Medium 199 with 100 nM 125 I- 59 Fe₂Tf. After incubation for specified times at 37°C, cells were rinsed with PBS pH 7.4 and exposed to two acid/neutral wash steps to remove surface-bound Tf. One acid/neutral wash step consisted of 10 min of incubation with 25 mM NaAc/150 mM NaCl/2 mM CaCl₂ pH 4.5 followed by 10 min of incubation with PBS pH 7.4, both incubations on ice. Cells were lysed in Complete® protease

inhibitor cocktail. Radioactivity and protein were determined in the lysates. The amount of radioactivity in cell lysates that were only incubated for 30 min at 4°C was taken as a measure for non-specific binding to cells and dishes and subtracted from the total radioactivity.

2.8.2 Uptake of ^{125}I - $^{59}\text{Fe}_2\text{Tf}$ by trophoblast cells cultured on a permeable filter

Cells were cultured for 48 h, washed with PBS pH 7.4 and preincubated with M199 containing 0.5 mg/ml BSA and either 0.5 mg/ml ovalbumin (medium A) or 0.5 mg/ml human diferric Tf (medium B) for 1 h at 37°C as described by Gottlieb et al. (29). The upper and lower compartment contained respectively 0.7 and 0.45 ml medium in order to have the same level of fluid in both compartments to avoid pressure differences. To avoid stratification of diffused ^{125}I - $^{59}\text{Fe}_2\text{Tf}$ at the receptor side of the filter, the media were regularly mixed during incubations. Incubation was started by changing the medium on one side of the filter by prewarmed medium containing 100 nM ^{125}I - $^{59}\text{Fe}_2\text{Tf}$. Incubation occurred at 37°C. For incubation longer than 1 h, the medium from the side opposite that to which the labelled ligand had been added was replaced every hour with fresh medium. At fixed time points, medium was removed, membrane filters were put on ice and washed with ice-cold PBS. Filters were then treated with an acid/neutral wash as described for uptake experiments with cells cultured on plastic dishes. Radioactivity in the filters was counted in a Packard gamma counter. Cell-specific radioactivity was determined as the difference between the average radioactivities associated with medium A and medium B incubations.

2.9 Uptake of gold-labelled diferric Tf (Au-Tf) by cultured trophoblast cells

2.9.1 Coupling of 6 nm gold to Tf

Human diferric Tf was bound to 6 nm gold particles (Aurion) according to the manufacturer's instructions. The optimal pH for gold conjugate preparation is considered to be approximately 0.5 pH unit higher than the iso electric point (IEP) of the protein that is to be labelled (IEP of hTf is approximately 5.5). To be ascertained that iron stays bound to Tf we used a pH of 1.0 unit higher than the IEP. For each preparation the minimal amount of Tf required to stabilize the sol was determined. Depending on the result of this determination an amount of human diferric Tf was dissolved in 1 ml 5 mM NaHCO_3 pH 7.4. To this solution 10 ml of the 6 nm gold sol (pH 6.5) was added under continuous stirring. This suspension was left to stand for 10 min, 1.1 ml 10 % BSA (pH 9.0) was added and left to stand for another 10 min. To remove unbound Tf and gold-aggregates, the suspension was centrifuged at 100,000 g for 1 h. The supernatant was removed, the pellet washed with PBS containing 0.5 % BSA (pH 8.0), loaded on a linear 10-30 % glycerol gradient and centrifuged at 80,000 g for 1 h. The Au-Tf band was collected, frozen in liquid nitrogen and stored at -20°C. Before use, the solution was dialyzed against DMEM with 0.1 % BSA overnight at 4°C.

2.9.2 Incubation of membrane-grown trophoblast cells with Au-Tf

Cells were cultured on a permeable membrane. After 48 h of culture, cells were washed with PBS pH 7.4 and preincubated with DMEM containing 0.1 % BSA and 0.5 % ovalbumin. Cells were incubated with Au-Tf on either the microvillous (upper compartment) or the basal (lower compartment) side.

Incubation on upper side of the membrane

Cells were incubated with 1 μ g Au-Tf in 0.25 ml DMEM containing 0.1 % BSA on the upper side of the membrane and 0.5 ml DMEM containing 0.1 % BSA and 100 μ g of human diferric Tf in the lower compartment, for 3 min at 37°C. The media were removed and respectively 0.25 and 0.5 ml DMEM containing 0.1 % BSA was added to the upper and lower compartment. Cells were further incubated for specified times to allow endocytosis of Au-Tf.

Incubation on lower side of the membrane

Cells were incubated with 2 μ g Au-Tf in 0.5 ml DMEM containing 0.1 % BSA in the lower compartment and 0.25 ml DMEM with 0.1 % BSA in the upper compartment, for 1 h at 4°C to saturate the basal TfRs with Au-Tf. Cells were washed twice with DMEM containing 0.1 % BSA (first with cold medium, second with medium of 37°C), prewarmed 0.5 ml DMEM with 0.1 % BSA and 0.25 ml DMEM with 0.1 % BSA and 60 μ g human diferric Tf were added to respectively the lower and upper compartments and cells were further incubated for specified times at 37°C to allow endocytosis of Au-Tf.

Endocytosis was stopped by placing the cells on ice and washing them with ice-cold PBS pH 7.4. The filters were fixed overnight at 4°C with standard fixation medium containing 1 % glutaraldehyde and 4 % formaldehyde.

2.10 Immunolocalization of TfRs

TfRs were visualized by postfixation preembedding immuno electron microscopy (IEM) using a protocol described by Hansen, Sandvig & van Deurs (30). After 48 h of culture, membrane-grown cells were washed with PBS pH 7.4 containing 0.5 % BSA and fixed with 2 % formaldehyde, 0.1 % glutaraldehyde in 0.1 M phosphatebuffer pH 7.4 for 30 min at 4°C. Cells were first incubated with 10 μ g/ml anti-TfR (mouse monoclonal antibody clone B3/25, Boehringer Mannheim) for 1 h at room temperature, fixed for 30 min at 4°C, second incubated with 1:20 (w/v) 10 nm gold-conjugated goat-anti-mouse antibody (Amersham, UK) and finally fixed overnight at 4°C. At the concentrations used, controls omitting the primary antibody were negative.

2.11 Electron microscopy

All samples were postfixed in a mixture of 1 % (w/v) OsO_4 and 1.5 % (w/v) $\text{K}_4\text{Fe}(\text{CN})_6$ for 30 min at 4°C. After washing with distilled water, samples were dehydrated in graded ethanols (respectively 50 %, 80 %, 90 % and twice 100 %, 15 min each step) and infiltrated with Epon (respectively 30 min 3:1 EtOH/Epon, 30 min 1:1 EtOH/Epon, three times 30 min pure Epon and finally overnight pure Epon, all steps at room temperature). Polymerization with Epon occurred overnight at 68°C. The Epon embedding fluid consisted of a mixture of 38 ml LX-112 (LADD Research Industries Inc., Burlington, USA), 26 ml dodecylsuccinic anhydride (DDSA) (Merck, FRG), 20 ml methyl nonborene 2,3-dicarboxylic anhydride (MNA) (Merck, FRG), and 1.5 ml 2,4,6-bis(dimethyl aminomethyl)-phenol (DMP30) (Merck, FRG).

Ultrathin sections were made with an Ultratome (LKB, Sweden), equipped with Diatome 1.5 mm diamond knives and collected on unfilmed 250 mesh copper grids. Contrast of the samples was enhanced by staining with uranyl acetate. Sections were studied in a Zeiss EM 209 transmission electron microscope (Zeiss, Oberhochen, FRG), with an integrated electron spectrometer. This instrument allows high-resolution imaging with energy-filtered electrons. For further details see Sorber et al. (31,32).

2.12 Transferrin synthesis by cultured trophoblast cells

2.12.1 Identification of transferrin mRNA by RT-PCR

Trophoblast cells were isolated as described and additionally immuno-purified. After 48 h of cell culture, RNA was isolated according to Chomczynski and Sacchi (33). About 0.72 µg RNA was reverse transcribed (RT) in a volume of 5 µl. A fifth part of the resulting cDNA was amplified by polymerase chain reaction (PCR). The PCR was performed in 20 µl PCR-mix, consisting of 1 x PCR-buffer (75 mM Tris-HCl pH 9.0, 20 mM $(\text{NH}_4)_2\text{SO}_4$, 0.01 % Tween 20), 2.0 mM MgCl_2 , 3.75 pmol each of Tf-specific primers Tf1 (5'-CGCTGGCTGGAACATCC-3') and Tf2 (5'-CTACGGAAAGTGCAGGCTTC-', Eurogentec), and 0.5 unit of Goldstar DNA polymerase. Using a DNA Thermal Cycler an initial denaturation step of 3 min at 96°C was followed by 45 cycles of amplification (30 s at 94°C, 30 s at 60°C, and 30 s at 72°C) and a final extension for 5 min at 72°C. Plasmid ptacRRTF3101 (34), containing Tf cDNA, was used as a positive control for PCR. As a negative control a RT-PCR was done without the addition of reverse transcriptase. The forward primer (Tf1) was located at nucleotides 1458-1474 of human Tf mRNA, whereas the reverse primer (Tf2) was located at nucleotides 2101-2120 (35). The size of the fragment amplified from Tf cDNA would therefore be 663 bp. The PCR-product from Tf cDNA was digested with either Pst I which would cut the PCR-product in two fragments of 50 bp and 613 bp, or Hind III, which would yield fragments of 412 bp and 251 bp. The PCR- and the digestion products were examined on 1 % agarose gels with

ethidium bromide staining. DNA molecular weight marker VI (Boehringer, Mannheim) was used as a standard.

2.12.2 De novo synthesis of transferrin

³⁵S-methionine pulse labelling

Cultured trophoblast cells were pulse-labelled with ³⁵S-methionine according to Starreveld et al. (3). At indicated culture times, cells were washed twice with ice-cold PBS. Pre-incubation in methionine-free medium for 1 h at 37°C was followed by incubation with 60-80 µCi translabelled ³⁵S-methionine (1089 Ci/mmol) per 1.5×10^6 cells for 2 h at 37°C. Cells were washed twice with PBS and lysed in 500 µl lysis buffer, consisting of 1 % Triton X-100, 1 mM PMSF and 0.5 U/ml aprotinin in PBS pH 7.4. The cell lysates were centrifuged at 10,000 g for 2 min. The supernatants were used for determination of both total protein synthesis and Tf synthesis.

Total protein synthesis

Total protein synthesis was determined as previously described (3). After addition of 0.1 ml distilled water and 0.1 ml ice-cold 20 % TCA to 20 µl supernatant of the cell lysates, samples were incubated for 10 min at 4°C and centrifuged at 1,500 g for 15 min. The pellets were washed with 0.5 ml 10 % TCA and subsequently vigorously mixed with 0.5 ml Soluene-350 (Packard, USA). Radioactivity was counted in a sample of 20 µl, after the addition of 10 ml Insta-gel Plus (Packard, USA), using an Isocap 300 counter. Total protein synthesis was expressed in dpm/mg protein.

Tf synthesis

In order to determine Tf synthesis, BSA (400 µg) and L-methionine (10^4 times pulse-label concentration) were added to the supernatants. After incubation with 50 µl rabbit-anti-hTf for 18 h at 4°C, the Tf-antiTf complex was precipitated with 50 µl Protein-A Sepharose CL4B (Pharmacia, Sweden) during 2 h of rotation at room temperature. The samples were spun down and the precipitates were washed four times with PBS containing 0.2 % sodium deoxycholate, 0.2 % Triton X-100, 1 mM PMSF and 1 mg/ml BSA. The final precipitates were boiled with electrophoresis sample buffer (4 ml distilled water, 1 ml 0.5 M Tris-HCl pH 6.8, 0.8 ml glycerol, 1.6 ml 10 % SDS, 0.4 ml 0.8 M DTT and 0.2 ml 1 vol. % bromophenol blue) for 5 min and centrifuged at 10,000 g for 2 min. The supernatants were electrophoresed (1 h, 200 V; Mini-Protean II Cell; BioRad, Richmond, USA) under reducing conditions using 10 % Tris-HCl gels (BioRad, Richmond, USA). After drying, the gels were exposed to Kodak X-OMAT AR films for one week. The autoradiographs were scanned with an Ultrosan XL Enhanced Laser Densitometer (Pharmacia LKB, Sweden) and peak surfaces of the Tf bands were determined in absorption units (AU) x basis (mm). The ratio of peak surface/total protein synthesis (AU x mm / dpm) was used as a measure for de novo Tf synthesis.

2.12.3 Estimation of transferrin content

The Tf content was estimated in both cultured and non-cultured immunopurified and non-immunopurified trophoblast cells. The procedure was performed at 4°C. The cells were washed twice with PBS, lysed in 0.5 ml distilled water containing 1 mM PMSF and sonified for 10 s on ice. Total cell protein was determined in the cell lysate using the Micro BCA Protein Assay Reagent (Pierce).

In order to estimate the Tf content, the lysate was centrifuged at 20,000 g for 10 min, the supernatants were filtered through 0.5 µm Millipore-GS filters and concentrated (Centriflow). The culture media were collected and centrifuged at 15,000 g for 10 min. PMSF was added to the supernatant to a final concentration of 1 mM. The media passed a 0.5 µm Millipore-GS filter and were concentrated. Both the cell lysates and culture media were subjected to electrophoresis (10 % Tris-HCl gels, BioRad, reducing conditions, 1 h, 200 V) and blotted on 0.2 micron nitro-cellulose membranes (1 h, 100 V, 250 mA, at 4°C, BioRad Trans-Blot Cell, Richmond, USA). Tf was identified with an Immuno-lite® assay kit (BioRad, Richmond, USA), using rabbit anti-hTf as primary and goat anti-rabbit IgG coupled to alkaline phosphatase as secondary antibody. The blots were exposed to photosensitive film for 15 min. The Tf bands were scanned with an Ultrosan XL Enhanced Laser Densitometer (Pharmacia LKB, Sweden) and the Tf content of the samples was calculated by reference to Tf standards processed simultaneously.

2.12.4 Heterogeneity of trophoblast transferrin

The sialic acid-dependent heterogeneity of Tf was assessed by isoelectric focusing using the PhastSystem with PhastGel pH 4-6.5 (Pharmacia LKB, Sweden) according to the protocol described by van Eijk and van Noort (24). Prior to focusing, the Tf samples were saturated with iron. After focusing the Tf bands were immunoprecipitated with 80 µl of rabbit anti-Tf (titre 2800 mg/l). The gels were washed with 0.15 M NaCl for 48 h and the Tf bands were visualized with a silver Protein Staining kit using the Phast System (Pharmacia). In the case of ¹²⁵I-labelled Tf, the gels were exposed to photosensitive films. Bands were scanned with an Ultrosan Enhanced Laser Densitometer (Pharmacia LKB, Sweden).

2.13 Uptake of non-Tf iron by cultured trophoblast cells

2.13.1 Stock-solutions of ⁵⁹Fe(III)nitrilotriacetate and ⁵⁹Fe-ascorbate

The ⁵⁹Fe(III)nitrilotriacetate (NTA) stock-solution was prepared from solutions consisting of ⁵⁹FeCl₃ in 0.1 M HCl and a four-fold excess of NTA in 20 mM HEPES/Tris pH 6.0. The solution was titrated to neutral pH by dropwise addition of 0.5 M NaOH.

The ^{59}Fe -ascorbate stock-solution was prepared by adding a five-fold molar excess of cold FeSO_4 in 0.1 M HCl and a twenty-fold molar excess of L-ascorbic acid to $^{59}\text{FeCl}_3$. After equilibration for 30 min at room temperature the pH was carefully brought to neutral (pH 7) with a saturated NaHCO_3 solution. All solutions were saturated with N_2 to prevent oxidation and depletion of ascorbate by molecular oxygen. For each experiment the stock-solutions were freshly prepared.

2.13.2 Non-Tf iron uptake by cultured trophoblast cells

After 48 h of culture, cells were washed with PBS pH 7.4, pre-incubated in serum-free M199 and incubated in uptake medium (150 mM NaCl and 25 mM HEPES pH 7.4) in the presence or absence of Fe(III)CN , 1 mM of Fe(III) chelator desferrioxamine (DFO) or 1 mM of Fe(II) chelators bathophenanthroline disulphonic acid (BPS) or ferrozine (FZ) at 37°C . Uptake was initiated upon addition of either $^{59}\text{Fe(III)NTA}$ or ^{59}Fe -ascorbate. After the desired incubation time, medium was removed, cells were cooled on ice and washed three times with 1 ml of ice-cold PBS pH 7.4 for 5 min and lysed in Complete[®] protease inhibitor cocktail. Radioactivity in the lysate was determined in a Packard gamma counter. Protein was determined according to Markwell et al. (21).

2.14 Ferriredutase assays

Reduction of ferricyanide (Fe(III)CN) was measured in a reaction mixture, containing 140 mM NaCl, 5 mM KCl, 1 mM MgCl_2 , 5 mM NaH_2PO_4 and 5 mM HEPES pH 7.4 with or without NADH or NADPH, and Fe(III)CN , by following the decrease in absorbance at 420 minus 500 nm with a Cary 1E spectrophotometer (extinction coefficient: 1 /mM/cm).

Cells. After 48 hr of culture, cells were washed with PBS pH 7.4 and incubated in reaction mixture at 37°C . The reaction was started by the addition of Fe(III)CN and terminated after the desired incubation period by cooling the cells on ice. The absorbance at 420 minus 500 nm was measured in the medium and compared to a control without cells.

Vesicles. The reaction was started by the addition of either 10 μl BMV (2.5 $\mu\text{g}/\mu\text{l}$) or 10 μl MMV (5.0 $\mu\text{g}/\mu\text{l}$) to 990 μl of the reaction mixture. The decrease in absorbance at 420 minus 500 nm was directly measured at 37°C . NADH oxidation was followed at 340 minus 430 nm (extinction coefficient: 6.22 /mM/cm). Kinetic parameters were determined for NADH and Fe(III)CN , using the Michaelis-Menten plot from Enzyfit curve-fitting program.

References

1. Dschida W & Bowman BJ (1995) The vacuolar ATPase: sulfite stabilization and the mechanism of nitrate inactivation. *Journal of Biological Chemistry*, 270:1557-1563.
2. Kliman HJ, Nestler JE, Sermasi E, Sanger JM & Strauss III JF (1986) Purification, characterization, and in vitro differentiation of cytotrophoblasts from human term placentas. *Endocrinology*, 118:1567-1582.
3. Starreveld JS, Kroos MJ, van Suijlen JDE, Verrijt CEH, van Eijk HG & van Dijk JP (1995) Ferritin in cultured human cytotrophoblasts: synthesis and subunit distribution. *Placenta*, 16:383-395.
4. Yui J, Garcia-Lloret M, Brown AJ, Berdan RC, Morrish DW, Wegmann TG & Guilbert LJ (1994) Functional long-term cultures of human term trophoblasts purified by column-elimination of CD9 expressing cells. *Placenta*, 15:231-246.
5. Starreveld JS, van Denderen J, Verrijt CEH, Kroos MJ & van Dijk JP (1998) Morphological differentiation of cytotrophoblasts cultured in Medium 199 and keratinocyte growth medium. *European Journal of Obstetrics & Gynecology and Reproductive Biology* (in press).
6. Booth AG, Olaniyan RO & Vanderpuye OA (1980) An improved method for the preparation of human placental syncytiotrophoblast microvilli. *Placenta*, 1:327-336.
7. Dicke JM, Verges D, Kelley LK & Smith CH (1993) Glycine uptake by microvillous and basal plasma membrane vesicles from term human placentae. *Placenta*, 14:85-92.
8. Kelley LK, Smith CH & King BF (1983) Isolation and partial characterization of the basal cell membrane of human placental trophoblast. *Biochimica et Biophysica Acta*, 734:91-98.
9. Richterich R, Colombo JP & Weber H (1962) Ultramikromethoden im klinischen Laboratorium. VII. Bestimmung der sauren prostata-phosphatase. *Schweizerische Medizinische Wochenschrift*, 47:1496-1500.
10. Williams LT, Jarett L & Lefkowitz RJ (1976) Adipocyte β -adrenergic receptors. Identification and subcellular localization by (-)-[3 H]dihydroalprenolol binding. *Journal of Biological Chemistry*, 251:3096-3104.
11. Milson DW, Rose FA & Dodgson KS (1972) The specific assay of arylsulphatase C, a rat liver microsomal marker enzyme. *Biochemical Journal*, 128:331-336.
12. Pennington RJ (1961) Biochemistry of dystrophic muscle. Mitochondrial succinate-tetrazolium reductase and adenosine triphosphatase. *Biochemical Journal*, 80:649-654.
13. Dallner G, Siekevitz P & Palade GE (1966) Biogenesis of endoplasmic reticulum membranes. II. Synthesis of constitutive microsomal enzymes in developing rat hepatocyte. *Journal of Cell Biology*, 30:97-117.

14. Schoot BM, Schoots AFM, De Pont JJHM, Schuurmans-Stekhoven FMAH & Bonting SL (1977) Studies on $(\text{Na}^+ + \text{K}^+)$ activated ATPase. XLI. Effects of N-ethylmaleimide on overall and partial reactions. *Biochimica et Biophysica Acta*, 483:181-192.
15. Kato M & Kako J (1987) Orientation of vesicles isolated from baso-lateral membranes of renal cortex. *Molecular and Cellular Biochemistry*, 78:9-16.
16. Bligh EG & Dyer WJ (1959) A rapid method of total lipid extraction and purification. *Canadian Journal of Biological Chemistry and Physiology*, 37:911-917.
17. Jansson T, Powell TL & Illsley N (1993) Non-electrolyte solute permeabilities of human placental microvillous and basal membranes. *Journal of Physiology*, 468:261-274.
18. Bartlett GR (1959) Phosphorus assay in column chromatography. *Journal of Biological Chemistry*, 234:466-468.
19. Fiske CH & Subbarow Y (1925) The colorimetric determination of phosphorus. *Journal of Biological Chemistry*, 66:375-400.
20. Morrison WR & Smith LM (1964) Preparation of fatty acid methyl esters and dimethylacetals from lipids with boron fluoride-methanol. *Journal of Lipid Research*, 5:600.
21. Markwell M-AK, Haas SM, Bieber LL & Tolbert NE (1978) A modification of the Lowry procedure to simplify protein determination in membrane and lipoprotein samples. *Analytical Biochemistry*, 87:206-210.
22. Lowry OH, Rosebrough NJ, Farr AL & Randall RJ (1951) Protein measurement with the Folin phenol reagent. *Journal of Biological Chemistry*, 193:265-275.
23. Van Noort WL, de Jong G & van Eijk HG (1994) Purification of isotransferrins by Concanavalin A Sepharose chromatography and preparative isoelectric focusing. *European Journal of Clinical Chemistry and Clinical Biochemistry*, 32:885-892.
24. Van Eijk HG & van Noort WL (1992) The analysis of human serum transferrins with the Phast-System: quantitation of microheterogeneity. *Electrophoresis* 13:354-358.
25. Van Noort WL & van Eijk HG (1990) Quantification of monosaccharides occurring in glycoproteins at subnanomole levels using an automated LC analyzer. *LC-GC International*, 3/5:50-52.
26. Laurell CB (1966) Quantitative estimation of proteins by electrophoresis in agarose gel containing antibodies. *Analytical Biochemistry*, 15:45-52.
27. Berczi A & Faulk WP (1992) Iron-reducing activity of plasma membranes. *Biochemistry International*, 28:577-584.

28. Van Dijk JP, van der Zande FGM, Kroos MJ, Starreveld JS & van Eijk HG (1993) Number and affinity of transferrin-receptors at the placental microvillous plasma membrane of the guinea pig: influence of gestational age and degree of transferrin glycan chain complexity. *Journal of Developmental Physiology*, 19:221-226.
29. Gottlieb TA, Ivanov IE, Adesnik M & Sabatini DD (1993) Actin microfilaments play a critical role in endocytosis at the apical but not the basolateral surface of polarized epithelial cells. *Journal of Cell Biology*, 120:695-710.
30. Hansen SH, Sandvig K & van Deurs B (1992) Internalization efficiency of the transferrin receptor. *Experimental Cell Research*, 199:19-28.
31. Sorber CWJ, de Jong AAW, den Breejen NJ & de Bruijn WC (1990) Quantitative energy-filtered image analysis in cytochemistry. I. Morphometric analysis of contrast-related images. *Ultramicroscopy*, 32:55-68.
32. Sorber CWJ, van Dort JB, Ringeling PC, Cleton-Soeteman MI & de Bruijn WC (1990) Quantitative energy-filtered image analysis in cytochemistry. II. Morphometric analysis of element-distribution images. *Ultramicroscopy*, 32:69-79.
33. Chomczynski P & Sacchi N (1987) Single-Step of RNA Isolation by Acid Guanidinium Thiocyanate-Phenol-Chloroform Extraction. *Analytical Biochemistry*, 162:156-159.
34. De Smit MH, Hoefkens P, de Jong G, van Duin J, van Knippenberg PH & van Eijk HG (1995) Optimized bacterial expression of nonglycosylated human transferrin and its half-molecules. *International Journal of Biochemistry and Cell Biology*, 27:839-850.
35. Yang F, Lum JB, McGill JR, Moore CM, Naylor SL, van Bragt PH, Baldwin WD & Bowman BH (1984) Human transferrin: cDNA characterization and chromosomal location. *Proceedings in National Academic Sciences of the USA*, 81:2752-2756.

3

Two models for placental transport studies:
purified membrane vesicles and trophoblast
cells in culture

3.1 General introduction

An important function of the placenta is its role in the exchange of compounds between mother and fetus. The placenta mediates transfer of nutrients from mother to fetus and reversely the transfer of waste products from fetus to mother. Several in vitro models can be used to study transfer across the placenta, such as perfused whole placenta or placental cotyledons, isolated membrane vesicles from the microvillous and basal membranes or in vitro cultures of either choriocarcinoma cell lines or freshly isolated trophoblast cells. All these models have their own advantages and disadvantages.

General mechanisms involved in placental transfer can easily be studied with the perfused placenta. This model enables the determination of the preferential transport direction. However, the perfused placenta is not suitable for studying specific transport phenomena, particularly not at cellular or molecular level. Membrane vesicles from syncytiotrophoblast microvillous and basal membranes are very useful to study basic characteristics of transport systems. They allow to separately study specific transport mechanisms on the two membranes. However, the effect of intracellular metabolism cannot be studied with this model. A good model to investigate placental transport in relation to its metabolism are the cultured trophoblast cells. Nevertheless, a combination of models is preferred for investigation of mechanisms involved in placental transport.

In this report we describe two models for placental transport studies: isolated microvillous and basal membrane vesicles and cultured trophoblast cells.

3.2 Isolation and characterization of microvillous and basal membrane vesicles.

3.2.1 Introduction

The human placental syncytiotrophoblast forms the main barrier between mother and fetus. Membrane vesicles are a good model to examine transport mechanisms on microvillous and basal plasma membranes. Nowadays it is possible to isolate both membranes from the same placental tissue. The vesicle preparations need to be well characterized before use. In this chapter we describe in detail the characteristics of our membrane preparations, which have been used in further studies.

3.2.2 Materials and Methods

Chemicals

[³H]-alanine was from Amersham Life Science (Buckinghamshire, UK). Rabbit polyclonal antibody to the 67 kD subunit of *Neurospora* V-ATPase was kindly supplied by Dr. B.J. Bowman, University of California. Goat anti-rabbit IgG coupled to alkaline phosphatase was from BioRad (Richmond, USA).

Tissue source

Normal human term placentae were obtained from the department of Obstetrics and Gynaecology, Dijkzigt University Hospital Rotterdam, within 30 min after spontaneous vaginal delivery.

Preparation of membrane vesicles

Both microvillous and basal membrane vesicles were isolated from the same human term placenta as described in 2.3.1. Microvillous membrane vesicles (MMV) were isolated according to Dicke et al. (1) based on the method of Booth, Olanyian and Vanderpuye (2). Basal membrane vesicles (BMV) were isolated according to the method of Kelley, Smith and King (3) as modified by Dicke et al. (1). The final pellets were resuspended in phosphate buffered saline (PBS; containing 136.9 mM NaCl, 2.7 mM KCl, 8.1 mM Na_2HPO_4 and 1.4 mM KH_2PO_4) at pH 7.4, frozen in liquid nitrogen and stored at -80°C until use.

Placental tissue homogenate was prepared by homogenizing villous tissue in 250 mM sucrose/50 mM Tris/1 mM EDTA (see 2.3.1).

Protein determination

Protein was determined by a modification (4) of the Lowry method (5).

Marker enzyme activities

Alkaline phosphatase activity (6) was determined as marker for microvillous membranes, and the binding of dihydroalprenolol (7) as marker for basal membranes. Activities of arylsulphatase (8), NADPH-dependent cytochrome c reductase (9) and succinate dehydrogenase (10) were determined as markers for respectively lysosomes, endoplasmic reticulum and mitochondria. The activities of the membrane preparations (/mg protein) were compared to enzyme activities of placental tissue homogenate (/mg protein). These determinations are described in detail in 2.3.2.

Orientation of membrane vesicles

The orientation of membrane vesicles was determined as described in 2.3.3. Orientation of MMV was determined by assaying the alkaline phosphatase activity with and without previous treatment of the vesicles with 0.1 % saponin. Orientation of BMV was determined by assaying the Na^+K^+ -ATPase activity (11) after treatment of the vesicles with or without 0.1 % saponin or 40 mM valinomycin (12). The amount of inside-out vesicles could be determined in the presence of valinomycin.

Uptake of [^3H]-alanine

Uptake of [^3H]-alanine was measured in the presence of either a Na^+ - or a K^+ -gradient using a rapid filtration technique. For these experiments, vesicles were resuspended in 300 mM mannitol/10 mM HEPES/2 mM Tris pH 7.4. Uptake was started by the addition of

10 μ l (approximately 70 μ g) vesicles to 40 μ l of extravesicular medium containing 0.1 mM [3 H]-L-alanine in 200 mM mannitol, 10 mM HEPES, 2 mM Tris pH 7.4 and either 50 mM NaCl or 50 mM KCl. Incubations were carried out for 15 sec – 60 min at 37°C. Uptake was stopped by the addition of 2.5 ml ice-cold stop solution (300 mM mannitol/10 mM HEPES/2 mM Tris pH 7.4), samples were filtered under vacuum through two glass-fibre filters GF/C (Whatman, UK) and filters were washed three times with 2.5 ml stop solution. Filters were counted for radioactivity in a Packard liquid scintillation counter.

Electron microscopy

Membrane vesicles were fixed in suspension in a mixture of 4 % glutaraldehyde and 4 % formaldehyde in 0.1 M phosphate buffer (pH 7.4) overnight at 4°C. After centrifugation at 90,000 g for 30 min, pellets were washed with PBS pH 7.4, postfixed in a mixture of 1 % (w/v) OsO₄ and 1.5 % K₄Fe(CN)₆ at 4°C, dehydrated through graded alcohols, and embedded in Epon. Ultrathin sections, stained with uranyl acetate, were examined in a Zeiss EM 902 transmission electron microscope (Zeiss, Oberkochen, FRG).

Gel electrophoresis of membrane vesicles

Membrane vesicles were subjected to SDS polyacrylamide gel electrophoresis (PAGE) under reducing conditions as described in detail in 2.3.4. Samples were run on 4–20 % gradient Tris-HCl polyacrylamide gels (BioRad, Richmond, USA). In order to demonstrate the presence of vacuolar ATPase (V-ATPase), vesicles were subjected to SDS-PAGE on a 10 % homogenous ready gel (BioRad) under reducing conditions. After blotting on nitro-cellulose, V-ATPase was identified with an Immunolite[®] assay kit (BioRad) using a rabbit polyclonal antibody to the 67 kD subunit of *Neurospora* V-ATPase as primary and goat anti-rabbit IgG coupled to alkaline phosphatase as secondary antibody (see 2.3.4). As a control the blot was incubated with pre-immune serum.

Determination of membrane cholesterol and phospholipid contents

Lipids were extracted according to the method of Bligh and Dyer (13). The extracted samples were saponified in a mixture of 95 % ethanol/3.3 % KOH and extracted with hexane (14). Total cholesterol content was measured in either untreated membrane vesicles or in extracted lipids, using a cholesterol test from Boehringer (Mannheim, FRG). Total phosphorus content was determined according to a modification (15) of the method of Fiske and Subbarow (16). Samples were heated in H₂SO₄/HClO₄/distilled water (1.5:1.5:1.0), cooled and the phosphorus content was spectrophotometrically measured using ammoniummolybdate as reagent. See 2.3.5 for detailed descriptions of these procedures.

Fatty acid analysis in phospholipids

Fatty acid analysis was performed as described in 2.3.6. In short: Phospholipids were separated by thin layer chromatography on Kieselgel 60 F254 plates (Merck, Darmstadt,

Germany). Phospholipid spots were scraped off and the fatty acids were transmethyalted with 14 % boronfluoride in methanol according to the method of Morrison and Smith (17). The fatty acid methyl esters were separated and quantified by capillary gas liquid chromatography on a CP-Sil88 column (WCOT, 50 m x 0.25 mm, 0.20 µm film; Chrompack, NL) in a Chrompack CP9000 capillary gas chromatograph. The fatty acid methyl esters were identified by comparing their retention times to those of authentic standards (Alltech Ass., Deerfield, IL, USA).

3.2.3 Results

Marker enzyme activities of microvillous and basal membranes

Approximately 37 and 21 mg of protein was recovered for MMV and BMV respectively, starting with 100 g human term placental tissue. The enrichments of binding and enzyme activities (/mg protein), relative to whole placental tissue homogenate, are given in Table 3.1. Contamination of the membrane preparations with the opposite membranes or with subcellular organelles was very small.

Table 3.1

Enrichments of binding and enzyme activities (/mg protein), relative to the activities (/mg protein) of whole placental tissue homogenates.

	BMV	MMV
Alkaline phosphatase	2.7 ± 1.1 (n=24)	19.3 ± 4.6 (n=24)
Dihydroalprenolol binding	28.6 ± 6.5 (n=11)	1.8 ± 0.2 (n=4)
Arylsulphatase	2.0 ± 0.8 (n=21)	1.2 ± 0.4 (n=22)
NADPH cyt c reductase	1.4 ± 0.4 (n=11)	0.7 ± 0.3 (n=11)
Succinate dehydrogenase	0.8 ± 0.6 (n=8)	0.14 ± 0.07 (n=8)

Orientation of membrane vesicles

With the alkaline phosphatase assay, with or without previous treatment of the vesicles with 0.1% saponin, we could discriminate between inside-out MMV and either unsealed vesicles or right-side-out MMV. As a result we found $88 \pm 7\%$ (n=4) of MMV to be right-side-out or unsealed and 12 % to be inside-out. For BMV, discrimination between inside-out, right-side-out and unsealed vesicles was possible using the Na^+K^+ -ATPase assay with or without previous treatment of the vesicles with saponin or valinomycin. The major part of

BMV was either right-side-out or unsealed, namely, $28 \pm 8 \%$ was right-side-out, $60 \pm 8 \%$ unsealed and $12 \pm 6 \%$ was inside-out.

Uptake of [^3H]-alanine

The isolated membrane vesicles were functionally validated by measuring the Na^+ -gradient dependent uptake of [^3H]-alanine. MMV revealed an overshoot above equilibrium uptake in the presence of an inwardly directed Na^+ -gradient (not shown). [^3H]-Alanine uptake by BMV was stimulated in the presence of an inwardly directed Na^+ -gradient, but an overshoot was not seen.

Electron micrographs

Figure 3.1 shows electron micrographs of MMV and BMV preparations. The membrane preparations contained round or tubular smooth membrane structures. A large part of the membrane structures seemed vesicular. The sizes of the vesicles varied widely. The preparations were relatively free of subcellular structures.

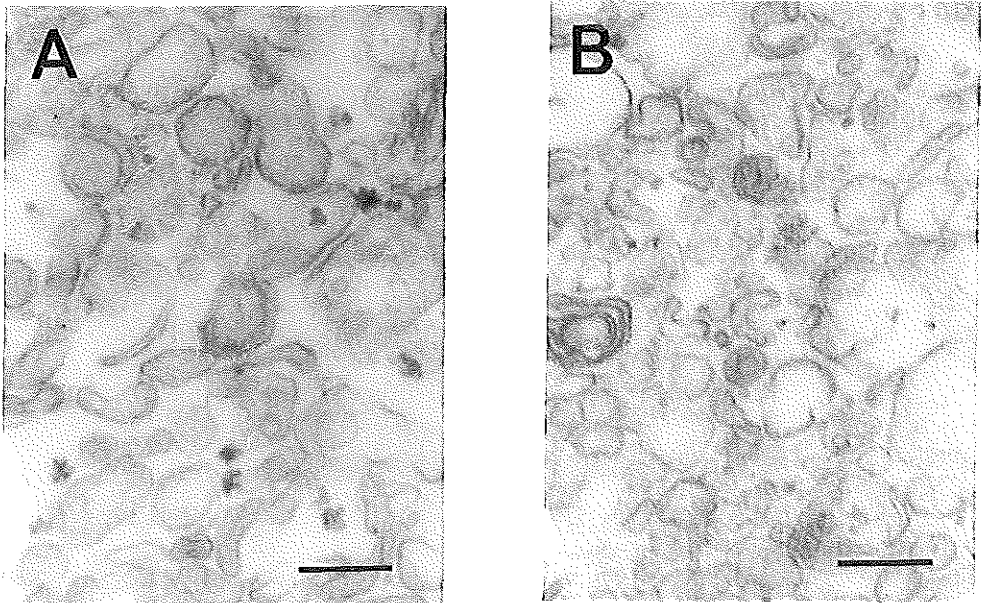


Figure 3.1

Electron micrographs of MMV (3.1A) and BMV (3.1B). Samples were prepared as described in Materials and Methods. (bar = $0.25 \mu\text{m}$).

Membrane protein profiles

To further characterize both MMV and BMV preparations, the vesicles were subjected to SDS gelelectrophoresis under reducing conditions. Figure 3.2 displays different protein patterns for MMV and BMV preparations. Most protein bands were seen in both MMV and BMV preparations, although some proteins significantly differed in their relative concentrations (indicated by arrows and arrowheads for respectively BMV and MMV specific protein bands). Using a polyclonal antibody to the 67 kD subunit of *Neurospora* V-ATPase, two specific bands of respectively 70 and 45 kD were visualized in Western blots of MMV and BMV (Figure 3.3). With Western blots of gels run under native non-reducing conditions, we found that both bands were subunits of a high molecular weight complex (not shown). The response was specific since incubation with pre-immune serum in stead of the polyclonal antibody did not show the specific bands of 70 and 45 kD. These results suggested the presence of V-ATPase in MMV and BMV.

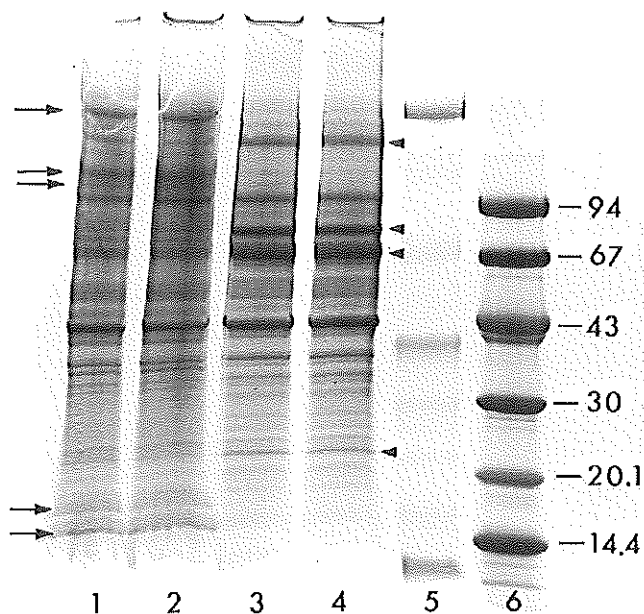


Figure 3.2

Comparison of plasma membrane proteins from MMV and BMV by SDS gelelectrophoresis. Approximately 50 μ g of protein from MMV and BMV were put on 4-20 % gradient polyacrylamide gel (BioRad, Richmond, USA). Lane 1 and 2: BMV; lane 3 and 4: MMV; lane 5: Kaleidoscope prestained standards (BioRad); lane 6: low molecular weight marker (Pharmacia, Sweden). Arrows indicate BMV specific proteins and arrowheads indicate proteins enriched in MMV preparations.

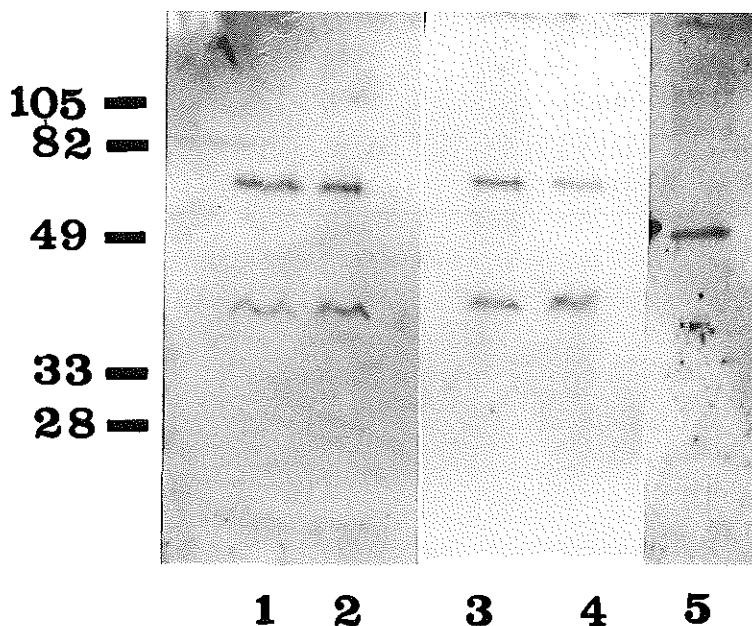


Figure 3.3

*Western blot of MMV (lanes 1,2,5) and BMV (lanes 3,4) subjected to SDS-PAGE on a 10 % homogenous gel under reducing conditions and blotted on nitro-cellulose. The blot was cut in two parts: one part was incubated with rabbit polyclonal antibody to the 67 kD subunit of *Neurospora* V-ATPase (lane 1-4), the other part with pre-immune serum (lane 5). The bands were visualized using the Immunolite[®] assay kit with goat anti-rabbit IgG coupled to alkaline phosphatase as secondary antibody.*

Membrane cholesterol and phospholipid contents

The cholesterol and phospholipid contents of MMV and BMV are shown in Table 3.2. The ratio of cholesterol content in lipid extract with respect to that in untreated membrane vesicles was used as a measure for the recovery of lipid extraction (approximately 85 %). The cholesterol content of BMV was 1.2 times higher compared to MMV. The content of phospholipids was also higher in BMV (1.4 times compared to MMV), therefore resulting in a cholesterol/phospholipid ratio that was not significantly different between the two vesicle preparations.

To further analyze the phospholipid content of both membrane preparations, we performed fatty acid analysis of total phospholipids. As shown in Figure 3.4, MMV and BMV revealed no significant differences in fatty acid composition (represented as mol %) of total phospholipids.

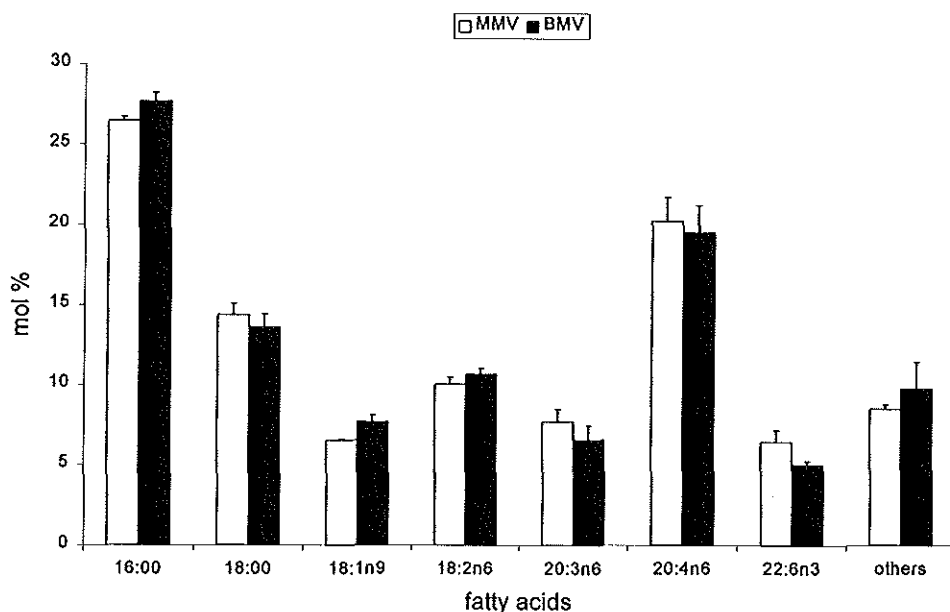
Table 3.2

Cholesterol and phospholipid contents in isolated MMV and BMV (nmol/mg protein).

Membrane	cholesterol (n = 9)	phospholipids (n = 4)	cholesterol/ phospholipid (n = 4)
MMV	371.9 ± 35.8 *	447.8 ± 50.1 *	0.88 ± 0.17 **
BMV	439.5 ± 39.4	609.4 ± 69.9	0.78 ± 0.07

* $P < 0.05$ versus BMV (unpaired two-tailed Student's *t*-test)

** not significantly different from BMV

**Figure 3.4**

Fatty acid analysis of total phospholipids from MMV and BMV. Fatty acids with a mol % above 2 % are presented in this figure. All other fatty acids are combined in the last bar. The mol % of polyunsaturated fatty acids was 46.7 ± 1.1 for MMV and 44.4 ± 2.2 for BMV. The ratio of saturated/unsaturated fatty acids was 0.81 ± 0.04 and 0.84 ± 0.06 for respectively MMV and BMV.

3.2.4 Discussion

Membrane vesicles provide a good model system to investigate specific transport mechanisms. Vesicles can be isolated from both maternal-facing microvillous and fetal-facing basal membranes and transport mechanisms on either of these membranes can separately be studied. Studies with membrane vesicles allow manipulation of the composition of solution (e.g. osmolarity, pH) inside and outside the vesicles. Transport of substrates across membranes can be investigated by (pre-)incubating the vesicles with labelled substrates and measuring either influx into or efflux from the vesicles. Vesicles can then be separated from the external medium by means of rapid filtration. To distinguish transport of the substrate from binding to the membrane surface, equilibrium uptake can be measured with varying osmolarities of the incubation medium. The intravesicular volume changes as the osmolarity outside the vesicles changes. Consequently the amount of substrate within the vesicles alters, whereas binding to the membrane surface does not alter. Another purpose of vesicle studies can be the investigation of plasma membrane associated enzyme systems. For all these studies it is important to know the purity and orientation of the membrane preparations.

In this report we describe the characteristics of MMV and BMV isolated from the same human term placenta. The vesicles were isolated according to Dicke et al. (1), based on the methods of Booth, Olaniyan and Vanderpuye (2) and Kelley, Smith and King (3) respectively. We showed that MMV were 19-fold enriched in alkaline phosphatase activity, whereas BMV were 28-fold enriched in dihydroalprenolol binding. These results were similar to those described by other researchers (2,3,18-22). Contamination of basal membranes in our MMV preparations and the opposite contamination of microvillous membranes in the BMV preparations was low (1.8-fold and 2.7-fold enrichments of dihydroalprenolol binding and alkaline phosphatase activity respectively in MMV and BMV preparations). Contamination of subcellular organelles such as lysosomes, endoplasmic reticulum and mitochondria was very small.

For most experiments it is essential to know the orientation of the vesicle preparations. For MMV we revealed that 12 % of the vesicles was inside-out and therefore 88 % was either right-side-out or unsealed. BMV were 28 % right-side-out, 60 % unsealed and 12 % inside-out. Illsley et al. (21) and Eaton and Oakey (22) previously determined vesicle orientation by measuring the binding of Concanavalin A to their vesicle preparations before and after lysis by repeated freeze-thawing in liquid nitrogen. They showed that about 90 % of MMV and either 73 % (21) or 90 % (22) of BMV was right-side-out. However, as with the alkaline phosphatase assay the Concanavalin A binding assay cannot discriminate between vesicles that are right-side-out or unsealed. For BMV this is possible with the Na^+K^+ -ATPase assay. Given these facts, our results agreed with the results previously described. For the interpretation of vesicle studies, the orientation of the vesicles must be kept in mind. It can for example be very difficult to determine the polarity of certain enzyme systems.

To examine the functional validity of our membrane preparations, we measured the uptake of [^3H]-alanine as described for microvillous and basal membranes (23,24). Uptake of [^3H]-alanine was stimulated by an inwardly directed Na^+ -gradient and MMV even revealed an overshoot above equilibrium uptake. Our results were in agreement with those described and they suggested the functionality of our membrane preparations.

We compared the proteins of microvillous and basal plasma membranes by SDS-electrophoresis under reducing conditions. A lot of proteins were common to both membranes, although significant differences were observed in their relative concentrations. BMV for example contained some low molecular weight proteins, which were considered as good markers for basal membranes (25,26). Vanderpuye and Smith (25) identified a 66 kD protein as placental alkaline phosphatase. In our electrophoresis we observed a major band of approximately 68 kD in the MMV fraction. If this band would represent the alkaline phosphatase, it would predominantly be present in the MMV fraction. This would agree with the enzymatic determination of alkaline phosphatase activity, which was much higher in MMV compared to BMV. With respect to iron uptake some proteins have previously been described: mobilferrin with a molecular mass of 56 kD (27,28) and the proton pore subunit of V-ATPase with a molecular mass of approximately 17 kD (29). Mobilferrin is homologous to calreticulin (30), which was previously isolated from human term placental tissue and was partly characterized (31). V-ATPase was shown in MMV from human term placenta (32). In the present study we visualized a 70 kD and a 45 kD band in Western blots of MMV and BMV, incubated with a rabbit polyclonal antibody to the 67 kD subunit of *Neurospora* V-ATPase. This suggested the presence of V-ATPase in both the microvillous and basal membrane of human term placenta. The 70 kD subunit might be identical to one of the cytosolic subunits of the V-ATPase and the 45 kD subunit might represent a trans-membrane subunit of V-ATPase (review: 33).

The fluidity of plasma membranes is a major determinant in regulating transport processes. Membrane fluidity essentially depends upon the cholesterol/phospholipid ratio: a decrease in this ratio results in an increase in fluidity. Our results revealed no significant differences in cholesterol/phospholipid ratio between MMV and BMV preparations, although both cholesterol and phospholipid contents were higher in BMV. Our results differ from previous reported results (14,34), which revealed that the cholesterol content was significantly less in basal membranes. Lafond, Ayotte and Brunette (34) found that the phospholipid content in basal membranes was higher compared to microvillous membranes, just as we observed with our membrane vesicles. However, the cholesterol/phospholipid ratio was significantly higher in their microvillous membranes compared to their basal membranes. These differences in results might be explained by a different preparation of particularly the basal membrane vesicles. Our vesicles were prepared by sonification of tissue that was separated from microvillous membranes after stirring in isotonic solution. Lafond, Ayotte and Brunette (34) and Jansson, Powell and Iilsley (14) separated their basal membranes from microvillous membranes after the Mg^{2+}

precipitation step and further purified them on either a Ficoll or sucrose gradient. Therefore, the starting material for purification of BMV is quite different.

Further analysis of total phospholipids from our membrane vesicles was performed by fatty acid analysis (Figure 3.4). Our results were comparable to those reported for total human placental phospholipids (35).

In summary, we isolated MMV and BMV from the same human term placenta. Both preparations were relatively free from contamination of the opposite membrane or subcellular organelles. The vesicles were able to take up [^3H]-alanine, which was stimulated by an inwardly directed Na^+ -gradient. With MMV an overshoot above equilibrium was observed, suggesting the functionality of the membrane vesicles. We showed significant differences between the protein profiles of the two preparations after SDS-electrophoresis. Both the cholesterol and phospholipid contents were higher for BMV compared to MMV, resulting in a cholesterol/phospholipid ratio that was not significantly different for the membrane preparations. Thus we characterized in detail the membrane preparations, which were used in further studies.

3.3 Description of trophoblast cells in culture.

3.3.1 Introduction

Purified membrane vesicles are a suitable model to investigate the characteristics of transport carriers on microvillous and basal membranes of placental trophoblast. However, in order to study trans-syncytiotrophoblast transfer and its interaction with intracellular metabolism, an intact cell preparation is needed. The cell preparation must consist of predominantly pure trophoblast cells. Contamination with other cell types may lead to properties of the cell culture that are not characteristic for trophoblast cells. In vivo, cytotrophoblast cells differentiate to form a syncytiotrophoblast layer. For studies with cultured trophoblast cells it is important to be acquainted with the morphological and biochemical differentiation state of the cells. Conditions of cell preparation and culture may play a role in differentiation (recent review: 36,37). In this report we will describe the isolation, purification and in vitro differentiation of trophoblast cells. With respect to these points we will discuss our own cultures.

3.3.2 Isolation and purification of trophoblast cells.

The method of Kliman et al. (38) is the most widely used method for the isolation of trophoblast cells. This method involves trypsin-DNase I digestion of villous tissue followed by Percoll gradient centrifugation. Cells obtained by this procedure are mononuclear, appear round and are not contaminated to a significant extent with endothelial cells, fibroblasts or macrophages, as demonstrated by the lack of immunocytochemical staining

with anti-vimentin (intermediate filament protein, present in endothelial cells and fibroblasts) and anti-ACT (marker for macrophages). The isolated cells do not stain for the β -subunit of human chorionic gonadotropin (hCG), human placental lactogen (hPL), human pregnancy-specific β_1 -glycoprotein (SP₁) and cytokeratin. In situ, the villous syncytiotrophoblast and not the cytotrophoblast stains for these markers, suggesting that the isolated cells are cytotrophoblast cells rather than fragments of syncytiotrophoblast (38,39).

We isolated trophoblast cells according to the method of Kliman et al. (38) except for the addition of 1 mM CaCl₂ and 0.8 mM MgSO₄ to the enzyme solution (40). The obtained cell population consisted of at least 95 % predominantly mononucleated trophoblast cells, as revealed by immunolabelling studies using mouse-anti-vimentin, mouse-anti-cytokeratin and FITC-labelled rabbit anti-mouse IgG (40,41). Moreover, 96 % of freshly isolated cells reacted with trophoblast-specific monoclonal antibody ED 341 (42). Only 3.5 % of freshly isolated cells reacted with cytotrophoblast-specific monoclonal antibody ED 235, possibly because this antigen is susceptible to the trypsinization procedure (42). The major contaminants of isolated trophoblast cells are fibroblasts and macrophages, which can be removed by selective immuno-absorption using anti-CD9 antibodies (43,44). Our trophoblast cells were purified by indirect immunopurification using mouse anti-human CD9 as primary and goat anti-mouse IgG bound to Dynabeads as secondary antibody (45). The final cell population contained mononuclear cells that were able to fuse during culture. Cells were cultured either on 35 mm Falcon culture dishes (Greiner and Sohne, FRG) or on 0.45 μ m microporous membrane filters (Millicell-HA culture plate inserts, Millipore) at 37°C in humidified 5 % CO₂/95 % air.

3.3.3 Differentiation of cultured trophoblast cells

In vivo, cytotrophoblast cells differentiate into syncytiotrophoblast. This involves both morphological and biochemical differentiation. Morphologically, cytotrophoblast cells aggregate and fuse to form multinucleated syncytia. Biochemical differentiation includes the synthesis and/or secretion of hormones such as hCG, hPL, progesterone and oestrogen and the expression of for example placental alkaline phosphatase, SP₁ and interferon.

In vitro, isolated human placental cytotrophoblast cells differentiate into syncytiotrophoblast during culture, although morphological and biochemical differentiation do not necessarily coincide. It has for example been shown that epidermal growth factor (EGF) and cyclic AMP enhance hormone secretion and other biochemical differentiation processes without enhancing syncytium formation (39,46-48). For experiments with cultured trophoblast cells it is important to determine the differentiation state of these cells, morphologically as well as biochemically.

Morphological differentiation

The syncytiotrophoblast is formed by fusion of mononuclear, quite undifferentiated cytotrophoblast cells, containing relatively few subcellular organelles. The differentiated

syncytiotrophoblast is multinucleated, metabolically active and contains a high concentration of all kind of organelles. The outer surface of the syncytium is covered by microvilli that are surrounded by maternal blood (review: 49). Morphological differentiation is specific in the way that cytotrophoblast cells only fuse with other trophoblast cells, possibly only with syncytiotrophoblast, and not with other fetal cells (50).

In vitro, isolated cells attach to the culture dishes, aggregate and fuse to form large multinucleated complexes during culture (38). In order to make contact cells have to move over the culture surface. Under standard culture conditions there is a requirement for serum or extracellular matrix proteins to allow cellular movement and therefore to allow aggregation and fusion (review: 37). In suspension, serum is not required for aggregation, probably because shaking is sufficient to facilitate cell contact (50). Aggregated cytotrophoblast cells are coupled by numerous junctional complexes, such as desmosomes. This junctional communication is stimulated by hCG and 8-bromo-cyclic AMP (51). Desmosome formation can be visualized by desmoplakin staining using immunofluorescence microscopy. Freshly cultured cytotrophoblast cells show a punctuate staining pattern of desmoplakin throughout the whole cytoplasm. Upon cell aggregation desmoplakin is redistributed and becomes located at intercellular boundaries, consistent with desmosome formation. After further differentiation a pavement-like pattern of desmoplakin staining can be observed (41,47). Other characteristics of syncytia are the covering of the apical surface with microvilli and the appearance of cytoplasmic organelles and structures.

Figure 3.5 shows the morphology of trophoblast cells cultured on a permeable filter for 48 h. The cells are polarized with the basal membrane grown into the filter and the apical membrane, containing lots of microvilli, free at the upper side (Figure 3.6). Clathrin coated pits and vesicles are present on both sides of the cells. The cells have a well developed cytoskeleton and contain organelles such as the golgi system, mitochondria, rough and smooth endoplasmic reticulum, which seem active. Sometimes, multivesicular bodies are found. Figure 3.7 shows some specialized regions between two cells (arrows), which might be junctional complexes like desmosomes or tight junctions. The electron micrographs (Figures 3.5 - 3.7) clearly show the presence of cellular aggregates in 48 h cultures. They also show that cells within the aggregates are in contact with each other by means of several junctional complexes. Desmoplakin staining using immunofluorescence microscopy (visualizing desmosomes) has revealed that about 15 % of the 48 h cultured cells is still mononuclear, 30 % of the nuclei is present in aggregates and approximately 55 % of the nuclei is present in syncytia (41).

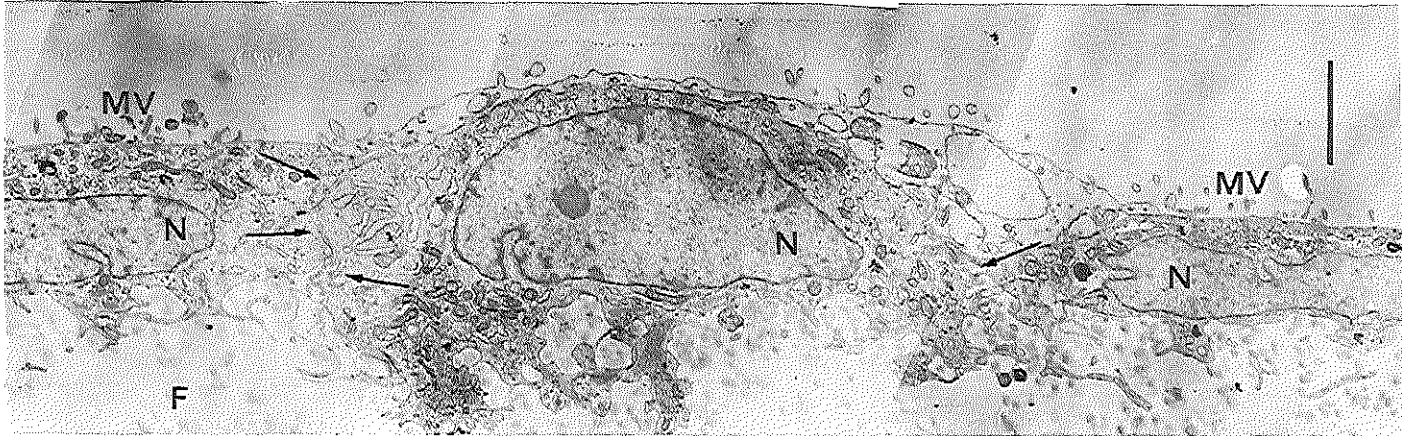


Figure 3.5

Electron micrograph of trophoblast cells grown on a permeable nitro-cellulose filter. Cells were cultured for 48 h. An aggregate of three cells is seen. The basal side of the cells is grown into the filter (F), whereas the microvilli (MV) on the apical membrane are free at the upper side. N refers to the nucleus of a cell. Notice the structured regions at places of cell fusion (arrows). (bar = 2.0 μm)

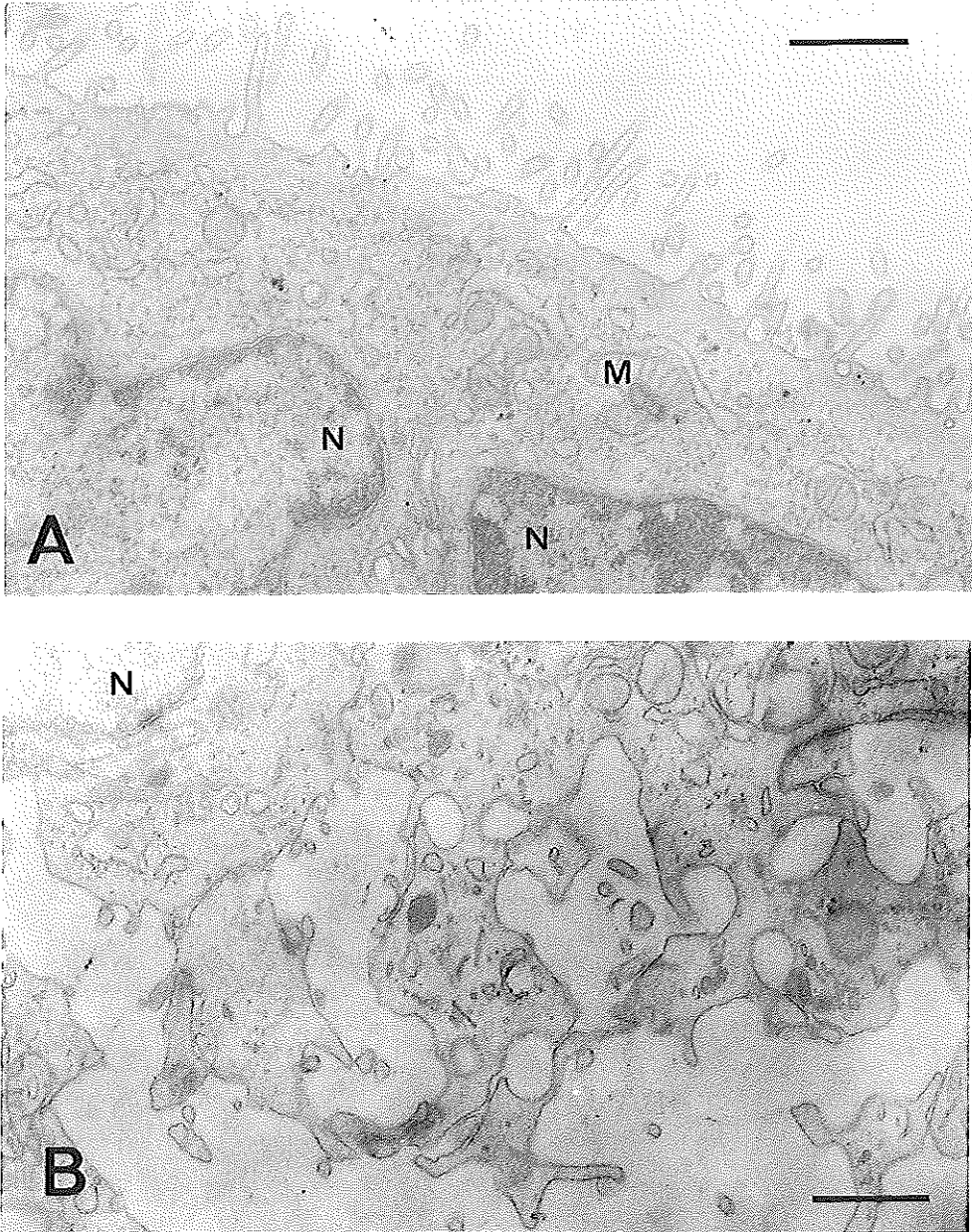


Figure 3.6

Electron micrographs of trophoblast cells, cultured for 48 h on a permeable membrane. Figure 3.6A shows the microvillous membrane. The membrane contains a lot of villi. Clathrin coated pits, coated vesicles, mitochondria and part of the nucleus are seen. Notice the absence of intracellular membranes, suggesting real syncytia. Figure 3.6B shows the basal side of the cell, which is grown into the filter. N refers to a nucleus and M refers to a mitochondrion (bar = 1.0 μm).

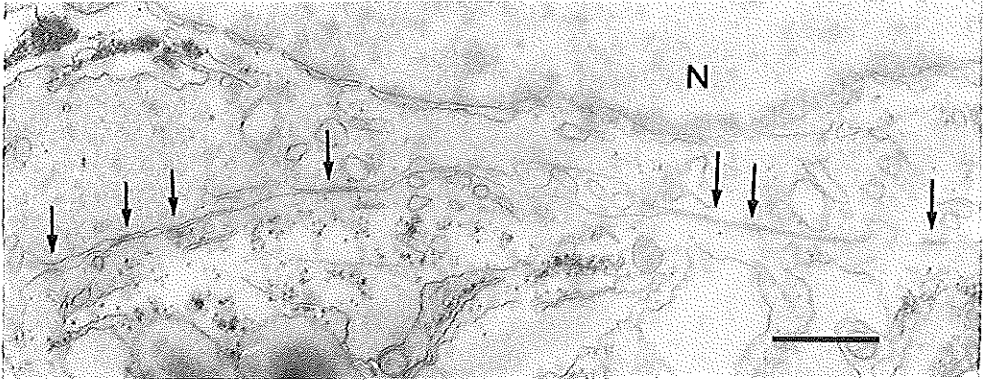


Figure 3.7

Electron micrograph showing an intercellular border between trophoblast cells, cultured for 48 h. Arrows point to specialized regions, which might be junctional complexes like desmosomes or tight junctions. N refers to the nucleus (bar = 1.0 μm).

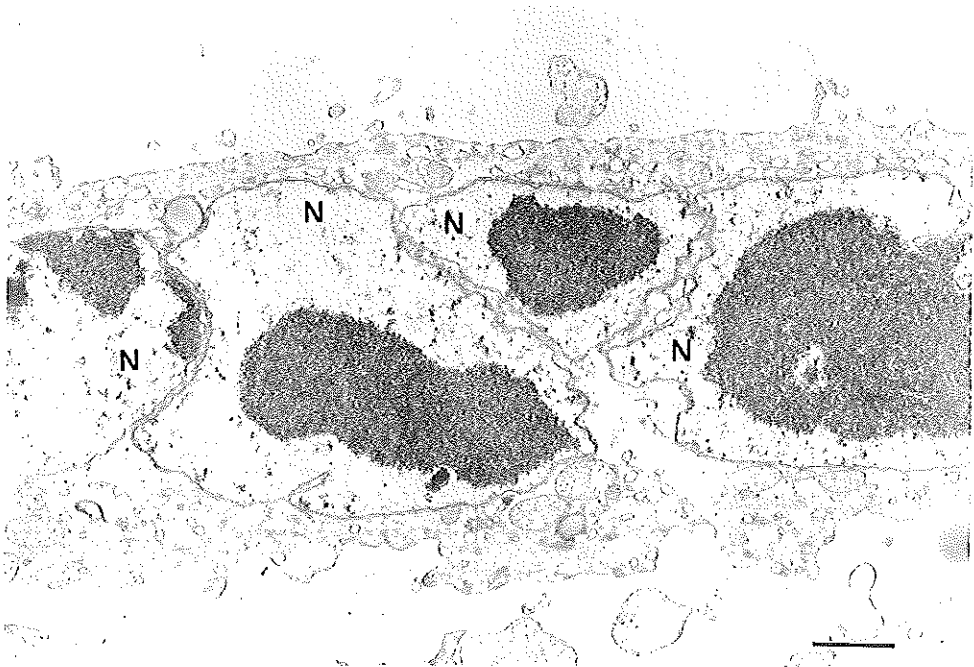


Figure 3.8

Electron micrograph of trophoblast cells, cultured for 66 h. Four nuclei with condensed chromatin can be seen. The intercellular borders are completely lost, as well as the microvilli on the upper membrane. N refers to a nucleus (bar = 1.5 μm).

If cells are cultured for a longer time (66 h), most of the intercellular borders completely disappear, resulting in large multinuclear syncytial complexes (Figure 3.8). However, the long cultured cells also reveal apoptotic changes: the nuclei show condensed chromatin; cytoplasmic organelles lose their distinctive profiles; mitochondria are swollen and their cristae are disrupted; the cell exhibits membrane blebbing and microvilli are lost. The features of these cells correspond to the features of apoptotic human placental syncytiotrophoblast cells, as previously described by Nelson et al. (52).

With respect to morphological differentiation it is very important to culture cells long enough to obtain syncytiotrophoblast-like structures, although not too long, since apoptosis has to be avoided.

Biochemical differentiation

As mentioned above biochemical differentiation of trophoblast cells involves the expression and synthesis of specific hormones such as hCG, hPL and progesterone and the expression of specific proteins as placental alkaline phosphatase and SP₁. The most widely used determinant for the differentiation state of cultured trophoblast cells is the ability of cells to synthesize and secrete hCG and hPL. Proliferating, relatively undifferentiated, cytotrophoblast cells do not express hCG or hPL. In the initial state of differentiation, cytotrophoblast cells start to express the α -subunit of hCG. In a second stage, where multinucleated intermediates may be involved, synthesis of β hCG is induced. As the multinucleated cells differentiate into real syncytium, the synthesis of β hCG may stop and synthesis of hPL is started (53). Further differentiation include a series of apoptotic events, leading to loss of multinucleated cells, which in turn leads to a decline in the levels of hCG (54). The synthesis of hCG and hPL by cultured trophoblast cells can be stimulated by epidermal growth factor (EGF) and cyclic AMP (39,46-48). Trophoblast cells cultured on uncoated surfaces in the absence of serum, and therefore not able to fuse into syncytium, also secrete hCG. This secretion can be stimulated by 8-bromo-cyclic AMP (39). Thus, single mononuclear trophoblast cells may be able to express endocrine functions of syncytiotrophoblast, suggesting that syncytium formation is not a prerequisite for biochemical differentiation. Another differentiation marker is the expression of TfRs. It has been shown that TfRs are expressed on the villous syncytiotrophoblast whereas they are absent from the villous cytotrophoblast (55). Bierings et al. (40) have shown that cultured human term trophoblast cells express TfRs and that expression increases during culture, in parallel with the increase in the number of cell aggregates and syncytia. However, mononucleated cells are still present after 60 to 70 h of culture and they express TfRs as well.

The observation that biochemical and morphological differentiation are not necessarily coupled, is used as an argument for the hypothesis that the primary cell population consists at least partly of mononuclear syncytiotrophoblast fragments. This could explain the syncytiotrophoblast characteristics in the primary mononuclear cells. Moreover, these

cells remains unclear until specific markers for cyto- and syncytiotrophoblast have been discovered.

Although the origin of the isolated trophoblast cells can be discussed, it is clear that cells cultured for 48 h mainly consist of syncytiotrophoblast-like structures with syncytiotrophoblast-like biochemical characteristics.

References

1. Dicke JM, Verges D, Kelley LK & Smith CH (1993) Glycine uptake by microvillous and basal plasma membrane vesicles from term human placentae. *Placenta*, 14:85-92.
2. Booth AG, Olaniyan RO & Vanderpuye OA (1980) An improved method for the preparation of human placental syncytiotrophoblast microvilli. *Placenta*, 1:327-336.
3. Kelley LK, Smith CH & King BF (1983) Isolation and partial characterization of the basal cell membrane of human placental trophoblast. *Biochimica et Biophysica Acta*, 734:91-98.
4. Markwell M-AK, Haas SM, Bieber LL & Tolbert NE (1978) A modification of the Lowry procedure to simplify protein determination in membrane and lipoprotein samples. *Analytical Biochemistry*, 87:206-210.
5. Lowry OH, Rosebrough NJ, Farr AL & Randall RJ (1951) Protein measurement with the Folin phenol reagent. *Journal of Biological Chemistry*, 193:265-275.
6. Richterich R, Colombo JP & Weber H (1962) Ultramikromethoden im klinischen Laboratorium. VII. Bestimmung der sauren Prostata-phosphatase. *Schweizerische Medizinische Wochenschrift*, 47:1496-1500.
7. Williams LT, Jarett L & Lefkowitz RJ (1975) Adipocyte β -adrenergic receptors. Identification and subcellular localization by (-)-[3 H]dihydroalprenolol binding. *Journal of Biological Chemistry*, 251:3096-3104.
8. Milson DW, Rose FA & Dodgson KS (1972) The specific assay of arylsulphatase C, a rat liver microsomal marker enzyme. *Biochemical Journal*, 128:331-336.
9. Dallner G, Siekevitz P & Palade GE (1966) Biogenesis of endoplasmic reticulum membranes. II. Synthesis of constitutive microsomal enzymes in developing rat hepatocyte. *Journal of Cell Biology*, 30:97-117.
10. Pennington RJ (1961) Biochemistry of dystrophic muscle. Mitochondrial succinate-tetrazolium reductase and adenosine triphosphatase. *Biochemical Journal*, 80:649-654.
11. Schoot BM, Schoots AFM, De Pont JJHM, Schuurmans-Stekhoven FMAH & Bonting SL (1977) Studies on ($\text{Na}^+ + \text{K}^+$) activated ATPase. XLI. Effects of N-ethylmaleimide on overall and partial reactions. *Biochimica et Biophysica Acta*, 483:181-192.
12. Kato M & Kako J (1987) Orientation of vesicles isolated from baso-lateral membranes of renal cortex. *Molecular and Cellular Biochemistry*, 78:9-16.
13. Bligh EG & Dyer WJ (1959) A rapid method of total lipid extraction and purification. *Canadian Journal of Biochemistry and Physiology*, 37:911-917.
14. Jansson T, Powell TL & Illsley NP (1993) Non-electrolyte solute permeabilities of human placental microvillous and basal membranes. *Journal of Physiology*, 468:261-274.

15. Bartlett GR (1959) Phosphorus assay in column chromatography. *Journal of Biological Chemistry*, 234:466-468.
16. Fiske CH & Subbarow Y (1925) The colorimetric determination of phosphorus. *Journal of Biological Chemistry*, 66:375-400.
17. Morrison WR & Smith LM (1964) Preparation of fatty acid methyl esters and dimethylacetals from lipids with boron fluoride-methanol. *Journal of Lipid Research*, 5:600-608.
18. Smith CH, Nelson DM, King BF, Donohue TM, Ruzycski SM & Kelley LK (1977) Characterization of a microvillous membrane preparation from human placental syncytiotrophoblast: a morphologic, biochemical, and physiologic study. *American Journal of Obstetrics and Gynecology*, 128:190-196.
19. Khalfoun B, Degenne D, Arbeille-Brassart B, Gutman N & Bardos P (1985) Isolation and characterization of syncytiotrophoblast plasma membrane from human placenta. *FEBS Letters*, 181:33-38.
20. Glazier JD, Jones CJP & Sibley CP (1988) Purification and Na⁺ uptake by human placental microvillous membrane vesicles prepared by three different methods. *Biochimica et Biophysica Acta*, 945:127-134.
21. Illsley NP, Wang ZQ, Gray A, Sellers MC & Jacobs MM (1990) Simultaneous preparation of paired, syncytial, microvillous and basal membranes from human placenta. *Biochimica et Biophysica Acta*, 1029:218-226.
22. Eaton BM & Oakey MP (1994) Sequential preparation of highly purified microvillous and basal syncytiotrophoblast membranes in substantial yield from a single human placenta: inhibition of microvillous alkaline phosphatase activity by EDTA. *Biochimica et Biophysica Acta*, 1193:85-92.
23. Johnson LW & Smith CH (1988) Neutral amino acid transport systems of microvillous membrane of human placenta. *American Journal of Physiology*, 254:C772-C780.
24. Hoeltzli SD & Smith CH (1989) Alanine transport systems in isolated basal plasma membrane of human placenta. *American Journal of Physiology*, 256:C630-C637.
25. Vanderpuye OA & Smith CH (1987) Proteins of the apical and basal plasma membranes of the human placental syncytiotrophoblast: immunochemical and electrophoretic studies. *Placenta*, 8:591-608.
26. Eaton BM & Oakey MP (1997) Image analysis of protein profiles from paired microvillous and basal syncytiotrophoblast plasma membranes from term human placenta and characterization of IgG binding to membrane vesicles. *Placenta*, 18:569-576.
27. Conrad ME, Umbreit JN, Moore EG, Peterson RDA & Jones MB (1990) A newly identified iron binding protein in duodenal mucosa of rats. Purification and characterization of mobilferrin. *Journal of Biological Chemistry*, 265:5273-5279.

28. Conrad ME & Umbreit JN (1993) A concise review: iron absorption - The mucin-mobilferrin-integrin pathway. A competitive pathway for metal absorption. *American Journal of Hematology*, 42:67-73.
29. Li CY, Watkins JA, Hamazaki S, Altazan JD & Glass J (1995) Iron binding, a new function for the reticulocyte endosome H⁺-ATPase. *Biochemistry*, 34:5130-5136.
30. Conrad ME, Umbreit JN & Moore EG (1993) Rat duodenal iron-binding protein mobilferrin is a homologue of calreticulin. *Gastroenterology*, 104:1700-1704.
31. Houen G & Koch C (1994) Human placental calreticulin: purification, characterization and association with other proteins. *Acta Chemica Scandinavica*, 48:905-911.
32. Simon BJ, Kulanthaivel P, Burckhardt G, Ramamoorthy S, Leibach FH & Ganapathy V (1992) Characterization of an ATP-driven H⁺ pump in human placental brush-border membrane vesicles. *Biochemical Journal*, 287:423-430.
33. Forgac, M (1989) Structure and function of vacuolar class of ATP-driven proton pumps. *Physiological Reviews*, 69:765-796.
34. Lafond J, Ayotte N & Brunette MG (1993) Effect of (1-34) parathyroid hormone-related peptide on the composition and turnover of phospholipids in syncytiotrophoblast brush border and basal plasma membranes of human placenta. *Molecular and Cellular Endocrinology*, 92:207-214.
35. Bayon Y, Croset M, Chirouze V, Tayot JL & Lagarde M (1993) Phospholipid molecular species from human placenta lipids. *Lipids*, 28:631-636.
36. Bloxam DL, Bax CMR & Bax BE (1997) Culture of syncytiotrophoblast for the study of human placental transfer. Part I: isolation and purification of cytotrophoblast. *Placenta*, 18:93-98.
37. Bloxam DL, Bax BE, & Bax CMR (1997) Culture of syncytiotrophoblast for the study of human placental transfer. Part II: production, culture and use of syncytiotrophoblast. *Placenta*, 18:99-108.
38. Kliman HJ, Nestler JE, Sermasi E, Sanger JM & Strauss III JF (1986) Purification, characterization, and in vitro differentiation of cytotrophoblasts from human term placentas. *Endocrinology*, 118:1567-1582.
39. Kliman HJ, Straus III JF, Kao LC, Caltabiano S & Wu S (1991) Cytoplasmic and biochemical differentiation of the human villous cytotrophoblast in the absence of syncytium formation. *Trophoblast Research*, 5:297-309.
40. Bierings MB, Adriaansen HJ & van Dijk JP (1988) The appearance of transferrin receptors on cultured human cytotrophoblast and in vitro-formed syncytiotrophoblast. *Placenta*, 9:387-396.

41. Starreveld JS, van Denderen J, Verrijt CEH, Kroos MJ & van Dijk JP (1998) Morphological differentiation of cytotrophoblasts cultured in medium 199 and keratinocyte growth medium. *European Journal of Obstetrics & Gynecology and Reproductive Biology*, 79:205-210.
42. Bierings M, Jones C, Adriaansen H & van Dijk JP (1991) Transferrin receptors on cyto- and in vitro formed syncytiotrophoblast. *Trophoblast Research*, 5:349-362.
43. Morrish DW, Shaw ARE, Seehafer J, Bhardwaj D & Paras MT (1991) Preparation of fibroblast-free cytotrophoblast cultures utilizing differential expression of the CD9 antigen. In *Vitro Cellular and Developmental Biology*, 27A:303-306.
44. Yui J, Garcia-Lloret M, Brown AJ, Berdan RC, Morrish DW, Wegmann TG & Guilbert LJ (1994) Functional, long-term cultures of human term trophoblasts purified by column-elimination of CD9 expressing cells. *Placenta*, 15:231-246.
45. Starreveld JS, Kroos MJ, van Suijlen JDE, Verrijt CEH, van Eijk HG & van Dijk JP (1995) Ferritin in cultured human cytotrophoblasts: synthesis and subunit distribution. *Placenta*, 16:383-395.
46. Kao LC, Caltabiano S, Wu S, Strauss JF & Kliman HJ (1988) The human villous cytotrophoblast: interaction with extracellular matrix proteins, endocrine function, and cytoplasmic differentiation in the absence of syncytium formation. *Developmental Biology*, 130:693-702.
47. Douglas GC & King BF (1989) Isolation of pure villous cytotrophoblast from term human placenta using immunomagnetic microspheres. *Journal of Immunological Methods*, 119:259-268.
48. Morrish DW, Dakour J, Li H, Xiao J, Miller R, Sherburne R, Berdan CR & Guilbert LJ (1997) In vitro cultured human term cytotrophoblast: a model for normal primary epithelial cells demonstrating a spontaneous differentiation program that requires EGF for extensive development of syncytium. *Placenta*, 18:577-585.
49. Jones JP & Fox H (1991) Ultrastructure of the normal human placenta. *Electron Microscopy Reviews*, 4:129-178.
50. Babalola GO, Coutifaris C, Soto EA, Kliman HJ, Shuman H & Strauss III JF (1990) Aggregation of dispersed human cytotrophoblastic cells: lessons relevant to the morphogenesis of the placenta. *Developmental Biology*, 137:100-108.
51. Cronier L, Hervé JC, Délèze J & Malassiné A (1997) Regulation of gap junctional communication during human trophoblast differentiation. *Microscopy Research and Technique*, 38:21-28.
52. Nelson DM (1996) Apoptotic changes occur in syncytiotrophoblast of human placental villi where fibrin type fibrinoid is deposited at discontinuities in the villous trophoblast. *Placenta*, 17:387-391.

53. Boime I (1991) Human placental hormone production is linked to the stage of trophoblast differentiation. *Trophoblast Research*, 5:57-60.
54. Muyan M & Boime I (1997) Secretion of chorionic gonadotropin from human trophoblasts. *Placenta*, 18:237-241.
55. Bulmer JN, Morrison L & Johnson PM (1988) Expression of the proliferation markers Ki67 and transferrin receptor by human trophoblast populations, *Journal of Reproductive Immunology*, 14:291-302.

4

Binding of human isotransferrin variants to
microvillous and basal membrane vesicles from
human term placenta

Based on:

Verrijt CEH, Kroos MJ, van Noort WL, van Eijk HG &
van Dijk JP

Placenta (1997) 18:71-77

4.1 Introduction

The fetus requires a large amount of iron during the course of gestation. Iron is actively transported from mother to fetus across the placenta. The major source of iron in human placental iron transport is maternal transferrin (Tf).

Tf shows microheterogeneity based on the variation in the structure of the N-linked glycan chains (1,2). During pregnancy, the complexity of the carbohydrate chains of Tf increases in maternal guinea pig serum (3) as well as in maternal human serum (4), whereas the complexity of Tf in fetal serum is reduced.

Tf-mediated iron transport involves transferrin receptors (TfRs), which are present both on the maternal-facing microvillous plasma membrane (5,6) and on the fetal-facing basal plasma membrane (7) of human placental syncytiotrophoblast. Léger et al. (8) showed that the affinity of Tf for TfRs on the microvillous membrane decreases as the complexity of the Tf glycan chains increases.

In the present study, we investigated the binding of isoTf variants to TfRs on microvillous and basal membrane vesicles, isolated from the same human term placenta. We studied the binding of the following purified human diferric isotransferrins: bi-bi-antennary tetra-sialo Tf (bb Tf), bi-tri-antennary penta-sialo Tf (bt Tf) and tri-tri-antennary hexa-sialo Tf (tt Tf).

4.2 Materials and Methods

Chemicals

Human serum Tf was purchased from Behringwerke (Marburg an Lahn, Germany). Rabbit anti-human Tf antibody (titre = 2800 mg/l) was from DAKO (Denmark). Na¹²⁵I was obtained from Amersham (Buckinghamshire, UK).

Tissue source

Normal human term placentae were obtained from the department of Obstetrics and Gynaecology, University Hospital Rotterdam/Dijkzigt, within half an hour after spontaneous vaginal delivery.

Isolation and characterization of membrane vesicles

Both microvillous and basal membrane vesicles were isolated from the same human term placenta (see 2.3.1 in Chapter 2 for a detailed description of the isolation). Microvillous membrane vesicles (MMV) were isolated according to the method of Booth, Olaniyan and Vanderpuye (9), modified by Dicke et al. (10). Basal membrane vesicles (BMV) were isolated according to a modification (10) of the method of Kelley, Smith and King (11). The final

pellets were resuspended in PBS pH 7.4. Membrane protein was determined according to Markwell et al. (12).

As shown in Chapter 3, MMV were enriched 19-fold in alkaline phosphatase and BMV were enriched 28-fold in dihydroalprenolol binding. Contamination of lysosomes, endoplasmic reticulum and mitochondria was low.

Orientation of MMV was determined by assaying the alkaline phosphatase activity with and without previous treatment of the vesicles with 0.1% saponin. Orientation of BMV was determined by assaying the Na^+K^+ -ATPase activity (13) after treatment of the vesicles with or without 0.1% saponin or 40 nM valinomycin (14). We found that MMV were 88 % either right-side-out or unsealed and 12 % of MMV was inside-out. For BMV we found that 28 % was right-side-out, 60 % unsealed and 12 % inside-out (Chapter 3).

Isolation of transferrin variants

The Tf variants (bb, bt and tt Tf) were isolated from human serum Tf by Concanavalin A Sepharose chromatography and preparative isoelectric focusing (15). The subfractions were checked on sialic acid content by isoelectric focusing, using PhastGels IEF pH 4-6.5 (16). The molar proportions of the sugars from the Tf variants were determined (17). This procedure is described more detailed in 2.5.

Labelling of diferric transferrin with ^{125}I

Diferric Tf was labelled with ^{125}I as described in 2.6.2. The final specific activity ranged from 2.3×10^4 - 6.1×10^4 cpm/pmol Tf.

Estimation of endogenous transferrin

The amount of endogenous Tf in the membrane preparations was estimated using the Laurell-rocket immunoelectrophoresis (18) as described in 2.7.1. Rabbit anti human Tf was used as the antibody. The precipitates were stained with Coomassie Brilliant Blue R250. The amount of Tf in membrane vesicles was determined by comparing with Tf standards.

Transferrin binding assay

For each experiment, membrane vesicles (MMV and BMV) from the same human term placenta were used. The assay for Tf binding is described in detail in 2.7.2. In short: Membrane vesicles were washed respectively with an acidic and an alkaline buffer to remove Tf bound to TfRs (19) and incubated with ^{125}I -labelled isoTf variants for 1 h at 4°C. The vesicle suspension was centrifuged, washed with PBS without resuspending the pellet, and centrifuged again (20). The final pellet was dissolved in 2 ml 1 % SDS and radioactivity was determined. The data were evaluated by a non-linear curve-fit program, using the Langmuir equation for equilibrium binding ($B = [\text{Bmax} * x] / [x + K_d]$ + non-specific binding), where B is the fraction of Tf that is bound, Bmax is the saturation level for specific binding, x is the

concentration of Tf in the incubation medium, K_d is the concentration of Tf at which half-maximal specific saturable binding is achieved, and the non-specific binding is a linear function of x . Non-specific binding was experimentally determined in the presence of a 100-fold molar excess of unlabelled human isoTf variants. The limited amounts of especially bt and tt isoTf made it impossible to routinely assess non-specific binding in this way. Since the experimentally determined specific binding corresponded with the specific binding calculated by the non-linear curve-fit program, we further used the latter method. Both the maximal binding and the affinity constant ($K_a = 1/K_d$) of the isoTf variants were determined.

Data analysis

Data were analyzed by Multifactor Analysis of Variance (ANOVA) procedure, followed by paired Student's *t*-test, using Statgraphics' computer program (Table 4.1 and left part of Table 4.2). S.d. values for K_a ratios (right part of Table 4.2) were derived from the coefficient of variation for a ratio, *Coeff.Var.(nu/de)* which was calculated as

$$\begin{aligned} \text{Coeff.Var.}^2(\text{nu/de}) &= \text{Coeff.Var.}^2(\text{nu}) + \text{Coeff.Var.}^2(\text{de}) \\ &\quad - [2 \times r \times \text{Coeff.Var.}(\text{nu}) \times \text{Coeff.Var.}(\text{de})] \end{aligned}$$

where *Coeff.Var.(nu)* and *Coeff.Var.(de)* are the coefficients of variation and *r* the correlation coefficient for numerator (nu) and denominator (de) (21).

For the K_a ratios, unpaired two-tailed Student's *t*-tests were performed and the following test value was employed: $U = (X - Y) / \sqrt{s.d.^2 X / n_X + s.d.^2 Y / n_Y}$, with $(n_X + n_Y - 2)$ degrees of freedom for determination of *P*-values (21).

4.3 Results

Purification of serum isoTf variants

The sialic acid contents of the isoTf variants were checked by isoelectric focusing. The number of sialic acids was respectively 4, 5, and 6 per Tf for the different isoTf variants (results not shown). The isoTf variants were checked on carbohydrate molar proportions. The molar mannose and galactose contents were 5.6, 5.7 and 5.6 mol mannose and 4.0, 5.3 and 7.2 mol galactose per mol protein of tetra-, penta- and hexa-sialo Tf. These results make clear that the isolated isoTf variants were: bi-bi-antennary tetra-sialo Tf (bb Tf), bi-tri-antennary penta-sialo Tf (bt Tf) and tri-tri-antennary hexa-sialo Tf (tt Tf) (see Chapter 1, Figure 1.1).

Estimation of endogenous Tf

Microvillous and basal membrane vesicles contained up to 2.5 and 1.2 μg Tf / mg protein, as estimated by Laurell-rocket immunoelectrophoresis. After washing the vesicles according to Berczi and Faulk (19), the amount of Tf per mg protein reduced to approximately 60 % in relation to the unwashed vesicles (Figure 4.1). When the vesicles were extensively washed

with both 3M KCl and with the procedure according to Berczi and Faulk (19), a lot of protein was lost with no further purification. The enrichments of enzyme activities did not improve and the amount of endogenous Tf did not further decrease (Figure 4.1).

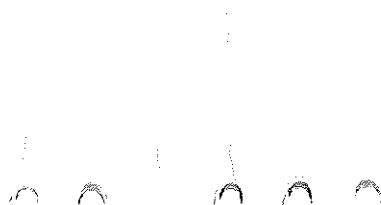


Figure 4.1

Laurell-rocket immunoelectrophoresis in 1% agarose with 1% Triton X-100 and 30 ml of anti human Tf (titre:2800 mg/l). Samples contained 4 µg/µl protein and 12 µl of the samples was put on gel. Lane 1: unwashed BMV; lane 2: BMV washed according to Berczi and Faulk (19); lane 3: BMV washed both with 3 M KCl and according to Berczi and Faulk (19); lane 4: unwashed MMV; lane 5: MMV washed according to Berczi and Faulk (19); and lane 6: MMV washed both with 3 M KCl and according to Berczi and Faulk (19).

Binding of isoTf variants to microvillous and basal membrane vesicles

The specific binding of each of the isoTf variants to both MMV and BMV was saturable in the range of the Tf concentrations used. The non-specific binding never exceeded 10 % of total binding. Figure 4.2 gives the result of one experiment for bb Tf binding to MMV (A) and to BMV (B). Similar binding curves were obtained for each study. The Scatchard plots were deduced from the fitted binding curves, resulting in an alternative presentation of the calculated specific binding.

Table 4.1 lists the numbers of TfRs on MMV and BMV, which were determined according to the Langmuir equation. ANOVA revealed that the number of TfRs was not influenced by the isoTf variants, whereas the influence of the membrane preparation (BMV versus MMV) was highly significant ($P < 0.001$). Since the large variations in number of TfRs were due to interplacental variations, we compared data from the same human term placenta

to investigate the differences in number of TfRs on MMV and BMV. The number of TfRs on MMV was 6.1 ± 2.4 (mean \pm s.d.) times higher than the number of TfRs on BMV, independent of the isoTf used (paired Student's *t*-test, $P < 0.01$; $n = 15$).

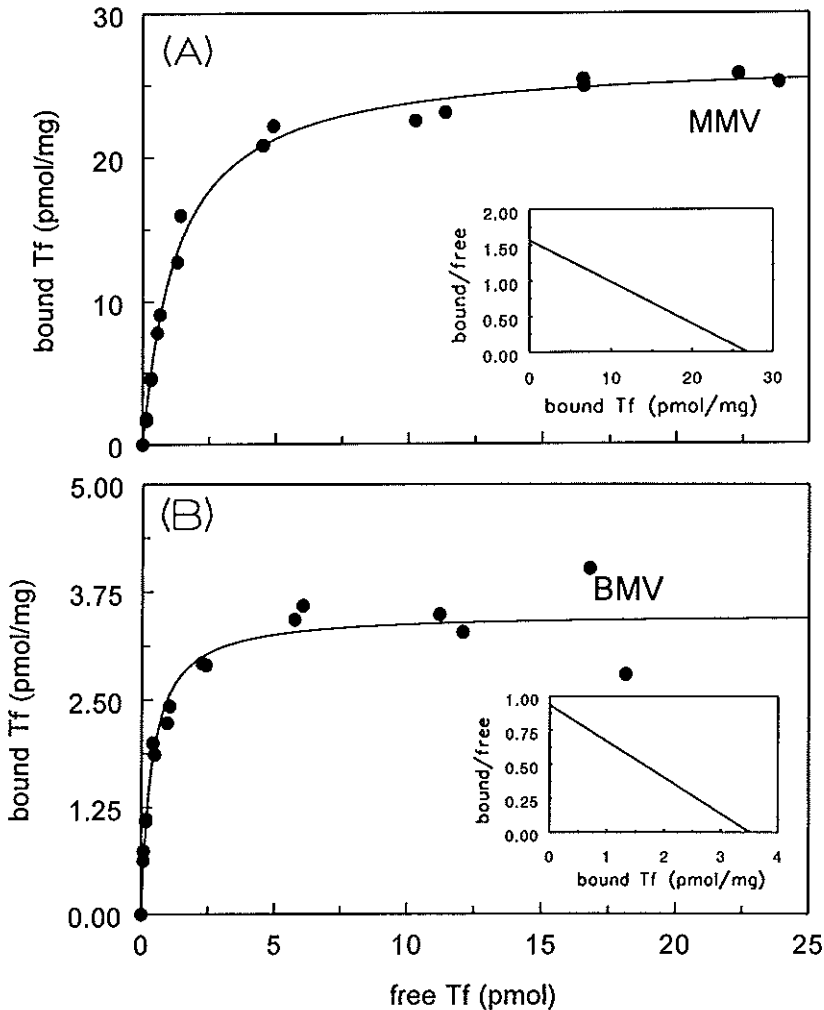


Figure 4.2

Specific equilibrium binding of diferric bb Tf to MMV (A) or to BMV (B) from the same human term placenta. Washed membrane vesicles (75 μ g for MMV and 100 μ g for BMV) were incubated with various concentrations of diferric 125 I-Tf. After 1 h of incubation, vesicle suspensions were centrifuged, pellets were dissolved in 1% SDS and binding was measured and analyzed by a nonlinear curve fit program, using the Langmuir equation ($r = 0.99$). Free Tf refers to the Tf concentration in the incubation medium, bound Tf refers to the amount of Tf that is bound to the membrane vesicles, and bound/free is the quotient of the amount of bound Tf (pmol) and the amount of Tf (pmol) in the incubation medium. The Scatchard plots are deduced from the fitted binding curve, giving another presentation of the results. Data are from one out of five experiments with five different placentae.

Table 4.1
Number of TfRs on MMV and BMV

membrane	TfRs [#]		
	bb [*]	bt [*]	Tt [*]
MMV	1.4x10 ¹³	1.3x10 ¹³	1.2x10 ¹³
s.d.	0.7x10 ¹³	0.7x10 ¹³	0.7x10 ¹³
BMV	2.7x10 ¹² **	2.5x10 ¹² **	2.4x10 ¹² **
s.d.	1.8x10 ¹²	1.7x10 ¹²	1.7x10 ¹²

The numbers of TfRs for each isoTf variant (mean ± s.d. from five experiments with five different membrane preparations) were determined according to the Langmuir equation.

#) number of TfRs / mg membrane protein

**) The number of TfRs was not influenced by the isoTf variants (ANOVA)*

***) P<0.01 vs MMV (Student's paired t-test)*

Table 4.2
K_a values and K_a ratios of TfRs on MMV and BMV

membrane	K _a (nM)			K _a ratio		
	bb	bt	tt	bb/bt	bb/tt	bt/tt
MMV	0.16	0.11	0.10	1.45 ^{b,c}	1.59 ^c	1.09
s.d.	0.05	0.03	0.03	0.06	0.10	0.03
BMV	0.58 ^a	0.43 ^a	0.37 ^a	1.36 ^{b,c}	1.57 ^c	1.16
s.d.	0.15	0.12	0.10	0.11	0.04	0.08

The K_a values for each isoTf variant (mean ± s.d. from five experiments with five different membrane preparations) were determined according to the Langmuir equation. The influence of the isoTf variants is reflected by the K_a ratios, which were determined for experiments with membrane preparations from one placenta and are presented as mean ± s.d. from five experiments with five different membrane preparations.

a) P<0.01 vs MMV (Student's paired t-test)

b) P<0.05 vs bb/tt (unpaired two-tailed Student's t-test)

c) P<0.05 vs bt/tt (unpaired two-tailed Student's t-test)

The affinity constants are shown in the left part of Table 4.2. The large s.d.s are due to differences in binding when membrane preparations from different placentae were used. According to the ANOVA procedure, the K_a values were significantly influenced by both the origin of membrane preparation ($P < 0.001$) and the isoTf variants ($P < 0.05$) on the K_a of the TfR. For all isoTf variants, the K_a of TfRs on BMV was 3.9 ± 0.4 (mean \pm s.d.) times higher than the K_a of TfRs on MMV from the same human term placenta (paired Student's *t*-test, $P < 0.01$; $n=15$). The K_a values for the isoTf variants showed no significant differences (paired Student's *t*-test), because the differences caused by different placentae were larger than the differences caused by the isoTf variants. To further determine the influence of isoTf variants on the K_a values, we used K_a ratios (bb : bt, bb : tt and bt : tt). The ratios were determined for experiments with membrane preparations from one placenta. The right part of Table 4.2 shows the K_a ratios as mean \pm s.d. from five experiments with five different membrane preparations. The K_a ratios of the isoTf variants were significantly different (unpaired two-tailed Student's *t*-test, $P < 0.05$) and show that the K_a for bb Tf $>$ K_a for bt Tf and tt Tf, and the K_a for bt Tf $>$ K_a for tt Tf.

4.4 Discussion

During pregnancy, there is a shift to Tfs with more complex carbohydrate chains in maternal serum and less complex carbohydrate chains in fetal serum (2,3,22). Léger et al. (8) showed a decrease in affinity constants of TfRs on microvillous membranes as the number of Tf triantennary glycan chains increased. In this study we investigated the binding of purified human diferric isoTf variants to TfRs on both MMV and BMV from the same human term placenta, and the effect of increasing complexity of Tf on number and affinity of these receptors. In order to diminish the effect of endogenous Tf, the binding assays were performed after extensive washing of the membrane vesicles.

Each of the isoTf variants showed saturable binding to TfRs on both MMV and BMV. The number of TfRs was comparable for each isoTf variant with a sixfold higher number of TfRs on MMV compared with BMV. Since 88 % of both MMV and BMV were either right-side-out or unsealed, 88 % of the TfRs of both MMV and BMV were accessible for Tf. Therefore, vesicle orientation gives no explanation for the observed differences in the number of TfRs. Vanderpuye et al. (7) demonstrated a twofold higher binding capacity of TfRs on microvillous membranes compared with TfRs on basal membranes. The number of TfRs on microvillous membranes (1.3×10^{13}) was thousandfold higher than that observed by Léger et al. (8), but comparable with that estimated by Vanderpuye et al. (7). Because endogenous Tf was still present in the membrane suspensions of Léger et al. (8), it was possible that the seroTf variants added were not able to displace all receptor-bound endogenous Tf, resulting in an underestimation of the number of TfRs.

The affinity of Tf for TfRs on BMV was higher than that for TfRs on MMV. Similar differences were observed by Vanderpuye et al. (7) who supposed that these differences were the result of differences in endogenous Tf content. Tsunoo and Sussman (23) showed endogenous Tf affected the binding of Tf to its receptor. It would behave like a competitive inhibitor, and therefore, lower the experimentally determined receptor affinities. In the present study we tried to completely remove endogenous Tf by washing with respectively acidic and an alkaline buffer according to Berczi and Faulk (19). However, only about 60 % of the endogenous Tf could be removed (Figure 4.1). Another method to remove endogenous Tf from membranes is treatment with chaotrope (24). Washing our membrane vesicles with 3 M KCl resulted again in no more than 60 % reduction of endogenous Tf (results not shown). Even washing with either 3 M KCl or 0.3 M ammonium thiocyanate followed by washing according to Berczi and Faulk (19) did not further decrease the amount of endogenous Tf (Figure 4.1, lane 3 and 6). Therefore, we supposed that the endogenous Tf left represented non-exchangeable Tf and did not disturb the Tf binding assays. The differences in affinity of Tf for TfRs on MMV and BMV might be due to the heterogeneity of the TfRs. Differences in glycosylation pattern of human placental TfRs has been shown to be greatly influenced by glycosylation (26). Another explanation could be the difference in microenvironment surrounding the TfRs on microvillous and basal membranes. The number of available TfRs in bone marrow cells was influenced by changes in lipid fluidity (27). Recently, DiGiulio et al. (28) reported differences in binding capacity of human placental TfRs in different liposomes. Although they did not show significant differences in affinity constants, they made it clear that the microenvironment plays a crucial role in the binding behaviour of the TfR. In Chapter 3 we showed that both the cholesterol and the phospholipid content were higher in BMV compared to MMV (Table 3.2). These differences might play a role in the affinities of Tf binding to TfRs on BMV and MMV.

For TfRs on both MMV and BMV, a decrease in affinity constant was observed as bb Tf was replaced by bt Tf or tt Tf, but these differences are probably too small to be of physiological importance ($K_d \ll [\text{diferric Tf}]$). Léger et al. (8) showed up to sixfold decrease in affinity constant with an increasing number of Tf triantennary glycan chains. However, their membrane suspensions contained endogenous Tf, which might have disturbed the binding assays.

Iron transport across the placenta is unidirectional from mother to fetus. Only iron and not maternal Tf is transferred from mother to fetus (review: 29). TfRs are virtually absent on placental endothelial cells (30), suggesting that iron may reach the fetal circulation via a non-receptor-mediated process. In trophoblast-like BeWo cells, which were stimulated to form syncytia, it was shown that due to differences in post-endocytotic sorting, 25 % of diferric ^{125}I -Tf was transcytosed from microvillous to basal direction and 16 % in the reversed direction (31). These data explained that under steady state conditions the distribution of TfRs on the basolateral surface is about double that on the apical surface

(31). In our study, we found six times as much TfRs on MMV than on BMV, which could indicate merely unidirectional transcytosis in basal to microvillous direction, in combination with limited TfR recycling at the basal membrane. This way of TfR sorting would be important if *denovo* synthesized TfRs were preferentially trafficked to the basal membrane, and then enter the recycling pathway at the microvillous membrane after transcytosis. A possible additional function of the TfR at the basal membrane, *in situ*, could be to regulate the re-uptake of maternal Tf that reached the fetal side. The observed higher affinities of TfRs on BMV support this hypothesis. If indeed TfRs on basal membranes are not involved in iron transfer across this membrane, a Tf-independent transport mechanism for iron, released from the endosomes, has to be postulated in the basal membrane.

In conclusion, the number of TfRs on MMV was six-fold higher than that on BMV, with a higher affinity of Tf for TfRs on BMV. For both membrane preparations, a slight decrease in affinity was shown as bb Tf was replaced by bt Tf or tt Tf. However, these differences are probably not of physiological importance.

References

1. Spik G, Bayard B, Fournet B, Strecker G, Bourquelet S & Montreuil J (1975) Studies on glycoconjugates. LXIV. Complete structure of two carbohydrate units of human serotransferrin. *FEBS Letters*, 50:296-299.
2. De Jong G, van Dijk JP & van Eijk HG (1990) The biology of transferrin. Critical review. *Clinica Chimica Acta*, 190:1-46.
3. Bierings MB, Heeren JWA, van Noort WL, van Dijk JP & van Eijk HG (1987) Pregnancy and guinea-pig iso-transferrin -isolation and characterization of both isotransferrins. *Clinica Chimica Acta*, 165:205-217.
4. De Jong G & van Eijk HG (1988) Microheterogeneity of human serum transferrin. A biological phenomenon studied by isoelectric focusing on immobilized pH gradients. *Electrophoresis*, 165:205-211.
5. Wada HG, Hass PE & Sussman HH (1979) Transferrin receptor in human placental brush border membranes. Studies on the binding of transferrin to placental membrane vesicles and the identification of a placental brush border glycoprotein with high affinity for transferrin. *Journal of Biological Chemistry*, 254:12629-12635.
6. Loh TT, Higuchi DA, van Bockxmeer FM, Smith CH & Brown EB (1980) Transferrin receptors on the human placental microvillous membrane. *Journal of Clinical Investigation*, 65:1182-1191.
7. Vanderpuye OA, Kelley LK & Smith CH (1986) Transferrin receptors in the basal plasma membrane of the human placental syncytiotrophoblast. *Placenta*, 7:391-403.
8. Léger D, Campion B, Decottignies J-P, Montreuil J & Spik G (1989) Physiological significance of the marked increased branching of the glycans of human serotransferrin during pregnancy. *Biochemical Journal*, 257:231-238.
9. Booth AG, Olaniyan RO & Vanderpuye OA (1980) An improved method for the preparation of human placental syncytiotrophoblast microvilli. *Placenta*, 1:327-336.
10. Dicke JM, Verges D, Kelley LK & Smith CH (1993) Glycine uptake by microvillous and basal plasma membrane vesicles from term human placentae. *Placenta*, 14:85-92.
11. Kelley LK, Smith CH & King BF (1983) Isolation and partial characterization of the basal cell membrane of human placental trophoblast. *Biochimica et Biophysica Acta*, 734:91-98.
12. Markwell M-AK, Haas SM, Bieber LL & Tolbert NE (1978) A modification of the Lowry procedure to simplify protein determination in membrane and lipoprotein samples. *Analytical Biochemistry*, 87:206-210.

13. Schoot BM, Schoots AFM, De Pont JJHM, Schuurmans-Stekhoven, FMAH & Bonting SL (1977) Studies on $(\text{Na}^+ + \text{K}^+)$ activated ATPase. XLI. Effects of N-ethylmaleimide on overall and partial reactions. *Biochimica et Biophysica Acta*, 483:181-192.
14. Kato M & Kako J (1987) Orientation of vesicles isolated from baso-lateral membranes of renal cortex. *Molecular and Cellular Biochemistry*, 78:9-16.
15. Van Noort WL, de Jong G & van Eijk HG (1994) Purification of isotransferrins by Concanavalin A Sepharose chromatography and preparative isoelectric focusing. *European Journal of Clinical Chemistry and Clinical Biochemistry*, 32:885-892.
16. Van Eijk HG & van Noort WL (1992) The analysis of human serum transferrins with the Phast-System: quantitation of microheterogeneity. *Electrophoresis* 13:354-358.
17. Van Noort WL & van Eijk HG (1990) Quantification of monosaccharides occurring in glycoproteins at subnanomole levels using an automated LC analyzer. *LC-GC International*, 3/5:50-52.
18. Laurell CB (1966) Quantitative estimation of proteins by electrophoresis in agarose gel containing antibodies. *Analytical Biochemistry*, 15:45-52.
19. Berczi A & Faulk WP (1992) Iron-reducing activity of plasma membranes. *Biochemistry International*, 28:577-584.
20. Van Dijk JP, van der Zande FGM, Kroos MJ, Starreveld JS & van Eijk HG (1993) Number and affinity of transferrin-receptors at the placental microvillous plasma membrane of the guinea pig: influence of gestational age and degree of transferrin glycan chain complexity. *Journal of Developmental Physiology*, 19:221-226.
21. Armitage P & Berry G (1987) *Statistical Methods in Medical Research*. Oxford: Blackwell.
22. Van Dijk JP, van Noort WL, Kroos MJ, Starreveld JS & van Eijk HG (1991) Isotransferrins and pregnancy: a study in the guinea pig. *Clinica Chimica Acta*, 203:1-16.
23. Tsunoo H & Sussman HH (1983) Placental transferrin receptor. Evaluation of the presence of endogenous ligand on specific binding. *Journal of Biological Chemistry*, 258:4118-4122.
24. Galbraith RM, Werner P, Kantor RRS & Galbraith GMP (1981) Studies of the interaction between human transferrin and specific receptors on the trophoblast membrane. *Placenta (supplement 3)*:48-59.
25. Orberger G, Geyer R, Stirn S & Tauber R (1992) Structure of the N-linked oligosaccharides of the human transferrin receptor. *European Journal of Biochemistry*, 205:257-267.

26. Hunt RC, Riegler R & Davis AA (1989) Changes in glycosylation alter the affinity of the human transferrin receptor for its ligand. *Journal of Biological Chemistry*, 264:9643-9648.
27. Muller C & Shinitzky M (1979) Modulation of transferrin receptors in bone marrow cells by changes in lipid fluidity. *British Journal of Haematology*, 42:355-362.
28. Di Giulio A, D'Andrea G, Saletti MA, Impagnatiello A, D'Alessandro AM & Oratore A (1994) The binding of human serum transferrin to its specific receptor reconstituted into liposomes. *Cellular Signalling*, 6:83-90.
29. Van Dijk JP (1988) Review article: Regulatory aspects of placental iron transfer - a comparative study. *Placenta*, 9:215-226.
30. Lang I, Hartmann M, Blaschitz A, Dohr G, Skofitsch G & Desoye G (1993) Immunohistochemical evidence for the heterogeneity of maternal and fetal vascular endothelial cells in human full-term placenta. *Cell & Tissue Research*, 274:211-218.
31. Cerneus DP, Strous GJ & van der Ende A (1993) Bidirectional transcytosis determines the steady state distribution of the transferrin receptor at opposite plasma membrane domains of BeWo cells. *Journal of Cell Biology*, 122:1223-1230.

5

Accumulation and release of iron in polarly
cultured trophoblast cells

5.1 Introduction

Iron is an essential element for growth and development. The fetal demand for iron increases during pregnancy. At the end of pregnancy, an amount of 5 mg iron per day is transported across the human placenta. The major pathway for placental iron uptake is receptor-mediated endocytosis of maternal diferric transferrin (Tf) (1). Previous studies have shown that cultured trophoblast cells express Tf receptors (TfRs) (2) and take up diferric Tf by receptor-mediated endocytosis (3,4).

Trophoblast cells cultured on plastic dishes (cultured long enough to allow differentiation of the cells) were found to accumulate iron during incubation with diferric Tf (3,5). Since, *in vivo*, iron is transferred across the differentiated syncytiotrophoblast, accumulation was not expected. It could be argued that non-polarized cells do not express the mechanism for iron release and therefore accumulate iron. In the present study we looked at iron transfer in polarly cultured trophoblast cells, and found that they accumulated iron as well. It might be possible that, after release into the cytosol, part of the iron is actually transferred out of the cell, whereas the remaining part is accumulated in ferritin. In this case, the rate of iron uptake must exceed the rate of iron accumulation. We therefore assessed the initial rate of Tf mediated iron uptake and compared this rate with the rate of iron accumulation in the cells. We also determined whether intracellular iron was present as low molecular weight iron or incorporated in ferritin.

5.2 Materials and Methods

Tissue source

Normal human term placentae were obtained from the department of Obstetrics and Gynaecology, University Hospital Rotterdam/Dijkzigt, within 30 min after spontaneous delivery.

Isolation and culture of human term trophoblast cells

Trophoblast cells were isolated from human term placenta according to Kliman et al. (6), additionally purified by indirect immunopurification. Cells were cultured either on 35 mm Falcon culture dishes at a concentration of 1.5×10^6 cells in 2.5 ml culture medium, or on a permeable membrane (Millicell HA culture plate insert, 0.45 μ m pore size) at a concentration of 0.5×10^6 cells in 0.25 ml culture medium in humidified 5 % CO₂/95 % air at 37°C. After 48 h, the culture consisted of 17 % mononuclear cells, 21 % aggregates and 62 % syncytia (7). This procedure is described in detail in 2.2.

Labelling of transferrin with ⁵⁹Fe and ¹²⁵I

Apo Tf (in 0.1 M NaHCO₃ solution) was loaded with ⁵⁹Fe and labelled with ¹²⁵I as described in 2.5. The saturation of Tf with iron was checked by determination of the E₄₇₀ : E₂₈₀ ratio.

Uptake of ^{125}I - $^{59}\text{Fe}_2\text{Tf}$ by trophoblast cells cultured on a permeable filter

Uptake was measured as described in detail in 2.8.2. In short: Cells were cultured for 48 h, washed with PBS pH 7.4 and preincubated with M199 containing 0.5 mg/ml bovine serum albumin (BSA) and either 0.5 mg/ml ovalbumin (medium A) or 0.5 mg/ml human diferric Tf (medium B) as described by Gottlieb et al. (8). Cells were incubated at 37°C in medium A or B with 100 nM ^{125}I - $^{59}\text{Fe}_2\text{Tf}$ on one side of the cells. At fixed times, medium was removed, membrane filters were put on ice, rinsed with ice-cold PBS and subjected to two acid/neutral washes. Filters were counted for radioactivity in a Packard gamma counter. Cell-specific radioactivity was determined as the difference between the average radioactivities in the filters associated with incubations in either medium A or medium B.

Coupling of 6 nm gold to Tf

Human diferric Tf was bound to 6 nm gold particles (Aurion) according to the manufacturer's instructions, as described in 2.9.1.

Incubation of membrane-grown trophoblast cells with Au-Tf

After 48 h of culture on a permeable membrane, cells were washed with PBS pH 7.4, preincubated with DMEM containing 1 mg/ml BSA and 5 mg/ml ovalbumin and incubated with Au-Tf from either the microvillous (upper compartment) or the basal (lower compartment) side as described in 2.9.2. Endocytosis was stopped by placing the cells on ice. Filters were washed with icecold PBS pH 7.4 and fixed overnight at 4°C with standard fixation medium containing 1 % glutaraldehyde and 4 % formaldehyde. Samples were embedded in Epon and studied by electron microscopy (EM).

Immunolocalization of TfRs

TfRs were visualized by postfixation preembedding immuno electron microscopy (IEM) using a protocol described by Hansen, Sandvig & van Deurs (9). A detailed description of the procedure is found in 2.10. We used anti-TfR (mouse monoclonal antibody clone B3/25, Boehringer Mannheim) as primary and 10 nm gold-conjugated goat-anti-mouse IgG (Amersham, UK) as secondary antibody. At the concentrations used (10 $\mu\text{g/ml}$ anti-TfR and 1:20 (w/v) gold-conjugated anti-mouse-antibody), controls omitting the primary antibody were negative.

Electron microscopy

The methods for EM are described in 2.11. Samples were postfixated in a mixture of 1 % (w/v) OsO_4 and 1.5 % (w/v) $\text{K}_4\text{Fe}(\text{CN})_6$, dehydrated in graded ethanols and embedded in Epon. Ultrathin sections were collected on unfilmed 250 mesh copper grids, and studied in a Zeiss EM 209 transmission electron microscope. Contrast of the samples was enhanced by staining with uranyl acetate.

Uptake of ^{125}I - $^{59}\text{Fe}_2\text{Tf}$ by trophoblast cells cultured on plastic dishes

After 48 h of culture, cells were washed with PBS pH 7.4 and preincubated in M 199 containing 100 nM ^{125}I - $^{59}\text{Fe}_2\text{Tf}$ for 30 min at 4°C to saturate the surface TfRs. Without prior washing, the medium was replaced by prewarmed M 199 with 100 nM ^{125}I - $^{59}\text{Fe}_2\text{Tf}$ and cells were incubated at 37°C. After incubation, cells were rinsed with PBS pH 7.4 and exposed to two acid/neutral wash steps. Cells were lysed in Complete® protease inhibitor cocktail. Radioactivity and protein were determined in the lysates. The amount of radioactivity in cell lysates that were only incubated for 30 min at 4°C was taken as a measure for non-specific binding. See 2.8.1 for a more detailed description.

Separation of intracellular iron content

Cells were incubated for 4, 8 or 18 h at 37°C with 100 nM $^{59}\text{Fe}_2\text{Tf}$. After lysis, cell lysates were centrifuged at 1,000g for 10 min. The supernatant was loaded onto an ACA 34 Ultrogel (Pharmacia/LKB) column, equilibrated and eluted with 0.1 M Tris/0.5 M NaCl pH 8. Radioactivity in the separated fractions was counted in a Packard gamma counter.

Protein determination

Cellular protein was determined according to Markwell et al (10).

5.3 Results

Immunolocalization of TfRs

In order to investigate iron transfer in polarly cultured trophoblast cells we first determined whether TfRs are present at the cells and if they are able to endocytose diferric Tf. Previous experiments with microvillous and basal membrane vesicles from human term placenta showed that the number of TfRs on microvillous membranes was about six times higher than that on basal membranes (11). With postfixation preembedding IEM we visualized the distribution of surface TfRs on polarly cultured trophoblast cells. Cells were polarized with lots of microvilli on the upper cell membrane (Figure 5.1A), whereas the basal cell membrane, which was grown into the filter, lacked microvilli (Figure 5.1B). The number of TfRs on the microvillous side was considerably higher than the number of TfRs on the basal side of the cells (Figure 5.1), which agreed with the former results.

Uptake of Au-labelled Tf by membrane-grown trophoblast cells

We used diferric Au-Tf to visualize the uptake of Tf by polarly cultured trophoblast cells. As shown in Figure 5.2, Au-Tf was taken up from both the microvillous and the basal side of the cell. Au-Tf was present in coated pits, coated vesicles and tubular-like structures, possibly late endosomal structures. The number of coated pits and vesicles was higher at the microvillous compared to the basal side of the cell.

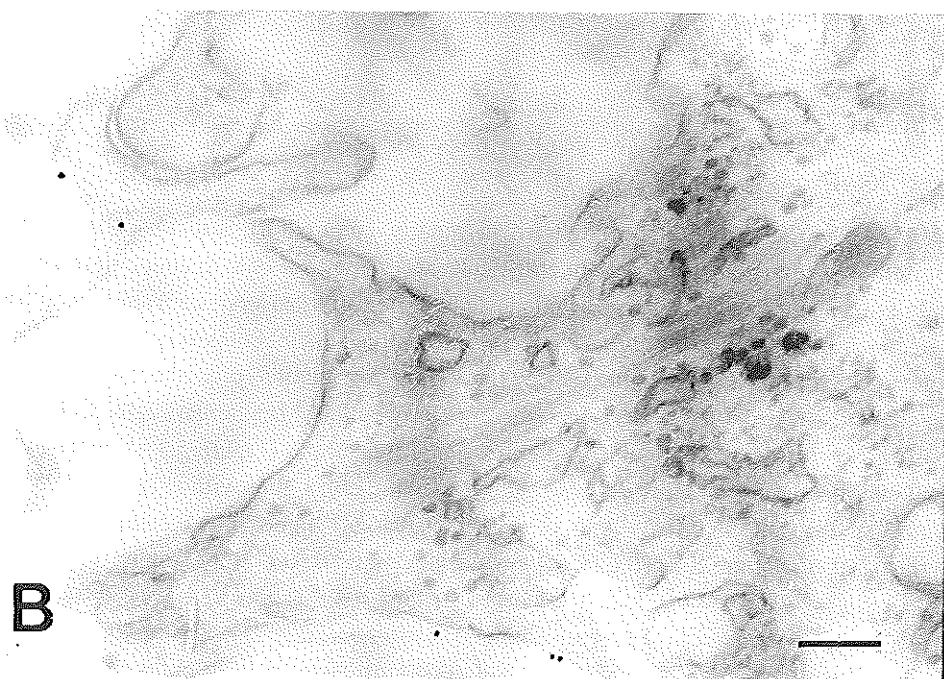
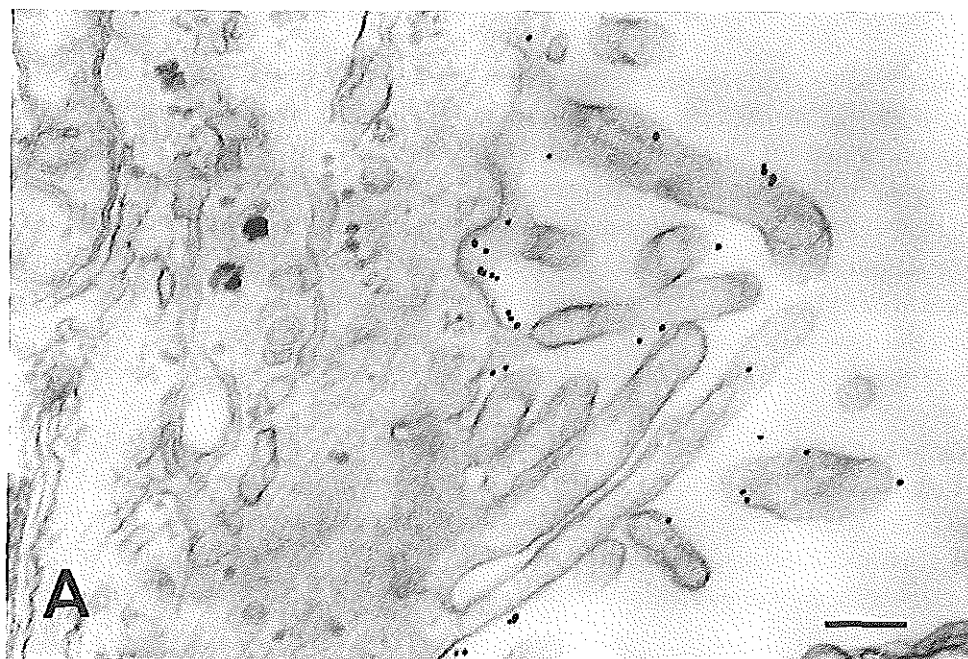


Figure 5.1

Distribution of surface TfRs on the microvillous (5.1A) and basal (5.1B) surface of polarly cultured trophoblast cells. TfRs were visualized by incubating fixed cells with monoclonal anti-TfR antibody and then with goat anti-mouse IgG coupled to 10 nm gold. (bar = 0.25 μ m)

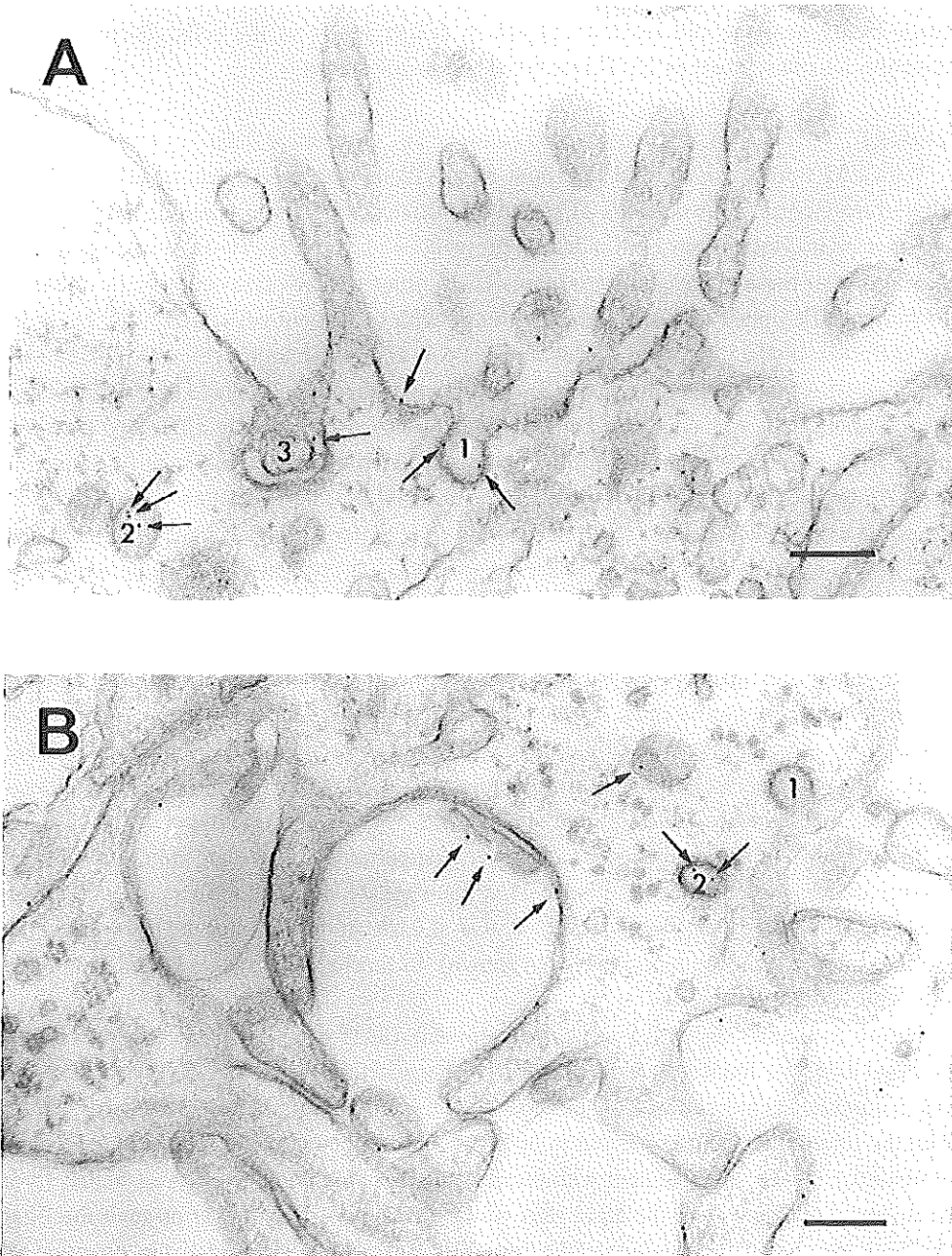


Figure 5.2

Electron micrographs showing the microvillous (5.2A) and basal (5.2B) surface of 48 h cultured trophoblast cells, which were incubated with 6 nm Au-conjugated Tf as described in the Methods section. Au-Tf (arrows) is shown near the cell surface, in coated pits (1), coated vesicles (2) and tubular-like structures (3). (bar = 0.25 μ m).

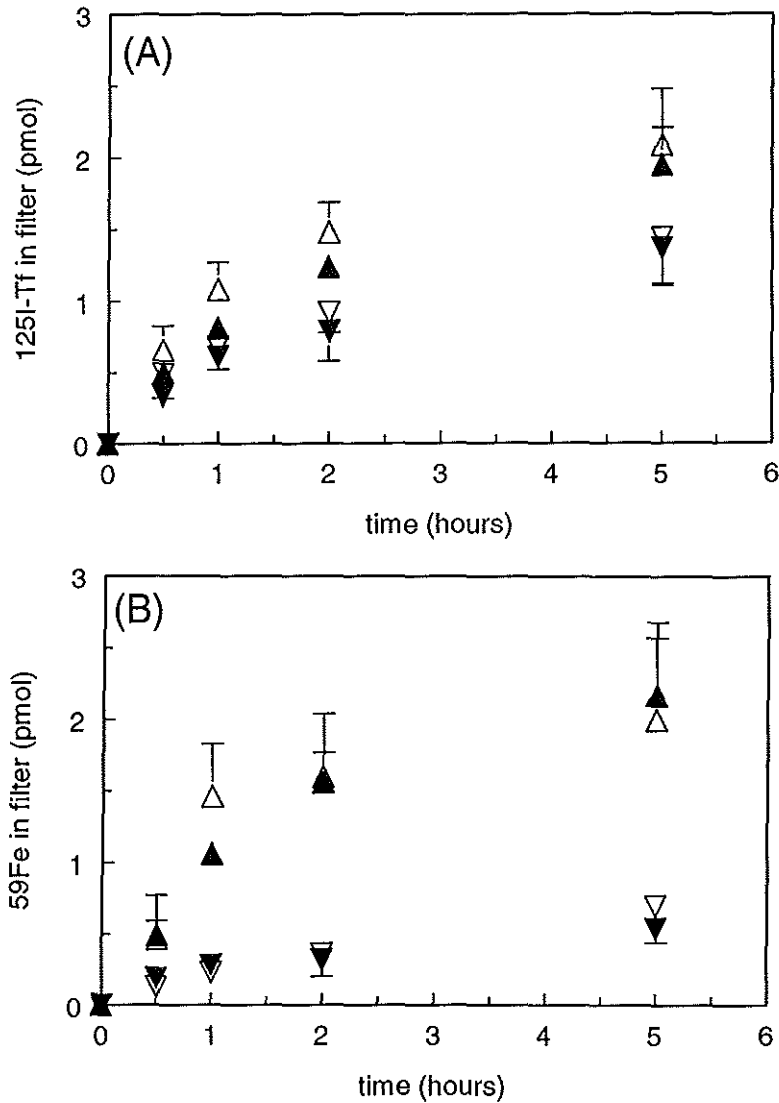
The processing of Au-Tf appeared limited to the cell periphery since Au-Tf was detected only near the cell surface and not in deeper layers of the cells. There was no indication for transcytosis of Tf. Tf was not found in lysosomes.

Uptake of ^{125}I - $^{59}\text{Fe}_2\text{Tf}$ by trophoblast cells cultured on a permeable filter

With EM studies we showed that both microvillous and basal membranes of polarly cultured trophoblast cells contains TfRs and that diferric Au-Tf was taken up by receptor-mediated endocytosis from both sides of the cell. With ^{125}I - $^{59}\text{Fe}_2\text{Tf}$ we investigated the contribution of these processes to iron transfer. In order to determine cell-specific instead of filter-specific uptake, we incubated the filters, with or without cells, with ^{125}I - $^{59}\text{Fe}_2\text{Tf}$ in two different media. Medium A contained BSA and ovalbumin, whereas medium B contained BSA and human diferric Tf (8). As shown in Figure 5.3, uptake of ^{125}I - $^{59}\text{Fe}_2\text{Tf}$ in filters without cells was equal for both media, allowing us to take the difference between uptake from medium A and uptake from medium B as a measure for cell-specific uptake in case of filters containing trophoblast cells. The amount of ^{125}I - $^{59}\text{Fe}_2\text{Tf}$ that was transported across the empty filter increased with incubation time. After 5 h of incubation with 100 nM ^{125}I - $^{59}\text{Fe}_2\text{Tf}$ in either the upper or lower compartment, a concentration of approximately 8 nM ^{125}I - $^{59}\text{Fe}_2\text{Tf}$ was reached at the opposite side. Since the $^{125}\text{I}/^{59}\text{Fe}$ ratio remained constant, we supposed that diferric Tf unchanged crossed the filter by diffusion.

Cell-specific uptake of ^{125}I - $^{59}\text{Fe}_2\text{Tf}$ was determined from both the microvillous and the basal side of 48 h cultured cells. As shown with empty filters there was some diffusion of radioactivity through the filter. Could the diffused radioactivity result in uptake of diferric Tf from the side opposite to that Tf was supplied to? To examine this question, membrane-grown cells were incubated for 60 min at 37°C with varying concentrations of ^{125}I - $^{59}\text{Fe}_2\text{Tf}$, up to 250 nM, in either the upper or lower compartment. For each concentration we determined the concentration of diferric Tf at the opposite side of the filters, as well as the cell-specific uptake. Our results revealed that uptake from the opposite side could be neglected in this concentration range (not shown). In further experiments we incubated the cells with 100 nM ^{125}I - $^{59}\text{Fe}_2\text{Tf}$.

Figure 5.4 shows the cell-specific uptake of diferric Tf from either the microvillous or the basal side. We found that intracellular ^{125}I -Tf reached a steady state level and that ^{59}Fe was accumulated, independent of the side ^{125}I - $^{59}\text{Fe}_2\text{Tf}$ was supplied to. Uptake of ^{125}I -Tf from the microvillous side appeared to be faster and reached a higher steady state level of intracellular ^{125}I -Tf. In agreement with these results, accumulation of ^{59}Fe was higher from the microvillous than from the basal side. Since diffusion of ^{125}I - $^{59}\text{Fe}_2\text{Tf}$ through the filter was high compared to cellular uptake, we were not able to determine the direction of transport out of the cell.

**Figure 5.3**

Uptake of $^{125}\text{I-Tf}(^{59}\text{Fe})_2$ in filters without cells. Filters were incubated for indicated times at 37°C with $100\text{ nM } ^{125}\text{I-Tf}(^{59}\text{Fe})_2$ in either medium A (▲, ▼) or medium B (△, ▽) from the upper (▲, △) or lower (▼, ▽) compartment. After acid/neutral washes, filters were counted for radioactivity. Figure 5.3A represents uptake of $^{125}\text{I-Tf}$ in the filter. Figure 5.3B represents uptake of ^{59}Fe . Results are mean values (\pm s.d.) from four experiments.

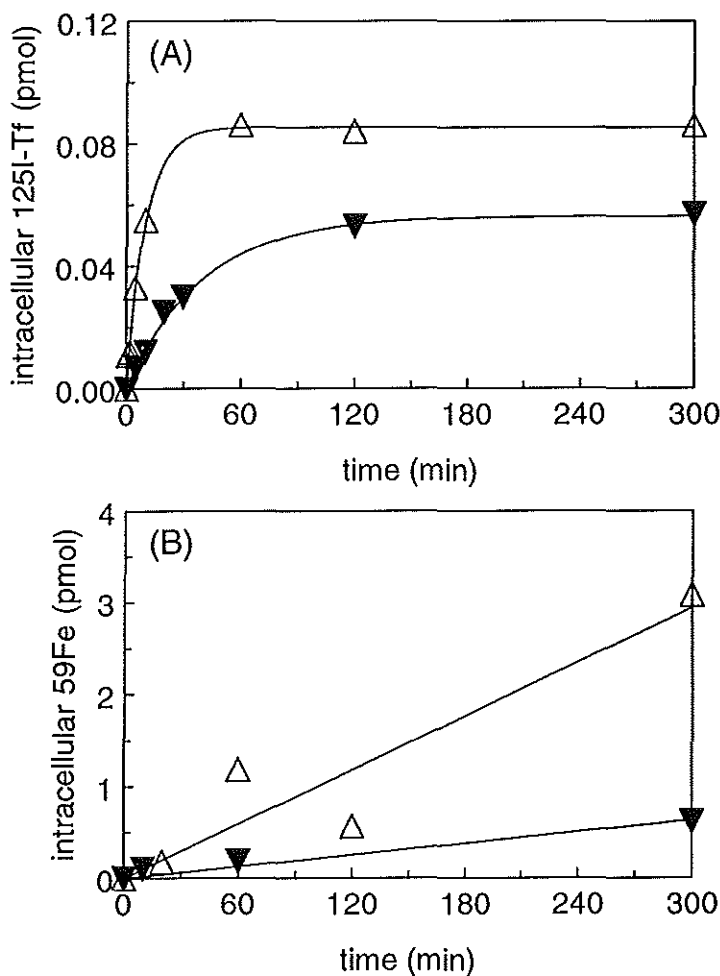


Figure 5.4

Uptake of $^{125}\text{I-Tf}(^{59}\text{Fe})_2$ by polarly cultured trophoblast cells. Cells were cultured for 48 h and incubated with 100 nM $^{125}\text{I-Tf}(^{59}\text{Fe})_2$ from either the upper (Δ) or lower (▼) compartment as described in the Methods section. Cell specific uptake was determined as the difference between uptake from medium A and uptake from medium B. Figure 5.4A represents uptake of $^{125}\text{I-Tf}$. Figure 5.4B represents uptake of ^{59}Fe . Results are from one representative experiment.

Uptake of ^{125}I - $^{59}\text{Fe}_2\text{Tf}$ by trophoblast cells on plastic dishes

Polarly as well as non-polarly cultured trophoblast cells accumulate iron. Can trophoblast cells transfer iron besides its accumulation? If so, the rate of iron uptake should exceed the rate of iron accumulation. In order to determine the initial rate of diferric Tf uptake, cells were preincubated with ^{125}I - $^{59}\text{Fe}_2\text{Tf}$ at 4°C to saturate the surface TfRs. Without prior washing, incubation at 37°C was started by the addition of prewarmed incubation medium, containing ^{125}I - $^{59}\text{Fe}_2\text{Tf}$. In this way, cells were able to immediately endocytose diferric Tf. Uptake of ^{125}I -Tf reached a steady state level (about 5 pmol/mg protein) after approximately 3 min, whereas ^{59}Fe was accumulated for at least 4 h (Figure 5.5).

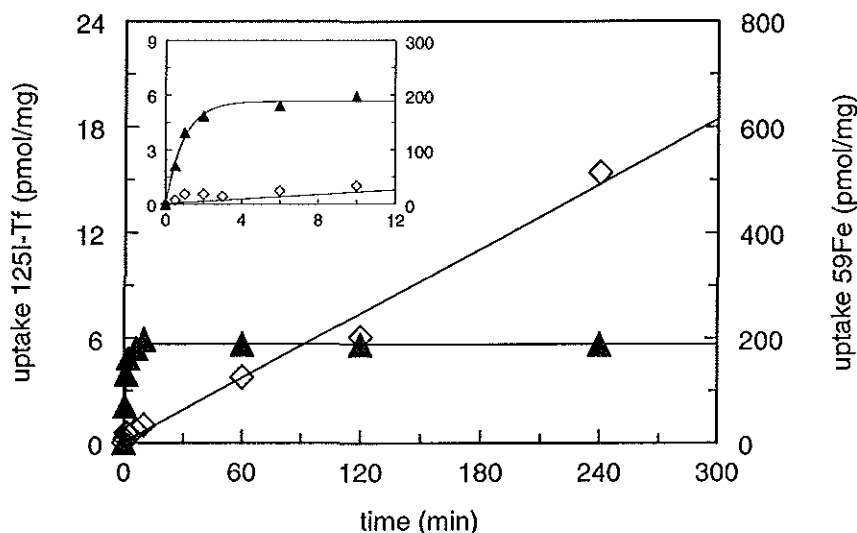


Figure 5.5

Uptake of ^{125}I -Tf(^{59}Fe)₂ by trophoblast cells cultured on plastic dishes. Cells were cultured for 48 h, preincubated with 100 nM ^{125}I -Tf(^{59}Fe)₂ at 4°C , washed with PBS and reincubated at 37°C with fresh medium containing 100 nM ^{125}I -Tf(^{59}Fe)₂. At the times shown, cells were placed on ice, rinsed with cold PBS and exposed to acid/neutral washes. Data are from one representative experiment. The inset shows uptake in the first minutes of incubation. The ^{125}I -Tf uptake reveals a one exponential curve fit [rate = steady state \times (1 - exp(-k \times t))] with steady state = 5.65 pmol/mg protein and k = 1.05 min⁻¹ for this experiment]. Initial uptake of ^{59}Fe is fast, followed by a slower linear uptake [rate = 1.516 + 2.044 \times t for this experiment] at least until four hours.

(\blacktriangle = ^{125}I , \diamond = ^{59}Fe)

The initial rate of ^{125}I -Tf uptake was determined for two independent experiments (respectively 5.9 and 2.6 pmol/mg protein/min). In the same experiments, we observed steady state rates of ^{59}Fe accumulation of respectively 2.1 and 1.1 pmol/mg protein/min. In order to determine whether intracellular iron was incorporated in ferritin or present as low molecular weight iron, we separated the intracellular iron pool by column chromatography. Table 5.1 shows that a small amount of iron was present as low molecular weight iron, the extent of which was relatively constant with time. The major part of intracellular iron was accumulated in ferritin, increasing with time.

Table 5.1

Intracellular iron pool after respectively 4, 8 and 18 h of incubation with 100 nM $^{59}\text{Fe}_2\text{Tf}$.

Incubation Time (h)	^{59}Fe in total lysate (pmol/mg cell protein)	^{59}Fe in ferritin (pmol/mg cell protein)	^{59}Fe as LMW iron (pmol/mg cell protein)
4	170	95	29
8	248	139	20
18	607	326	34

Cells were incubated with $^{59}\text{Fe}_2\text{Tf}$ for the indicated times. After lysis, cell lysates were counted for radioactivity, centrifuged and the supernatants were loaded on an ACA 34 Ultrogel column (see Materials and Methods). Over 96 % of radioactivity, loaded on the column, was recovered in the eluate. Radioactivity was determined in the separated fractions.

5.4 Discussion

The main process for placental iron uptake is receptor-mediated endocytosis of maternal diferric Tf (1). Previous studies showed that trophoblast cells in culture were able to take up diferric Tf by receptor-mediated endocytosis (3,4). Iron was accumulated in the cells, which was rather unexpected because differentiated syncytiotrophoblast cells should behave like a transfer epithelium with respect to iron. The syncytiotrophoblast is a polarized layer. It is possible that non-polarly cultured trophoblast cells lack the mechanism for iron transfer. We therefore investigated iron transfer in polarly cultured trophoblast cells.

With EM we showed that trophoblast cells cultured on a permeable membrane are polarized, with the basal membrane grown into the filter and the upper membrane containing lots of microvilli. With postfixation preembedding IEM we visualized the distribution of TFRs and observed a higher number of TFRs on the microvillous than on the basal cell membrane (Figure 5.1), corresponding to the results from studies with membrane vesicles (11). Diferric Au-Tf was taken up from both the microvillous and the basal side, probably by receptor-mediated endocytosis. In order to investigate iron transfer, the cells

were incubated with ^{125}I - $^{59}\text{Fe}_2\text{Tf}$. It was previously shown that polarly cultured BeWo cells took up iron from both sides of the cell (12). In the present study we showed endocytosis of diferric Tf from both the microvillous and the basal surface of polarly cultured trophoblast cells. Uptake of ^{125}I -Tf from the microvillous side was faster than from the basal side. Moreover, the steady state level of intracellular ^{125}I -Tf was higher in the case of uptake from the microvillous side. This agreed with the fact that iron is transferred from mother to fetus. However, as well as with non-polarly cultured trophoblast cells, iron was accumulated in polarly cultured trophoblast cells, independent of the side ^{125}I - $^{59}\text{Fe}_2\text{Tf}$ was supplied to. An explanation could be that part of the iron released from the endosomes into a labile iron pool is actually transferred out of the cell, whereas the remaining part is accumulated in ferritin. This means that the rate of iron uptake must exceed the rate of iron accumulation.

In order to estimate the initial rate of iron uptake we saturated all surface TfRs with ^{125}I - $^{59}\text{Fe}_2\text{Tf}$. To prevent dissociation of Tf from TfR, incubation was started by the addition of prewarmed medium containing ^{125}I - $^{59}\text{Fe}_2\text{Tf}$ without prior washing. In this way we could measure the initial rate of endocytosis with TfRs fully occupied with diferric Tf. The initial rates of ^{125}I -Tf uptake were 5.9 and 2.6 pmol/mg protein/min for two independent experiments. Because of the low specific activity we were not able to determine the initial rate of ^{59}Fe uptake. We assumed that the initial uptake rate of ^{59}Fe was equivalent to twice the initial uptake rate of ^{125}I -Tf (since one molecule of Tf can bind two atoms of iron). Taking this initial ^{59}Fe uptake rate as a measure for the rate of iron internalization during the entire incubation period, iron would be accumulated at a rate of respectively 11.8 and 5.2 pmol Fe/mg protein/min for the two independent experiments. We observed accumulation rates of respectively 2.1 and 1.1 pmol ^{59}Fe /mg protein/min at steady state conditions. These results suggested that about 80 % of internalized iron already was transported out of the cell. However, the rate of iron uptake was probably overestimated. In our experiments, the initial uptake rates were determined with fully occupied TfRs while it is predicted that at steady state only 25 % of the surface TfRs will be occupied with diferric Tf (Appendix in 5.5). The rate of endocytosis is given by $V_{\text{endo}} = k_2 \times [\text{TfFe}_2\text{-TfR}]_s$, with k_2 the rate constant for internalization of the surface $\text{TfFe}_2\text{-TfR}$ complex and $[\text{TfFe}_2\text{-TfR}]_s$ the concentration of surface TfRs occupied with diferric Tf. The rate of endocytosis at steady state will therefore be only 34 % of the initial rate of endocytosis. In our study we observed initial rates of endocytosis of 5.9 and 2.6 pmol/mg protein/min, which corresponded with initial iron uptake rates of 11.8 and 5.2 pmol/mg protein/min. Iron uptake in steady state conditions (34 % of the initial rate) can thus be estimated at 4.0 and 1.8 pmol/mg protein/min. The steady state rates for iron accumulation were 2.1 and 1.1 pmol/mg protein/min, respectively 53 and 61 % of the estimated uptake values. Therefore, about 47 and 39 % of internalized iron could be released from Tf into the cytosol and successively transported out of the cell. We further have to keep in mind that diferric Tf could be recycled without releasing all its iron into the cytosol. As shown in Table 5.1, iron was predominantly accumulated into ferritin and only a small part of ^{59}Fe was present as low

molecular weight (LMW) iron. The amount of LMW iron was relatively constant during incubation. We suggest that iron from this LMW iron pool might be transported out of the cell at a constant rate.

In summary, we found that TfRs were present on both the microvillous and the basal surface of cultured human term trophoblast cells and were able to endocytose diferric Tf. Iron was accumulated in the cells. Most of accumulated iron was incorporated in ferritin. The number of TfRs on the microvillous surface was higher than on the basal surface, resulting in higher rates of Tf endocytosis and iron accumulation on the microvillous side. The rate of ^{59}Fe accumulation at steady state was lower than the rate of ^{59}Fe uptake, as estimated from the initial uptake rate, suggesting that part of the iron released into the cytosol was transported out of the cell. Another explanation could be that not all iron was released from Tf during the endocytosis cycle.

5.5 Appendix

Ciechanover et al. (13) described the endocytic cycle of transferrin by a set of four differential equations:

1. $d[R] / dt = k_{-1}[R\text{-Tf.Fe}_2]_s - k_1[\text{Tf.Fe}_2][R]_s + k_0[R\text{-Tf}]_s$
2. $d[R\text{-Tf.Fe}_2]_s / dt = k_1[\text{Tf.Fe}_2][R]_s - (k_{-1} + k_2)[R\text{-Tf.Fe}_2]_s$
3. $d[R\text{-Tf}]_i / dt = k_2[R\text{-Tf.Fe}_2]_s - k_x[R\text{-Tf}]_i$
4. $d[R\text{-Tf}]_s / dt = k_x[R\text{-Tf}]_i - k_0[R\text{-Tf}]_s$

Tf.Fe ₂	: diferric Tf	s	: surface
R	: TfR	i	: intracellular
R-Tf	: apoTf-TfR complex		
R-Tf.Fe ₂	: diferric Tf-TfR complex		
k_1	: second order rate constant for binding of diferric Tf to surface TfRs.		
k_{-1}	: rate constant for dissociation of diferric Tf from surface TfRs.		
k_2	: rate constant for internalization of surface TfFe ₂ -TfR complex.		
k_x	: rate constant for dissociation of Fe and movement of apoTf-TfR complex to the cell surface.		
k_0	: rate constant for dissociation of apoTf from cell surface TfR.		

The second order rate constant k_1 can be modified to a pseudo first order rate constant by multiplication with the concentration of diferric Tf in the medium $[\text{Tf.Fe}_2]$ since this concentration stays constant during the incubation experiment. Thus $k = k_1[\text{Tf.Fe}_2] / \text{min}$.

Ciechanover et al. (13) found values of $k_1 = 3 \times 10^6$ l/mol/min, $k_{-1} = 0.1$ and $k_0 = 2.6 / \text{min}$. For k_2 and k_x we take respectively 0.18 /min and 0.19 /min as determined by

Starreveld et al. (4). The concentration of diferric Tf in our experiment was 100 nM, giving a value for k equal to $3 \times 10^6 \times 100 \times 10^{-9} = 0.3$ /min.

We solved the set of differential equations both analytically and by computer (Matlab: ode45 solver) for varying values of k , thus mimicking the response to changing Tf concentrations in the medium. Both methods gave the same results. Figure 5.6 shows the steady state values of $[R]_s$, $[R-Tf]_i$, $[R-Tf.Fe_2]_s$, and $[R-Tf]_s$ as a function of the concentration of Tf in the medium. The figure shows that at a diferric Tf concentration of 100 nM (the concentration used in our experiments) only 25% of the surface TfRs is occupied with diferric Tf. This leads to a strongly reduced rate of diferric Tf internalization when compared to the initial rate.

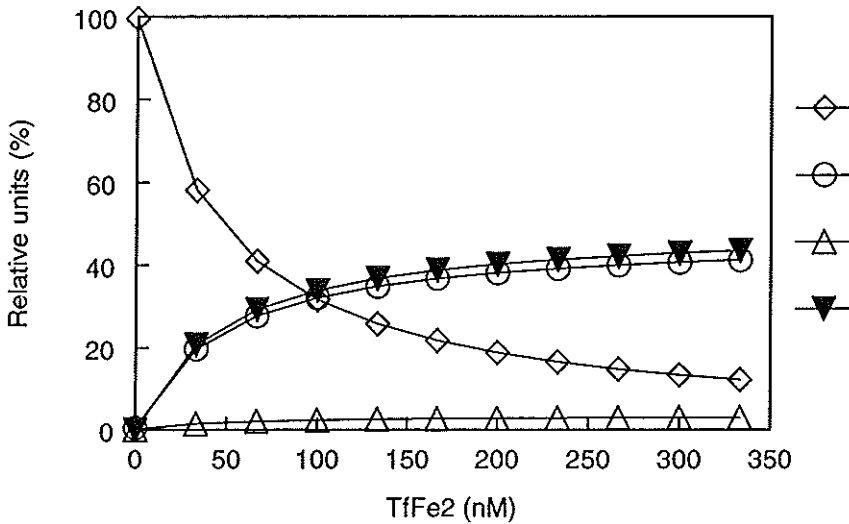


Figure 5.6

Steady state values of unoccupied surface TfRs (R_{surf}) (\diamond), intracellular TfRs containing apoTf ($RTf_{i.c.}$) (\circ), surface TfRs containing apoTf (RTf_{surf}) (\triangle) and surface TfRs containing diferric Tf ($RTfFe2_{surf}$) (\blacktriangledown), expressed in % of total receptor pool, as a function of the concentration of $TfFe_2$ in the medium. The values were determined by solving the differential equations as described in 5.5.

References

1. Van Dijk JP (1988) Review Article: regulatory aspects of placental iron transfer - a comparative study. *Placenta*, 9:215-226.
2. Bierings MB, Adriaansen HJ & van Dijk JP (1988) The appearance of transferrin receptors on cultured human cytotrophoblast and in vitro-formed syncytiotrophoblast. *Placenta*, 9:387-396.
3. Douglas GC & King BF (1990) Uptake and processing of ¹²⁵I-labelled transferrin and ⁵⁹Fe-labelled transferrin by isolated human trophoblast cells. *Placenta*, 11:41-57.
4. Starreveld JS, van Denderen J, Kroos MJ, van Eijk HG & van Dijk JP (1996) Effects of iron supplementation on iron uptake by differentiating cytotrophoblasts. *Reproduction Fertility and Development*, 8:417-422.
5. Starreveld JS, Kroos MJ, van Suijlen JDE, Verrijt CEH, van Eijk HG & van Dijk JP (1995) Ferritin in cultured human cytotrophoblasts: synthesis and subunit distribution. *Placenta*, 16:383-395.
6. Kliman HJ, Nestler JE, Sermasi E, Sanger JM & Strauss III JF (1986) Purification, characterization, and in vitro differentiation of cytotrophoblasts from human term placentae. *Endocrinology*, 118:1567-1582.
7. Starreveld JS, van Denderen J, Verrijt CEH, Kroos MJ & van Dijk JP (1998) Morphological differentiation of cytotrophoblasts cultured in medium 199 and keratinocyte growth medium. *European Journal of Obstetrics & Gynecology and Reproductive Biology*, 79:205-210.
8. Gottlieb TA, Ivanov IE, Adesnik M & Sabatini DD (1993) Actin microfilaments play a critical role in endocytosis at the apical but not the basolateral surface of polarized epithelial cells. *Journal of Cell Biology*, 120:695-710.
9. Hansen SH, Sandvig K & van Deurs B (1992) Internalization efficiency of the transferrin receptor. *Experimental Cell Research*, 199:19-28.
10. Markwell MAK, Haas SM, Bieber LL & Tolbert NE (1978) A modification of the Lowry procedure to simplify protein determination in membrane and lipoprotein samples. *Analytical Biochemistry*, 87:206-210.
11. Verrijt CEH, Kroos MJ, van Noort WL, van Eijk HG & van Dijk JP (1997) Binding of human isotransferrin variants to microvillous and basal membrane vesicles from human term placenta. *Placenta*, 18:71-77.
12. Cerneus DP & van der Ende A (1991) Apical and basolateral transferrin receptors in polarized BeWo cells recycle through separate endosomes. *Journal of Cell Biology*, 114:1149-1158.

13. Ciechanover A, Schwartz AL, Dautry-Varsat A & Loddish HF (1983) Kinetics of internalization and recycling of transferrin and the transferrin receptor in a human hepatoma cell line. *Journal of Biological Chemistry*, 258:9681-9689.

6

Transferrin in cultured human term trophoblast
cells

Synthesis and heterogeneity

Based on:

Verrijt CEH, Kroos MJ, Verhoeven AJM, van Eijk HG &
van Dijk JP

Molecular and Cellular Biochemistry (1997) 193:177-181

6.1 Introduction

The main site for Tf synthesis is the liver. Other -from a quantitative point of view- less important sites are the brain choroid plexus, Sertoli cells, brain glial-cells, fetal membranes and the placenta.

Tf mRNA was recently demonstrated in rat and mouse placental extracts (1,2). Moreover, rat placental cells in culture secrete Tf and secretion is stimulated by TNF (tumor necrosis factor) (3). It is not known which cell type is responsible for the synthesis and secretion of Tf.

The aim of this study is to investigate the ability of human trophoblast cells to synthesize Tf. We here report about de novo synthesis of Tf, the presence of Tf mRNA and the heterogeneity of Tf isolated from the cultured cells. Moreover we showed that the shift in isoelectric focusing pattern of trophoblast Tf was not due to a biochemical modification of serum Tf but originates from de novo synthesized Tf.

6.2 Materials and methods

Tissue source

Normal human term placentae were obtained from the department of Obstetrics and Gynaecology, University Hospital Rotterdam/Dijkzigt, within 30 min of spontaneous delivery.

Isolation and culture of trophoblast cells

Placentae were processed according to Kliman et al.(4) with slight modifications as described in detail in 2.2. For some experiments, the trophoblast cells, collected from the Percoll gradient, were additionally purified by indirect immunopurification using mouse anti-human CD9 as primary and goat anti-mouse IgG bound to Dynabeads as secondary antibody (5). About 1.5×10^6 cells were cultured in 35 mm diameter Falcon culture dishes (Greiner and Söhne, FRG) in 2.5 ml culture medium in humidified 5 % CO₂/95 % air at 37°C. After 48 h, the culture consisted of 17 % mononuclear cells, 21 % aggregates and 62 % syncytia (6).

Identification of Tf mRNA by RT-PCR

Trophoblast cells were isolated as described and additionally immunopurified. After 48 h of cell culture, RNA was isolated according to (7). RNA was reverse transcribed (RT) followed by polymerase chain reaction (PCR). Plasmid ptacRRTF3101 (8), containing Tf cDNA, was used as a positive control for PCR. As a negative control a RT-PCR was performed without the addition of reverse transcriptase. The forward primer (Tf1) was located at nucleotides 1458-1474 and the reverse primer (Tf2) at nucleotides 2101-2120 of human Tf mRNA (9). The size of the fragment amplified from Tf cDNA would be 663 bp. The PCR-

product from Tf cDNA was digested with either Pst I, yielding two fragments of 50 bp and 613 bp, or Hind III, which would yield fragments of 412 bp and 251 bp. The PCR- and the digestion products were examined on 1 % agarose gels with ethidium bromide staining. This procedure is described in detail in 2.12.1.

De novo synthesis of transferrin

De novo synthesis of Tf was determined as described in detail in 2.12.2.

Estimation of transferrin content

Tf content was determined in cell lysates and culture media as described in detail in 2.12.3.

Release of ^{125}I -Tf

Diferic serum Tf was labelled with ^{125}I as described in 2.6.2. After 24 h of culture, cells were incubated with diferic ^{125}I -Tf for 24 h. During this long incubation, cells were enabled to biochemically modify the serum Tf. Part of the cells were lysed in distilled water containing 1 mM PMSF. The other part was incubated with Medium 199 for 6 h, allowing release of Tf. Every h the medium was changed and collected. Both lysates and media were concentrated and the heterogeneity of Tf was determined.

Heterogeneity of trophoblast transferrin

The sialic acid-dependent heterogeneity of Tf was assessed by isoelectric focusing according to van Eijk & van Noort (10), as described in detail in 2.12.4. The isoelectric focusing patterns of serum Tf from non-pregnant women, maternal serum Tf at term pregnancy, umbilical cord serum Tf at term pregnancy and Tf from 48 h cultured trophoblast cells were compared. Moreover, the isoelectric focusing patterns of intracellular Tf and Tf released into the medium were compared to the pattern of ^{125}I -labelled serum Tf.

6.3 Results

To demonstrate Tf mRNA in immunopurified trophoblast cells cultured for 48 h, about 45 μg of total RNA was isolated from 5×10^7 plated cells. Figure 6.1 shows the result of one representative experiment (out of five independent experiments with three different trophoblast isolations). RT-PCR with Tf-specific primers Tf1 and Tf2 yielded a product with the expected length of 663 bp (lane 4, arrow). Both the water control and the RT-PCR without reverse transcriptase were negative (lanes 2 and 3). Digestion of the RT-PCR product with Pst I resulted in a product of 613 bp (lane 5) and digestion with Hind III yielded products of 412 bp and 251 bp (lane 6), as was expected.

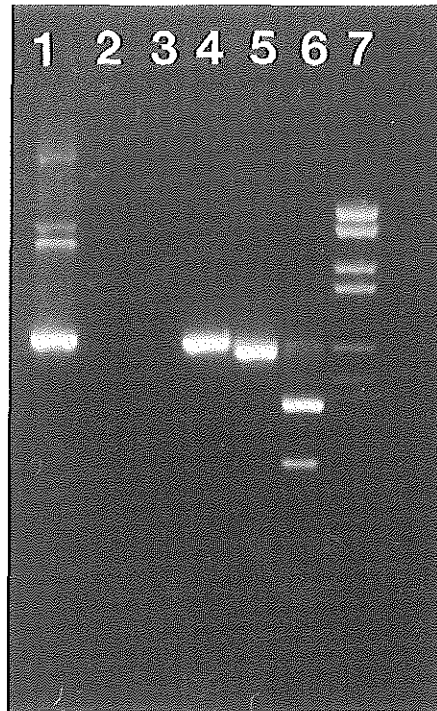


Figure 6.1

Identification of Tf mRNA in cultured trophoblast cells by means of RT-PCR.

After 48 h of culturing immunopurified human trophoblast cells, RNA was isolated, reverse transcribed, amplified by PCR and digested with either Pst I or Hind III. Lane 1: PCR of plasmid ptacRRTF3101 (8), with a length of 663 bp (clearest band, indicated with an arrow); lane 2: RT-PCR without reverse transcriptase; lane 3: negative control PCR with water; lane 4: RT-PCR of RNA from cultured trophoblast (663 bp, arrow); lane 5 and 6: respectively Pst I digest (613 bp) and Hind III digest of the RT-PCR product (412 bp and 251 bp); lane 7: DNA molecular weight marker VI (Boehringer).

Pulse-chase experiments showed that immunopurified cells translate Tf mRNA (Figure 6.2). The Tf locus at the Western blot was identified by a parallel run with ^{125}I -Tf. The radioactivity of the 80 kD band from the cell lysates originates from ^{35}S -labelled Tf because immunoprecipitation in the presence of excess non-labelled TfFe_2 suppressed the Tf-band, whereas the 96 kD band of the monomeric transferrin receptor (TfR) (our antibody also recognizes the Tf-TfR complex) was intensified (not shown). Table 6.1 makes clear that immunopurified cells, 48 h in culture, synthesize Tf and therefore translate Tf mRNA. This table also shows that the rate of Tf synthesis in non-immunopurified cells does not differ from that in immunopurified cells.

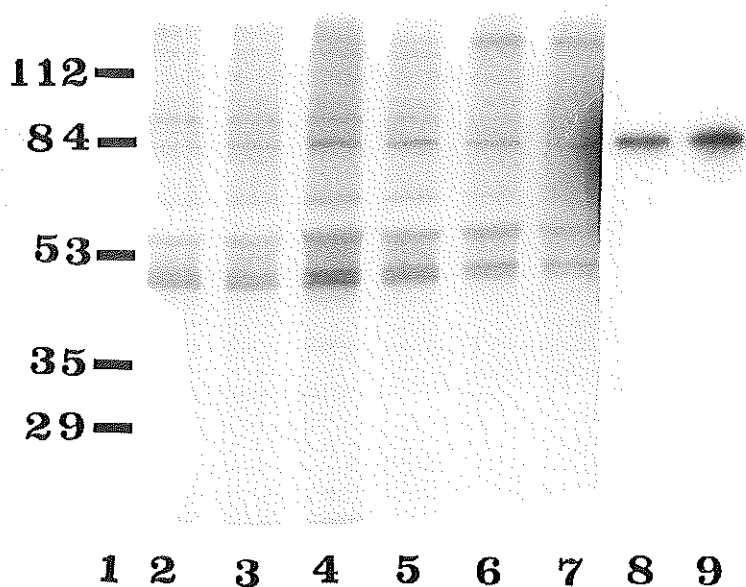


Figure 6.2

Table 6.1

De novo Tf synthesis by trophoblast cells 48 h in culture.

Treatment	Protein/dish (μg)	Total protein synthesis (dpm/mg) $\times 10^6$	Tf synthesis (AU \times mm/dpm) $\times 10^9$
Immunopurified	147.8 ± 18.4	56.3 ± 7.5	$17.3 \pm 4.7^*$
Non-immunopurified	164.3 ± 14.4	68.5 ± 9.4	$18.7 \pm 5.7^*$

*Tf synthesis was measured in 48 h cultured cells. After 24 h non-adherent cells were removed and culture was continued for another 24 h before de novo synthesis was assessed. After immunoprecipitation, electrophoresis and autoradiography (exposure time 14 d), the surfaces of the Tf bands (location identified by ^{125}I -Tf run simultaneously) were estimated by Laser densitometry. The peak surface is expressed in absorption units (AU) \times basis (mm). Total protein synthesis -assessed in triplicate- was expressed in dpm/mg cell protein. Peak surface/total protein synthesis (AU \times mm)/dpm was taken as a measure for de novo Tf synthesis. Six experiments; three with and three without immunopurification (for each experiment, lysates from three culture dishes were used). *: not statistically different (Student's t-test: $P > 0.1$)*

Figure 6.2.

De novo synthesis of Tf by trophoblast cells cultured for 3, 12 and 39 h.

Immunopurified cells were cultured for 3, 12 and 39 h. When cultured for 39 h, the medium was changed after 24 h. After three wash steps with cold PBS the cells were lysed (see Materials and Methods). Aliquots of each cell-lysate were precipitated with TCA and the radioactivity was assessed by liquid scintillation counting. For each sample, equal amounts of radioactivity were used for immunoprecipitation. After electrophoresis (10 % homogeneous SDS gels), the gels were dried and exposed to X-ray sensitive film. Lane 1: Molecular weight markers. Lane 2,3: culture time 3 h. Lane 4,5: culture time 12 h. Lane 6,7: culture time 39 h. Lane 8,9: ^{125}I -labelled TfFe₂.

Table 6.2

Transferrin content of culture medium and immunopurified cells. Influence of culture time.

Culture time (h)	Tot. cell protein (mg)	Tf cell lysate (μg)	Tf cell lysate (μg/mg)	Tf in medium (μg)
0	3.05±0.17	0.38±0.07	0.13±0.02*	-
3	1.80±0.16	0.34±0.03	0.19±0.02*	-
12	1.35±0.18	0.31±0.11	0.24±0.05*	0.17±0.06 **
48	1.19±0.05	0.34±0.07	0.28±0.06*	0.23±0.05 **

*Cells were cultured for the times indicated. The 12 and 48 h cultures were washed after respectively 3 and 24 h. The media of the last 9 h and 24 h of culture were collected. After indicated culture times, non-adherent cells were removed and the remaining cells were lysed. The lysates of ten culture dishes were used for each experiment. The media were centrifuged at 1,500 g for 5 min to remove intact cells. Media and cell lysates were filtered on 0.5 μm Micropore filters. After concentration (4°C), lysates and media were assessed for Tf by means of the Immuno-lite[®] procedure. Three experiments were performed each comprising 0, 3 and 12 h cultures. The 48 h cultures are data from three separate experiments. Mean ± s.d. *: ANOVA ($P < 0.01$) indicates that the cellular Tf content (μg/mg protein) increases during culture time. **: not significantly different (Student's t-test).*

Does Tf synthesis vary with cell culture time? We investigated Tf synthesis in immunopurified cells cultured for 3, 12 or 39 h. The results presented in Figure 6.2 show that Tf synthesis relative to total protein synthesis in 3 h cultures is less than in the 12 and 39 h cultures.

Does the cellular Tf content increase with culture time? Table 6.2 gives the Tf content of trophoblast cells cultured for 0, 3, 12 or 48 h, together with the Tf content of the culture medium. These data indeed show an increase of cellular Tf ($\mu\text{g}/\text{mg}$ cell protein) with culture time (ANOVA, $P < 0.01$). The amount of Tf recovered in the collected 12 and 48 h media did not differ significantly (Student's *t*-test).

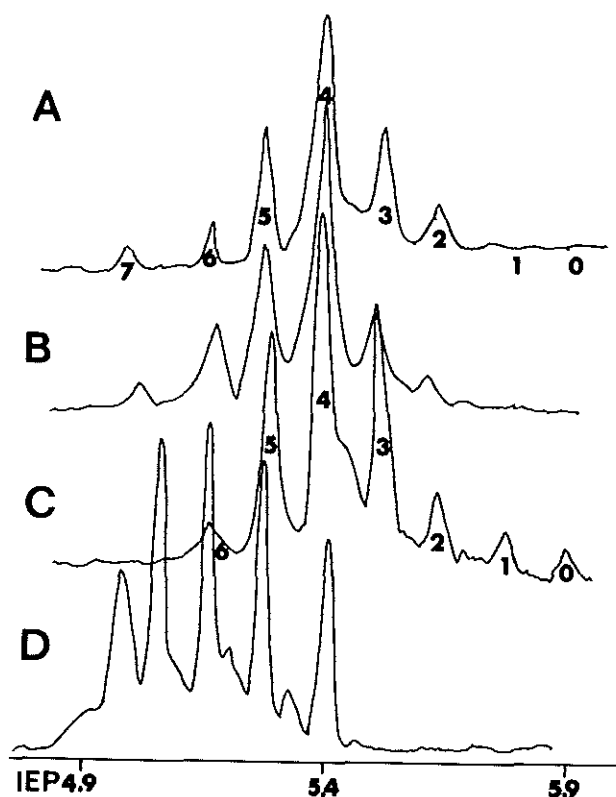


Figure 6.3. Densitometric scans of isoelectric focusing pattern of serum Tf from non-pregnant women (A), maternal serum Tf at term pregnancy (B), umbilical cord serum Tf at term pregnancy (C) and trophoblast Tf 48 h in culture (D). The given numbers characterize a specific isoTf fraction. The number 4 for instance, identifies the 4-sialo Tf fraction (4 sialic acids / Tf molecule). Result of one out of five independent but comparable experiments.

Figure 6.3 gives the isoelectric focusing pattern of serum Tf (non-pregnant women), maternal serum Tf (term pregnancy), fetal serum Tf and trophoblast Tf (cells 48 h in culture). Tf in cell lysates of isolated, non-cultured trophoblast cells had the same isoelectric focusing pattern as that of Tf from 48 h cultured cells (not shown). Compared to non-pregnant women,

the pattern of serum Tf from pregnant woman is displaced towards lower isoelectric points. The reverse is true for umbilical cord serum Tf. IsoTfs from cultured and non-cultured trophoblast cells are even more acidic than Tf from pregnant women at term. The shift in isoelectric focusing pattern of trophoblast Tf might be the result of biochemical modification of serum Tf. We therefore incubated trophoblast cells for 24 h with diferric ^{125}I -Tf, excubated for 6 h and compared the isoelectric focusing patterns of serum Tf, intracellular Tf and Tf released into the medium. No differences were observed in the X-ray patterns, whereas a shift to lower pH values was found in the protein isoelectric focusing patterns of intracellular Tf and Tf released into the medium (Figure 6.4). These results suggested that the shift in isoelectric focusing pattern was not due to biochemical modifications of serum Tf.

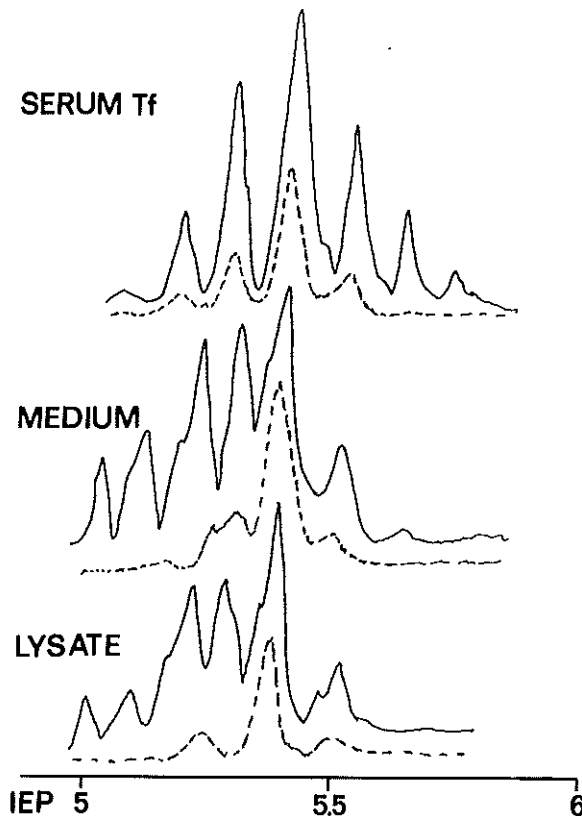


Figure 6.4

Densitometric scans of isoelectric focusing pattern of serum and trophoblast Tf. Cells were incubated with ^{125}I -labelled Tf for 24 h. Part of the cells was lysed, the other part was incubated in M199 allowing release of Tf (Materials and Methods). The ^{125}I -labelled serum Tf, collected media and lysates were subjected to isoelectric focusing. The Tf bands were visualized by autoradiography (dotted line) and silver staining (continuous line). Upper panel: ^{125}I -labelled serum Tf. Middle panel: Tf released into the medium. Lower panel: Tf in cell lysates prior to excubation.

6.4 Discussion

To assess the presence of Tf mRNA in trophoblast cells, we used RT-PCR techniques. RT-PCR, with Tf specific primers Tf1 and Tf2, of RNA from 48 h cultured trophoblast cells resulted in a product with the expected length of 663 bp (Figure 6.1, lane 4). Since genomic DNA would give higher molecular weight products (5 introns are present in genomic DNA in the region between primers Tf1 and Tf2) (9), the 663 bp product could only be the result of a PCR from cDNA. Digestion with either Pst I or Hind III further proved that the RT-PCR product was specifically arisen from Tf mRNA.

We previously showed that 48 h cultured immunopurified trophoblast cells are highly enriched with syncytiotrophoblast cells (6). All cell aggregates and syncytia produce hCG. Only 10 % of the single cell population (about 1 to 1.5 % of the total population) did not produce hCG and may represent non-trophoblast cells (6). Therefore, we can conclude that Tf mRNA is present in 48 h cultured human syncytiotrophoblast cells.

Our results also showed that Tf mRNA was translated by syncytiotrophoblast cells in culture (48 h). Immunopurification had no impact on Tf synthesis. This means that contaminating non-trophoblast cells did not contribute substantially to Tf synthesis.

Our observations are in conflict with those of Galbraith et al.(11). These authors could not demonstrate Tf synthesis in placental tissue cultures by radio-immunoelectrophoresis. An explanation could be that the tissue cultures were not sufficiently enriched with cyto- and syncytiotrophoblast cells and ^{14}C -lysine incorporation therefore did not reach the detection limit.

Tf synthesis is not an exclusive property of the differentiated syncytiotrophoblast cell. Immunopurified trophoblast cells cultured for 3 h already synthesize Tf. However, Tf synthesis, relative to total protein synthesis, was less in 3 h cultures compared to the 12 and 39 h cultures, suggesting that the state of cell differentiation might be a determinant factor.

Table 6.2 shows a decrease in total protein during culture, with similar amounts of Tf content. If we suppose that the loss of protein is caused by detachment of cells, we can compare the Tf content of the adherent cells relative to their protein content. Column four in Table 6.2 shows that the cellular Tf concentration ($\mu\text{g}/\text{mg}$ protein) increased during culture (ANOVA: $P < 0.01$). The data suggest that the amount of Tf recovered in the medium can be explained by cell release. The presence of a secretory component cannot be excluded yet.

The microheterogeneity pattern of Tf in the lysates of cultured trophoblast cells, as well as in the medium, was shifted to a lower range of isoelectric points compared to maternal and fetal serum Tf (Figure 6.3). This shift to lower pH values suggests that trophoblast Tf contains higher numbers of sialic acids per molecule, indicating a higher degree of complexity of their glycan chains (12). Since syncytiotrophoblast cells can take up iron-loaded serum Tf by receptor mediated endocytosis (13-15), part of the Tf detected in the cultured trophoblast cells could have originated from maternal or fetal serum. Because of both the method of cell

isolation (trypsin digestion will remove surface bound Tf) and the method of cell culture (medium replacements will deplete the intracellular receptor-bound Tf pool), this contribution will be negligible. Furthermore, we showed that endocytosed ^{125}I -labelled serum Tf was released unchanged from cultured trophoblast cells. The shift in isoelectric focusing pattern of trophoblast Tf was therefore not the result of biochemical modifications of serum Tf. Another source of Tf could be the 20 % FCS used in the culture medium. However, bovine Tf does not crossreact with anti-hTf (checked by radial immunodiffusion: results not shown), and therefore escapes detection in our Immuno-lite[®] assay. These results suggest that Tf detected in cultured trophoblast cells will be of trophoblast origin.

In summary, non-differentiated human term trophoblast cells as well as differentiated human term syncytiotrophoblast cells in culture synthesize Tf. Compared to both maternal and fetal serum Tf, term trophoblast Tf has a lower range of isoelectric points, indicating a higher decrease in complexity of the glycan chains. The isoTf pattern of intracellular Tf does not depend on the degree of trophoblast differentiation (culture time). The function of trophoblast Tf has yet to be elucidated.

References

1. Aldred AR, Dickson, PW, Marley, PD & Schreiber G (1987) Distribution of transferrin synthesis in brain and other tissues in the rat. *Journal of Biological Chemistry*, 262:5293-5297.
2. Yang F, Friedrichs WE, Buchanan JM, Herbert DC, Weaker FJ, Brock JH & Bowman BH (1990) Tissue specific expression of mouse transferrin during development and aging. *Mechanisms of Ageing and Development*, 56:1187-1197.
3. Boockfor FR, Harris SE, Barto JM & Bonner JM (1994) Placental cell release of transferrin: analysis by reverse hemolytic plaque assay. *Placenta*, 15:501-509.
4. Kliman HJ, Nestler JE, Sernasi E, Sanger JM & Strauss III JF (1986) Purification and in vitro differentiation of cytotrophoblasts from human term placentae. *Endocrinology*, 118:1567-1582.
5. Starreveld JS, Kroos MJ, Verrijt CEH, van Eijk HG & van Dijk JP (1995) Ferritin in Cultured Human Cytotrophoblasts: Synthesis and Subunit Distribution. *Placenta*, 16:383-395.
6. Starreveld JS, van Denderen J, Verrijt CEH, Kroos MJ & van Dijk JP (1998) Morphological differentiation of cytotrophoblasts cultured in Medium 199 and Keratinocyte growth medium. *European Journal of Obstetrics & Gynecology and Reproductive Biology* (in press).
7. Chomczynski P & Sacchi N (1987) Single-Step of RNA Isolation by Acid Guanidinium Thiocyanate-Phenol-Chloroform Extraction. *Analytical Biochemistry*, 162:156-159.
8. de Smit MH, Hoefkens P, de Jong G, van Duin J, van Knippenberg PH & van Eijk HG (1995) Optimized bacterial expression of nonglycosylated human transferrin and its half-molecules. *International Journal of Biochemistry and Cell Biology*, 27:839-850.
9. Yang F, Lum JB, McGill JR, Moore CM, Naylor SL, van Bragt PH, Baldwin WD & Bowman BH (1984) Human transferrin: cDNA characterization and chromosomal location. *Proceedings in National Academic Sciences of the USA*, 81:2752-2756.
10. van Eijk HG & van Noort WL (1992) The analysis of human transferrins with the PhastSystem: Quantitation of microheterogeneity. *Electrophoresis*, 13:354-358.
11. Galbraith GMP, Galbraith RM & Faulk WP (1980) Immunological studies of transferrin and transferrin receptor of human placental trophoblast. *Placenta*, 1:33-46.
12. de Jong G, van Dijk JP & van Eijk HG (1990) The Biology of Transferrin: A Critical Review. *Clinica Chimica Acta* 190:1- 46.

13. Eaton BM, Browne MJ & Contractor SF (1985) Transferrin mediated iron transport in the perfused isolated human placental lobule. *Contributions to Gynecology and Obstetrics*, 13:149-150.
14. Douglas GC & King BF (1990) Uptake and processing of ¹²⁵I labelled transferrin and ⁵⁹-Fe labelled transferrin by isolated human trophoblast cells. *Placenta*, 11:41-57.
15. Starreveld JS, van Denderen J, Kroos MJ, van Dijk JP & van Eijk HG (1996) The effect of iron supplementation on iron uptake by differentiating cytotrophoblasts. *Reproduction Fertility and Development*, 8:417-422.

7

Non-transferrin iron uptake by trophoblast cells
in culture

Significance of a NADH-dependent ferrireductase

Based on:

Verrijt CEH, Kroos MJ, Huijskes-Heins MIE, van Eijk HG &
van Dijk JP

Placenta (1998) in press

7.1 Introduction

A large amount of iron is transported across the placenta from mother to fetus during pregnancy. The major pathway for placental iron uptake is receptor-mediated endocytosis of diferric transferrin. The subsequent transfer of iron through the cytosol and across the basal plasma membrane is still unclear (1,2).

Besides its role in cellular iron uptake, Tf reduces the amount of free iron in plasma, and therefore reduces the possibility of iron-catalyzed formation of free radicals that may damage DNA, proteins and membrane lipids. Although receptor-mediated endocytosis of diferric Tf is the major pathway for cellular iron delivery, mechanisms for Tf-independent iron transport has often been described in recent years (review: 3). Tf-independent iron transport may be a supplementary pathway involved in maintaining low concentrations of free iron in plasma. An essential step in Tf-independent iron uptake seems to be the reduction of ferric iron to the ferrous state. The coupling of iron reduction and uptake has recently been described in cultured cells: HeLa (4), K562 (5), HepG2 (6), Caco-2 (7). The ferrireductase involved in Tf-independent iron uptake is probably a transmembrane NADH-ferricyanide oxidoreductase, which has previously been demonstrated in several cell types (8-12). After reduction, ferrous iron is transported across the plasma membrane.

Starrevelde et al. (13) have recently shown that trophoblast cells in culture are able to take up iron in the form of ferric ammonium citrate. The mechanism for this iron uptake has not been described however. In the present study we investigated the mechanism of non-Tf iron uptake in human term placenta. We measured the reduction of ferricyanide (Fe(III)CN) by cultured trophoblast cells and investigated cellular uptake of ^{59}Fe from $\text{Fe(III)nitilotriacetate}$ (Fe(III)NTA) and Fe-ascorbate , which is supposed to represent an equilibrium between Fe(II) and Fe(III) (14). Furthermore, we investigated the reduction of Fe(III)CN at microvillous membrane vesicles (MMV) and basal membrane vesicles (BMV), isolated from the same human term placenta. Since Tf-receptor mediated uptake is the obvious pathway for placental iron uptake, we suggest a role for Tf-independent iron transport in the transfer of iron across the basal membrane to the fetal side.

7.2 Materials and Methods

Tissue source

Normal human term placentae were obtained from the department of Obstetrics and Gynaecology University Hospital Rotterdam/Dijkzigt, within 30 min of spontaneous delivery.

Isotopes

$^{59}\text{FeCl}_3$ was obtained from DuPont, NEN Life Science Products (Boston, MA).

Isolation and culture of human term trophoblast cells

Human term placentae were processed according to Kliman et al. (15) with slight modifications (13). The isolated cell population was additionally purified by indirect immunopurification using mouse anti-human CD9 as primary and goat anti-mouse IgG bound to Dynabeads as secondary antibody (13). From 50 g (wet weight) placental villous tissue we obtained approximately 40×10^6 predominantly mononuclear cells. The viability was between 90 and 95 % as revealed by trypan blue exclusion. Immunolabelling studies using mouse-anti-vimentin, mouse-anti-cytokeratin (both from ICN immunobiologicals) and FITC-labelled rabbit anti-mouse IgG (DAKO, Denmark) demonstrated that over 96 % of the final cell population was of trophoblast origin. About 1.5×10^6 cells were cultured in 35 mm Falcon culture dishes (Greiner and Sohne, Germany) in 2.5 ml culture medium at 37°C in humidified 5 % CO_2 /95 % air. After 24 h, the cells were washed with phosphate buffered saline (PBS) and the medium was refreshed. After 48 h, the culture consisted of 17 % mononuclear cells, 21 % aggregates and 62 % syncytia (16). This procedure is described in detail in 2.2.

Isolation and characterization of membrane vesicles

Both MMV and BMV were isolated from the same human term placenta as described in 2.3.1. MMV were isolated according to the method of Booth, Olaniyan and Vanderpuye (17), modified by Dicke et al. (18). BMV were isolated according to a modification (18) of the method of Kelley, Smith and King (19). Vesicles were finally resuspended in PBS pH 7.4, unless mentioned otherwise. Membrane protein was determined by a modification (20) of the Lowry method (21). We previously showed (22) that, relative to tissue homogenate, MMV were enriched 19-fold in alkaline phosphatase, a microvillous membrane marker, and BMV were enriched 28-fold in dihydroalprenolol binding, a marker for the basal plasma membrane. Contamination of lysosomes, endoplasmic reticulum and mitochondria was low. MMV were found to be 88 % either right side out or unsealed and 12 % to be inside out. BMV showed 28 % of the vesicles to be right-side-out, 60 % unsealed and 12 % inside-out (22). A detailed characterization of our membrane preparations is shown in Chapter 3.

Ferrireductase assays

Fe(III)CN reduction was determined by following the decrease in absorbance at 420 minus 500 nm with a Cary 1E spectrophotometer (extinction coefficient: 1 /mM/cm), as described in detail in 2.14.

Cells. Cells were incubated in reaction mixture containing Fe(III)CN at 37°C. The reaction was stopped after fixed times by cooling the cells on ice. The absorbance at 420 minus 500 nm was measured in the medium and compared to a control without cells.

Vesicles. Either 10 µl BMV (2.5 µg/µl) or 10 µl MMV (5.0 µg/µl) was added to 990 µl reaction mixture. The decrease in absorbance at 420 minus 500 nm was directly measured at 37°C. NADH oxidation was followed at 340 minus 430 nm (extinction coefficient: 6.22 /mM/cm). Kinetic parameters were determined using the Michaelis-Menten plot from an Enzyfit curve-fitting program.

Stock solutions of $^{59}\text{Fe(III)NTA}$ and $^{59}\text{Fe-ascorbate}$

The stock-solutions were freshly prepared for each experiment as described in 2.13.1.

Uptake of non-Tf iron by trophoblast cells

This procedure is described in detail in 2.13.2. In short: Cells were preincubated in serum-free M199 and incubated in uptake medium with either $^{59}\text{Fe(III)NTA}$ or $^{59}\text{Fe-ascorbate}$ for specified times at 37°C. Cells were cooled on ice, washed and lysed. Radioactivity in the lysate was determined in a Packard gamma counter. Protein was determined according to Markwell et al. (20).

7.3 Results

Reduction of Fe(III)CN by trophoblast cells

Trophoblast cells (48 h in culture) were able to reduce Fe(III)CN. Cells were incubated with 100 µM Fe(III)CN in reaction medium at 37°C. After 1 h the decrease in absorbance at 420 minus 500 nm was measured in the medium (see Materials and Methods). The cells reduced Fe(III)CN at a rate of 226.8 ± 84.6 nmol/h/mg protein ($n=11$). As a control, we measured Fe(III)CN reduction in the culture medium to test whether detached cells or some secreted products of intact (or damaged) cells were responsible for the reductase activity. However, no reductase activity was detected in the culture medium. To determine the effect of superoxide anion on the Fe(III) reduction rate, we measured the 1 h reduction in the presence of 20 µg/ml superoxide dismutase (SOD). This resulted in a reduction rate of 186.1 ± 109.5 nmol/h/mg protein ($n=11$), which was not significantly different from the control rate.

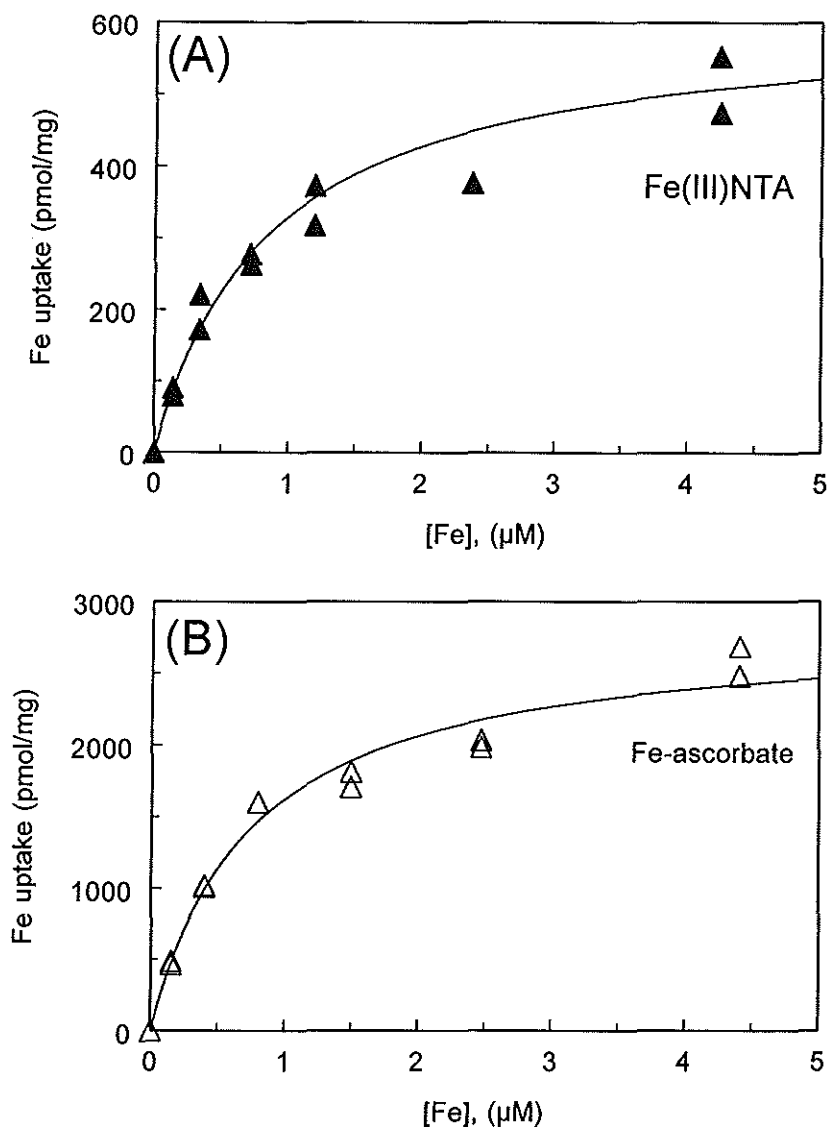


Figure 7.1

Uptake of ^{59}Fe from (A) Fe(III)NTA or (B) Fe-ascorbate . Cells were incubated with increasing concentrations of Fe for 5 min at 37°C . After incubation cells were washed, lysed and radioactivity was measured in the lysates. Uptake was concentration dependent and expressed as pmol/mg protein/5 min. Data are from one representative experiment. The curves are Michaelis-Menten fits: $(609.1 \cdot [\text{Fe}]) / (0.846 + [\text{Fe}])$ for Fe(III)NTA and $(2824.5 \cdot [\text{Fe}]) / (0.736 + [\text{Fe}])$ for Fe-ascorbate .

Uptake of non-Tf iron by cultured trophoblast cells

Starreveld et al. (13) showed that trophoblast cells were able to take up non-Tf iron. In the present study we measured uptake of ^{59}Fe from Fe(III)NTA and Fe-ascorbate by 48 h cultured trophoblast cells. Uptake of ^{59}Fe from both Fe(III)NTA and Fe-ascorbate was time-dependent and linear for the first 10 min at concentrations used in kinetic analysis (results not shown). To determine uptake kinetics of ^{59}Fe from Fe(III)NTA or Fe-ascorbate, trophoblast cells were incubated with increasing iron concentrations for 5 min at 37°C (Figure 7.1). It revealed saturation kinetics with a K_M of $0.96 \pm 0.65 \mu\text{M}$ ($n=5$) and a V_{\max} of $366 \pm 269 \text{ pmol/mg protein/5 min}$ ($n=5$) for $^{59}\text{Fe(III)NTA}$, and a K_M of $1.3 \pm 0.4 \mu\text{M}$ ($n=5$) and a V_{\max} of $4043 \pm 1955 \text{ pmol/mg protein/5 min}$ ($n=5$) for $^{59}\text{Fe-ascorbate}$. ACA 34 column chromatography of the lysates revealed that more than 80 % of the radioactivity was present in a soluble fraction, suggesting that uptake rather than binding was measured. Moreover, the ^{59}Fe was not incorporated into ferritin, but present as low molecular weight iron. Since uptake of ^{59}Fe from Fe-ascorbate was approximately 10 times higher than that from Fe(III)NTA, and we showed that our cells were able to reduce Fe(III)CN, we suggest that non-Tf iron transport might involve ferrireductase activity. To further examine this hypothesis we measured iron uptake in the presence or absence of the cell-impermeable Fe(III)CN, or the Fe(II)chelators bathophenanthroline disulphonic acid (BPS) or ferrozine (FZ).

Table 7.1

Effects of Fe(III)chelator DFO, Fe(II)chelators FZ and BPS, and of Fe(III)CN on iron uptake from Fe(III)NTA and Fe-ascorbate by trophoblast cells in culture.

	uptake (%)	
	$^{59}\text{Fe(III)NTA}$	$^{59}\text{Fe-ascorbate}$
Control	100	100
+ Fe(III)CN (0.1 mM)	61.5 ± 17.3 ($n=4$)	62.9 ± 6.4 ($n=3$)
+ FZ (1 mM)	61.6 ± 15.6 ($n=5$)	1.7 ± 1.0 ($n=3$)
+ BPS (1 mM)	148.6 ± 23.0 ($n=3$)	3.6 ± 0.8 ($n=3$)
+ DFO (1 mM)	20.6 ± 5.4 ($n=3$)	1.0 ± 0.7 ($n=3$)

Uptake of iron from $^{59}\text{Fe(III)NTA}$ or $^{59}\text{Fe-ascorbate}$ was measured for 5 min at 37°C as described in Materials and Methods. The control uptake of $^{59}\text{Fe(III)NTA}$ was $128 \pm 45 \text{ pmol/mg protein/5 min}$ ($n=5$) and for $^{59}\text{Fe-ascorbate}$ the control uptake corresponded with $2116 \pm 45 \text{ pmol/mg protein/5 min}$ ($n=5$). Data are presented as mean \pm s.d.

Table 7.1 shows that ^{59}Fe uptake from both Fe(III)NTA and Fe-ascorbate was inhibited by FZ. Since FZ only chelates Fe(II) (FZ was able to chelate Fe in the presence of ascorbate but not from Fe(III)NTA), we suggest that Fe from Fe(III)NTA was reduced before uptake. BPS inhibited ^{59}Fe uptake from Fe-ascorbate , however, it stimulated uptake from Fe(III)NTA . Fe(III)CN not only inhibited uptake of ^{59}Fe from Fe(III)NTA but also from Fe-ascorbate , suggesting tight coupling of reduction and transport. Superoxide dismutase (SOD) had a negligible effect on the uptake of $^{59}\text{Fe(III)NTA}$ in the presence or absence of either Fe(III)CN or FZ (results not shown), suggesting that superoxide anion did not play a role in reduction and uptake of Fe(III) by trophoblast cells.

Table 7.2

Requirements for reduction of Fe(III)CN by BMV and MMV.

vesicles	Fe(III)CN	NADH	Reduction Fe(III)CN (nmol/min/mg)	oxidation NADH (nmol/min/mg)
BMV	+	+	1667 ± 192 (n=10)	744 ± 49 (n=3)
MMV	+	+	496 ± 91 (n=10)	277 ± 24 (n=3)
BMV	+	—	36 ± 15 (n=5)	—
MMV	+	—	27 ± 8 (n=4)	—
BMV	—	+	8 ± 3 (n=4)	—
MMV	—	+	12 ± 5 (n=4)	—
—	+	+	2.5 ± 0.4 (n=5)*	—

Reduction of Fe(III)CN was directly measured by following the extinction at 420 minus 500 nm, in the presence of $200 \mu\text{M}$ Fe(III)CN , $100 \mu\text{M}$ NADH and either $25 \mu\text{g}$ of BMV or $50 \mu\text{g}$ of MMV. Oxidation of NADH was measured at 340 minus 430 nm. Oxidation of NADH was negligible in the absence of either Fe(III)CN , NADH or vesicles. Data are presented as mean \pm s.d.

** nmol/min*

Reduction of Fe(III)CN by BMV and MMV

We showed that trophoblast cells in culture were able to reduce Fe(III)CN and to take up ^{59}Fe from both Fe(III)NTA and Fe-ascorbate . To determine the site of iron reduction and subsequent transport, we investigated the possibility of iron reduction by BMV and MMV. Both BMV and MMV reduced Fe(III)CN in the presence of NADH. Reduction of Fe(III)CN in the presence of NADPH was negligible. Table 7.2 shows that Fe(III)CN could not be reduced in the absence of either NADH or the vesicles. Rotenone (inhibitor of mitochondrial reductase activity; $5\mu\text{M}$), dicoumarol (inhibits reductase activity from

microsomes; 20 $\mu\text{g/ml}$) and SOD (20 $\mu\text{g/ml}$) had no effect on the NADH-dependent reduction of Fe(III)CN (results not shown). NADH was oxidized in the presence of Fe(III)CN, NADH and vesicles and the ratio of Fe(III)CN reduction and NADH oxidation was 2.2:1 for BMV and 1.8:1 for MMV. Reduction of Fe(III)CN was dependent on the concentration of NADH (Figure 7.2) and Fe(III)CN (Figure 7.3). The kinetic parameters, derived from Michaelis-Menten plots, are listed in Table 7.3.

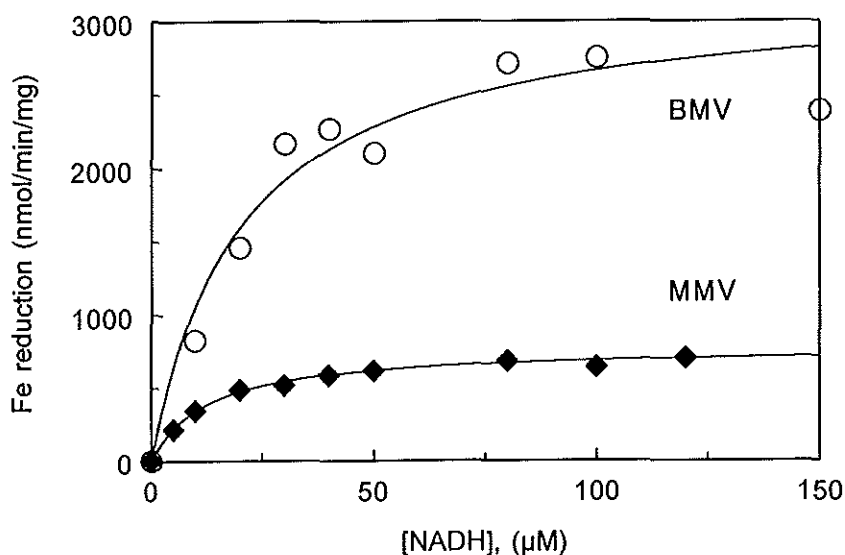


Figure 7.2

*NADH dependency of Fe(III)CN reduction by membrane vesicles. Reduction was measured in the presence of 150 μM Fe(III)CN, either 25 μg of BMV or 50 μg of MMV and increasing concentrations of NADH in a total volume of 1 ml. Kinetic parameters were determined using the Michaelis-Menten plot from the Enzyfit curve-fitting program. Shown are data from one representative experiment. The curves are Michaelis-Menten fits: $(3201.1 * [\text{Fe}]) / (20.08 + [\text{Fe}])$ for BMV and $(777.6 * [\text{Fe}]) / (12.58 + [\text{Fe}])$ for MMV.*

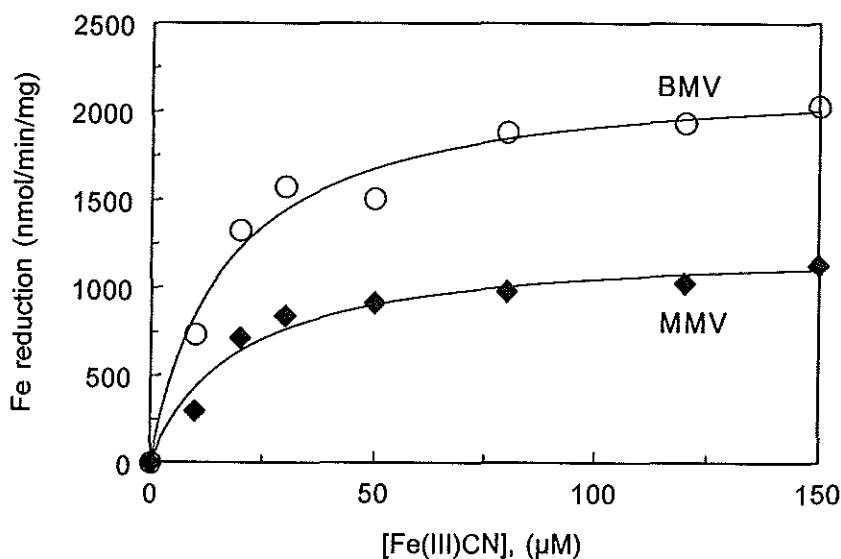


Figure 7.3

Effect of Fe(III)CN concentration on the rate of NADH-dependent Fe(III)CN reduction by membrane vesicles. Reduction of Fe(III)CN was measured in the presence of 150 μM NADH, either 25 μg of BMV or 50 μg of MMV, and increasing concentrations of Fe(III)CN in a total volume of 1 ml. Kinetic parameters were determined using the Michaelis-Menten plot from the Enzyfit curve-fitting program. Data are from one representative experiment. The curves are Michaelis-Menten fits: $(2216.9[Fe])/(16.16+[Fe])$ for BMV and $(1244.3*[Fe])/(18.98+[Fe])$ for MMV.*

Table 7.3

Kinetic parameters of Fe(III)CN reduction by BMV and MMV.

	NADH dependence		Fe(III)CN dependence	
	K_M (μM)	V_{max} (nmol/min/mg)	K_M (μM)	V_{max} (nmol/min/mg)
BMV	21.7 ± 5.5	2766 ± 693 *	22.5 ± 4.8	2781 ± 677 *
MMV	16.6 ± 5.4	1112 ± 351	21.2 ± 10.1	1135 ± 513

Data are derived from Michaelis-Menten plots (Figures 7.2 and 7.3) and presented as mean \pm s.d. from five experiments with five different membrane preparations.

** $P < 0.05$ versus MMV (unpaired two-tailed Student's *t*-test)*

7.4 Discussion

The major pathway for cellular iron uptake is receptor-mediated endocytosis of diferric Tf. Models other than receptor-mediated endocytosis have recently been described. Sun et al. (10) have identified a NADH diferric Tf reductase in liver plasma membranes, which may be involved in the transfer of iron across the plasma membrane or endocytic vesicles. From the reduction potentials of Tf-bound iron and cytosolic NADH, NADH-dependent reduction of Tf-bound Fe(III) seems not feasible. With respect to this point Thorstensen and Romslo (23) have suggested that diferric Tf may bind to receptors in close proximity to NADH-ferricyanide reductase. Through proton and electron fluxes the Tf-iron bond may be destabilized enabling the reduction of Fe(III). NADH-ferricyanide reductase may be involved in Tf-independent iron uptake (3 for a review). Klausner and Dancis (24) characterized a mechanism for Tf-independent iron uptake in *Saccharomyces cerevisiae*. It starts with the reduction of Fe(III) to Fe(II) by externally directed reductases Fre1p and Fre2p. This reduction is mediated by the oxidation of intracellular compounds. Ferrous iron is then transported across the membrane. Similarly, in higher eukaryotes, non-Tf ferric iron is reduced after which ferrous iron can be transferred across the membrane.

In human placenta, iron is taken up mainly by receptor-mediated endocytosis (1,25). Moreover, trophoblast cells in culture are able to take up non-Tf iron (13). In the present investigation, we showed that trophoblast cells in culture were able to take up ^{59}Fe from Fe(III)NTA and Fe-ascorbate, with a higher uptake of ^{59}Fe in the presence of ascorbate. Previously it was supposed that ascorbate would keep Fe in the reduced state (26). However, later investigations showed that, at pH 7, Fe is not necessarily in the reduced state in the presence of ascorbate (14,27). By means of Mössbauer spectroscopy, Dorey et al. (14) could not detect any Fe(II) at physiological pH in buffers containing ascorbate and oxygen. With spectrophotometric studies they showed that iron could be chelated by both Fe(III)chelator mimosine and Fe(II)chelator FZ, suggesting equilibrium between Fe(II) and Fe(III) in the presence of ascorbate in oxygenated solutions. This equilibrium is probably shifted to Fe(III), because of the favoured Fe(III)-ascorbate complex; however, Fe(III) is very easy reducible. Our results revealed that uptake of ^{59}Fe in the presence of ascorbate was inhibited by both DFO, a Fe(III)chelator and FZ, a Fe(II)chelator, which is in agreement with the suggestion of an equilibrium between the two oxidation states.

In view of the fact that our cells were able to reduce extracellular Fe(III)CN and that uptake of ^{59}Fe from Fe-ascorbate, with Fe(II) in equilibrium with Fe(III), was much higher than from Fe(III)NTA, we suggest that ferric iron is reduced before uptake by trophoblast cells. FZ, a Fe(II)-specific chelator, inhibited ^{59}Fe uptake from Fe-ascorbate as well as from Fe(III)NTA, further supporting the idea of Fe(III) reduction before uptake. BPS, another Fe(II)-chelator, inhibited uptake of ^{59}Fe from Fe-ascorbate as would be expected, however,

uptake of ^{59}Fe from Fe(III)NTA was stimulated in the presence of BPS. It is not clear why BPS stimulated the uptake of Fe(III) . It should be expected that BPS, just like FZ would inhibit both Fe(II) and Fe(III) uptake. With HepG2 cells, Randell et al. (6) showed that both BPS and FZ decreased uptake of Fe(III) . Han et al. (7) showed FZ- and BPS-inhibited iron uptake by Caco-2 cells in the presence of ascorbate and FZ-inhibited uptake of iron in the absence of ascorbate. They did not show the effect of BPS on Fe(III) uptake.

Uptake of ^{59}Fe from both Fe-ascorbate and Fe(III)NTA was inhibited by Fe(III)CN . Fe(III)CN is membrane impermeable and we showed that it could be reduced by our cells. Therefore, it probably inhibited Fe(III) uptake by inhibiting its reduction. The uptake of ^{59}Fe from Fe-ascorbate was also decreased in the presence of Fe(III)CN , suggesting that reduction and uptake were tightly coupled.

Thus, we demonstrated that trophoblast cells in culture could take up more ^{59}Fe from Fe-ascorbate than from Fe(III)NTA , the latter one probably preceded by reduction to Fe(II) . The necessity of iron reduction for uptake was previously shown for HepG2 cells (6), HeLa cells (4), Caco-2 cells (7,28) and K562 cells (5,29). From experiments with cells it was not clear which electron donors were responsible for iron reduction. To investigate the mechanism of Fe(III) reduction and whether a plasma membrane protein was involved, we studied reduction of membrane impermeable Fe(III)CN by MMV and BMV, isolated from human term placenta. We showed that both membranes were able to reduce Fe(III)CN in the presence of NADH. NADPH was not able to serve as an electron donor. Reduction was not due to contamination of mitochondria or microsomes, because rotenone and dicoumarol had no effect on the NADH-dependent reduction of Fe(III)CN by vesicles. Likewise SOD had no effect on the reductase activity, excluding the influence of oxide radicals.

Since our cells were able to reduce Fe(III)CN in the absence of extracellular NADH, we suggest a transmembrane ferrireductase activity with intracellular NADH serving as electron donor. Besides transmembrane redox systems, intracellular and extracellular redox systems have been described at plasma membrane (review: 9). With the membrane vesicles it was difficult to distinguish between transmembrane, intracellular and extracellular reductase activity, since a large part of the vesicles was unsealed (22). Therefore, the NADH-dependent ferrireductase could be a transmembrane system and play a role in extracellular reduction and subsequent uptake of non-Tf iron as suggested above. However, the ferrireductase could also be located on the intracellular side of the plasma membrane. Watkins et al. (30) demonstrated the presence of a NADH dehydrogenase on the outer membrane of endosomes. Since endosomes bud from plasma membranes, the presence of a NADH-dependent ferrireductase on the cytosolic side of the plasma membrane is very plausible. The mechanism of iron transport across the basal membrane is still unknown. A dynamic iron pool is present in the cytosol, from which iron can be transported, probably as low molecular weight iron (31). An intracellular NADH-dependent ferrireductase might

be involved in this iron transport by keeping cytosolic iron in the ferrous state. Ferrous iron can then be transported across the basal plasma membrane by still unknown channels. Our results, showing higher reduction of Fe(III)CN by BMV than by MMV are in agreement with this hypothesis.

In summary, we showed reduction of Fe(III)CN by trophoblast cells in culture. Since these cells revealed higher uptake of ^{59}Fe from Fe-ascorbate (assuming an equilibrium between Fe(II) and Fe(III)) than from Fe(III)NTA, reduction seemed to play a significant role in uptake of Fe(III). We investigated the mechanism of iron reduction by BMV and MMV, isolated from the same human term placenta. Reduction of Fe(III)CN was NADH-dependent and BMV reduced Fe(III)CN at a higher rate than MMV. The NADH-dependent ferrireductase might play a role in iron transfer across the basal membrane.

References

1. Van Dijk JP (1988) Review Article: regulatory aspects of placental iron transfer - a comparative study. *Placenta*, 9:215-226.
2. Harris ED (1992) New insights into placental iron transport. *Nutrition Reviews*, 50:329-337.
3. De Silva DM, Askwith CC & Kaplan J (1996) Molecular mechanisms of iron uptake in eukaryotes. *Physiological Reviews*, 76:31-47.
4. Jordan I & Kaplan J (1994) The mammalian transferrin-independent iron transport system may involve a surface ferrireductase activity. *Biochemical Journal*, 302:875-879.
5. Inman RS, Coughlan MM & Wessling-Resnick M (1994) Extracellular ferrireductase activity of K562 cells is coupled to transferrin-independent iron transport. *Biochemistry*, 33:11850-11857.
6. Randell EW, Parkes JG, Olivieri NF & Templeton DM (1994) Uptake of non-transferrin-bound iron by both reductive and nonreductive processes is modulated by intracellular iron. *Journal of Biological Chemistry*, 269:16046-16053.
7. Han O, Failla ML, Hill AD, Morris ER & Smith JC (1995) Reduction of Fe(III) is required for uptake of nonheme iron by Caco-2 cells. *Journal of Nutrition*, 125:1291-1299.
8. Goldenberg H, Crane FL & Morr  DJ (1979) NADH oxidoreductase of mouse liver plasma membranes. *Journal of Biological Chemistry*, 254:2491-2498.
9. Crane FL, Sun IL, Clark MG, Grebing C & L w H (1985) Transplasma-membrane redox systems in growth and development. *Biochimica et Biophysica Acta*, 811:233-264.
10. Sun IL, Navas P, Crane FL, Morr  DJ & L w H (1987) NADH diferric transferrin reductase in liver plasma membrane. *Journal of Biological Chemistry*, 262:15915-15921.
11. Thorstensen K (1988) Hepatocytes and reticulocytes have different mechanisms for the uptake of iron from transferrin. *Journal of Biological Chemistry*, 263:16837-16841.
12. B rczi A & Faulk WP (1992) Iron-reducing activity of plasma membranes. *Biochemistry International*, 28:577-584.
13. Starreveld JS, Kroos MJ, van Suijfen JDE, Verrijt CEH, van Eijk HG & van Dijk JP (1995). Ferritin in cultured human cytotrophoblasts: synthesis and subunit distribution. *Placenta*, 16:383-395.

14. Dorey C, Cooper C, Dickson DPE, Gibson JF, Simpson RJ & Peters TJ (1993) Iron speciation at physiological pH in media containing ascorbate and oxygen. *British Journal of Nutrition*, 70:157-169.
15. Kliman HJ, Nestler JE, Sermasi E, Sanger JM & Strauss III JF (1986) Purification, characterization, and in vitro differentiation of cytotrophoblasts from human term placentas. *Endocrinology*, 118:1567-1582.
16. Starreveld JS, van Denderen J, Verrijt CEH, Kroos MJ & van Dijk JP (1998) Morphological differentiation of cytotrophoblasts cultured in medium 199 and keratinocyte growth medium. *European Journal of Obstetrics & Gynecology and Reproductive Biology* (in press).
17. Booth AG, Olaniyan RO & Vanderpuye OA (1980) An improved method for the preparation of human placental syncytiotrophoblast microvilli. *Placenta*, 1:327-336.
18. Dicke JM, Verges D, Kelley LK & Smith CH (1993) Glycine uptake by microvillous and basal plasma membrane vesicles from term human placentae. *Placenta*, 14:85-92.
19. Kelley LK, Smith CH & King BF (1983) Isolation and partial characterization of the basal cell membrane of human placental trophoblast. *Biochimica et Biophysica Acta*, 734:91-98.
20. Markwell M-AK, Haas SM, Bieber LL & Tolbert NE (1978) A modification of the Lowry procedure to simplify protein determination in membrane and lipoprotein samples. *Analytical Biochemistry*, 87:206-210.
21. Lowry OH, Rosebrough NJ, Farr AL & Randall RJ (1951) Protein measurement with Folin phenol reagent. *Journal of Biological Chemistry*, 193:265-275.
22. Verrijt CEH, Kroos MJ, van Noort WL, van Eijk HG & van Dijk JP (1997) Binding of human isotransferrin variants to microvillous and basal membrane vesicles from human term placenta. *Placenta*, 18:71-77.
23. Thorstensen K & Romslo I (1988) Uptake of iron from transferrin by isolated rat hepatocytes. A redox-mediated plasma membrane process? *Journal of Biological Chemistry*, 263:8844-8850.
24. Klausner RD & Dancis A (1994) A genetic approach to elucidating eukaryotic iron metabolism. *FEBS Letters*, 355:109-113.
25. Douglas GC & King BF (1990) Uptake and processing of ¹²⁵I-labelled transferrin and ⁵⁹Fe-labelled transferrin by isolated human trophoblast cells. *Placenta*, 11:41-57.

26. Taqui Khan MM & Martell AE (1967) Metal ion and metal chelate catalyzed oxidation of ascorbic acid by molecular oxygen. I. Cupric and ferric ion catalyzed oxidation. *Journal of the American Chemical Society*, 89:4176-4185.
27. Plug CM, Dekker D & Bult A (1984) Complex stability of ferrous ascorbate in aqueous solution and its significance for iron absorption. *Pharmaceutisch Weekblad Scientific Edition*, 6:245-248.
28. Núñez MT, Alvarez X, Smith M, Tapia V & Glass J (1994) Role of redox systems on Fe^{3+} uptake by transformed human intestinal epithelial (Caco-2) cells. *American Journal of Physiology*, 267:C1582-C1588.
29. Inman RS & Wessling-Resnick M (1993) Characterization of transferrin-independent iron transport in K562 cells. *Journal of Biological Chemistry*, 268:8521-8528.
30. Watkins JA, Altazan JD, Elder P, Li CY, Nunez MI, Cui XX & Glass J (1992) Kinetic characterization of reductant dependent processes of iron mobilization from endocytic vesicles. *Biochemistry*, 31:5820-5830.
31. Van Dijk JP, van Kreel BK, & Heeren JWA (1985) Studies on the mechanisms involved in iron transfer across the isolated guinea pig placenta by means of bolus experiments. *Journal of Developmental Physiology*, 7:1-16.

8

General discussion

During human pregnancy, 250-300 mg iron is transferred across the placenta from mother to fetus. The amount of iron transfer increases during pregnancy and in the last trimester iron is transferred against a concentration gradient, with both the concentration and the iron saturation being higher in fetal plasma compared to maternal plasma (1,2). Iron transfer is unidirectional from mother to fetus. The major source of iron in man is maternal diferric Tf, which can be taken up by means of receptor-mediated endocytosis (2,3). *In vivo*, iron but not Tf is transferred to the fetus. ApoTf is recycled to the maternal side (4).

Serum Tf shows microheterogeneity based on the variation in the structure of N-linked glycan chains (5,6). The microheterogeneity pattern of Tf can be visualized by isoelectric focusing (7). During pregnancy, the isoelectric focusing pattern of maternal human serum Tf has shifted to lower pH values, suggesting an increase in the number of glycan chains and therefore an increase in the complexity of Tf (7-9). In contrast to maternal serum Tf, the complexity of human fetal serum Tf is reduced (Chapter 6). The presence of less sialylated Tfs in fetal serum may be due to the nearly absence of asialoglycoprotein receptors in mammalian fetal liver (10).

Can the observed changes in glycan chain complexity of Tf explain the increase of placental iron transfer during gestation? To address this question we studied the distribution and affinities of TfRs on both microvillous and basal membrane vesicles (MMV and BMV). The affinity of Tf for TfRs on both MMV and BMV was influenced by the complexity of Tf: K_a -values for Tf binding to TfRs on both MMV and BMV were decreased with increasing complexity of the Tf (Chapter 4). This excludes the possibility that the increase of placental iron transfer can partly be explained by the observed increase in glycan chain complexity of maternal Tf. In terms of the 'genetic conflict hypothesis' (11), our findings could be interpreted as maternal defence against excessive fetal iron extraction, which would be harmful for the mother.

The number of TfRs was higher on MMV than on BMV. The binding affinity was higher for TfRs on BMV (Chapter 4). The difference in affinity might be explained by a different microenvironment surrounding the TfRs. Microenvironment and membrane lipid fluidity might play a role in the binding behaviour of TfRs (12,13). In Chapter 3, we showed that both cholesterol and phospholipid content were higher in BMV compared to MMV. Another explanation might be a difference in the glycosylation pattern of microvillous and basal TfRs. Previous studies have shown that glycosylation of TfRs influences the affinity for Tf (14). Placental TfRs in diabetic pregnancies display an increased glycosylation, which is accompanied by a decreased affinity for Tf (15,16).

Because of the binding of Tf to both MMV and BMV, we argued that TfRs also are present on both membranes of the syncytiotrophoblast *in situ*. In order to investigate the functionality of both TfR populations, we used the model of the syncytiotrophoblast in polar culture. With EM studies, using mouse anti-TfR and Au-labelled anti-mouse IgG, we showed that TfRs were present on both microvillous and basal membranes of polarly cultured trophoblast cells (Chapter 5). Moreover, we showed that Au-labelled Tf was taken up by endocytosis from both sides of the cell. It is obvious that microvillous TfRs are

involved in placental uptake of maternal diferric Tf. The function of basal TfRs is still unclear. In BeWo cells, which are derived from a choriocarcinoma cell line and display trophoblast-like characteristics, 80 % of de novo synthesized TfRs was directly targeted to the basal surface. TfRs were redistributed by means of transcytosis (17). The population of basal TfRs in BeWo cells, as well as in the differentiated syncytiotrophoblast, might just be a relic of the sorting mechanism, characteristic for epithelial cells (18). Basal TfRs will not be involved in uptake of fetal serum Tf, since fetal Tf will probably not contact the basal TfRs. In contrast to the maternal blood, which is free in the villous space and therefore in direct contact with the placental syncytiotrophoblast, fetal blood is present in closed fetal capillaries and does not contact the syncytiotrophoblast (see Figures 1.3 and 1.4 in Chapter 1). A possible function of basal TfRs might be the regulation of the re-uptake of maternal Tf that has reached the fetal side, since, in vivo, iron and not Tf is transferred from mother to fetus.

The main site of Tf synthesis is the liver (19). Other, from a quantitative point of view, less important sites are the brain choroid plexus, Sertoli cells, brain glial cells, fetal membranes and the placenta. Tf mRNA has been detected in rat and mouse placental extracts (20-23). In the present study, we demonstrated the presence of Tf mRNA in cultured trophoblast cells from human term placenta. Moreover, we showed that the protein was synthesized and that de novo synthesized Tf was released from the cells (Chapter 6). Trophoblast Tf was different from both maternal and fetal serum Tf with respect to the isoelectric focusing pattern. As mentioned above, the isoelectric focusing pattern of human maternal serum Tf had shifted to lower pH values compared to normal serum Tf. However, trophoblast Tf was even more acidic than maternal serum Tf at term pregnancy, suggesting an even higher complexity. The function of trophoblast Tf still has to be elucidated, as well as the meaning of the shift in isoelectric focusing pattern. Placental Tf gene expression in rat has been shown to be increased throughout gestation and therefore coincides with increasing needs of the fetus (21,22), although it has been assumed that Tf synthesis in extrahepatic sites is not regulated by iron (24). It can be suggested that the placenta might be an additional source of Tf. Though, it is not clear whether an extra source of Tf really is needed at physiological conditions. Tf has been shown to stimulate the differentiation of cultured kidney mesenchyme (25). Tf also stimulates DNA synthesis both in proliferating and differentiating trophoblast cells from rat placenta (26,27). Syncytiotrophoblast Tf might therefore play a role in proliferation of cytotrophoblast and differentiation of syncytiotrophoblast. The latter postulated functions presume basolateral trafficking of trophoblast Tf, in which the glycan chains might be involved.

Besides Tf-mediated iron uptake, we showed that cultured trophoblast cells were able to take up iron independent from Tf (Chapter 7). Since, under physiological conditions, the level of Tf in maternal plasma is high enough to bind almost all iron, free iron is rarely found in maternal plasma. The Tf-independent iron uptake system will therefore not play an important role in the uptake of iron from maternal plasma (28). We showed that a NADH-dependent ferrireductase probably was involved in Tf-independent iron uptake. The activity

of this reductase was higher on BMV. We have suggested that this reductase plays a role in the transfer of cytosolic iron across the basal membrane. The orientation of the ferrireductase could not be determined in our membrane vesicles. The presence of the reductase on the cytosolic side of the plasma membrane is very plausible, since a NADH dehydrogenase has been found on the outer membrane of endosomes and endosomes bud from plasma membranes (29). When present on the intracellular side of plasma membranes, the ferrireductase may keep cytosolic iron in its reduced state. It has previously been demonstrated that the labile iron pool (LIP) in K562 cells mainly consists of ferrous iron (30). The intracellular redox state of cultured trophoblast cells (31) favours the presence of ferrous iron in the placental LIP. It has previously been shown that iron from the LIP can be transported out of the placenta, probably as low molecular weight iron (32). There is some evidence that iron removed out of the placenta is in the ferrous state (33). The transport of ferrous iron across the basal membrane might involve an iron carrier. A possible candidate for this iron carrier might be the 17 kD proton pore subunit of V-ATPase (34), which may be involved in iron transport across the endosomal membrane of reticulocytes (29,34,35). The presence of V-ATPase in MMV was demonstrated by Simon et al. (36). We indicated that V-ATPase also was present in BMV (Chapter 3). Another candidate as transporter for iron might be found in the family of integrins (37-39).

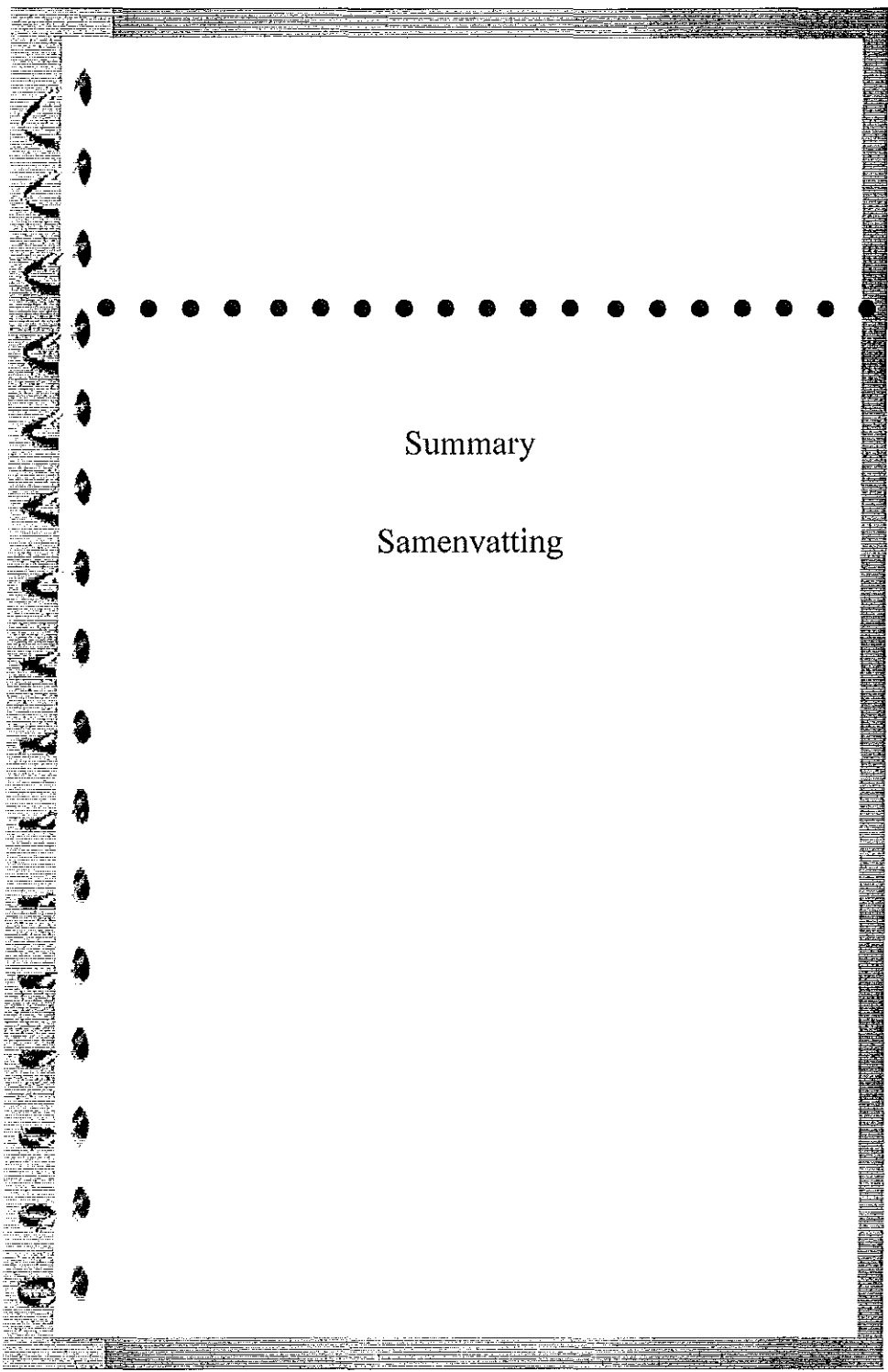
A model for placental iron transfer has to cope with some important facts: First, iron transfer is only in one direction, namely from mother to fetus. Iron but not maternal Tf is transferred to the fetus. Moreover, iron transfer is directed against a concentration gradient. Based on the results described in this thesis and considering the aspects above, we propose a descriptive model for iron transfer in human term placenta. The main barrier in placental transfer is the syncytiotrophoblast. At the maternal side, the microvillous membrane of the syncytiotrophoblast is in direct contact with maternal blood. Iron can be taken up from maternal diferric Tf by receptor-mediated endocytosis, involving the TfRs on the microvillous membrane. Acidification of the endosomes results in the loss of iron from Tf. Iron is then released from the endosomes into the LIP in the cytosol. ApoTf is recycled to the maternal side, which agrees with the fact that maternal Tf is not transcytosed. From the LIP, iron can either be accumulated into ferritin or transferred across the basal membrane to the fetal side. Both microvillous and basal membranes contain a NADH-dependent ferrireductase that may keep cytosolic iron in the reduced state. The activity of the basal ferrireductase was higher. After reduction, ferrous iron is transported across the basal membrane, probably involving an iron carrier. Active transport across the basal membrane as well as receptor-mediated endocytosis of maternal diferric Tf at the microvillous membrane can explain iron transfer against a concentration gradient. After iron reached the fetal side, it has to be transported to the fetal capillaries, in which it can bind to fetal Tf. The mechanisms for this are not clear yet. Not only the microvillous membrane, but also the basal membrane of the syncytiotrophoblast contains TfRs. However, since the number of TfRs at the microvillous membrane is higher, this does not have to be in conflict with the fact that iron is unidirectionally transferred from mother to fetus.

References

1. Van Dijk, JP (1977) Iron metabolism and placental transfer of iron in the term rhesus monkey (*Macaca mulatta*): a compartmental analysis. *European Journal of Obstetrics & Gynecology and Reproductive Biology*, 7:127-139.
2. Van Dijk JP (1988) Review Article: regulatory aspects of placental iron transfer - a comparative study. *Placenta*, 9:215-226.
3. Contractor SF & Eaton BM (1986) Role of transferrin in iron transport between maternal and fetal circulations of perfused lobule of human placenta. *Cell Biochemistry and Function*, 4:69-74.
4. Eaton BM, Browne MJ & Contractor SF (1985) Transferrin-mediated iron transport in the perfused isolated placental lobule. *Contributions to Gynecology & Obstetrics*, 13:149-150.
5. Spik G, Bayard B, Strecker G, Bouquelet S & Montreuil J (1975) Studies on glycoconjugates. LXIV. Complete structure of two carbohydrate units of human serotransferrin. *FEBS Letters*, 50:296-299.
6. De Jong G, van Dijk JP & van Eijk HG (1990) The biology of transferrin. *Clinica Chimica Acta*, 190:1-46.
7. De Jong G & van Eijk HG (1988) Microheterogeneity of human serum transferrin: a biological phenomenon studied by isoelectric focusing in immobilized pH gradients. *Electrophoresis*, 9:589-598.
8. Bierings MB, Heeren JWA, van Noort WL, van Dijk JP & van Eijk HG (1987) Pregnancy and guinea-pig isotransferrins - isolation and characterization of both isotransferrins. *Clinica et Chimica Acta*, 165:205-211.
9. Léger D, Campion B, Decottignies JP, Montreuil J & Spik G (1989) Physiological significance of the marked increased branching of the glycans of human serotransferrin during pregnancy. *Biochemical Journal*, 257:231-238.
10. Bujanover Y, Lebenthal E & Petell JK (1991) Reduced levels of galactose-terminated glycoproteins in rat serum during perinatal development. *Biology of the Neonate*, 60:45-51.
11. Haig D (1993) Genetic conflicts in human pregnancy. *The Quarterly Review of Biology*, 68:495-532.
12. Muller C & Shinitzky M (1979) Modulation of transferrin receptors in bone marrow cells by changes in lipid fluidity. *British Journal of Haematology*, 42:355-362.
13. Di Giulio A, D'Andrea G, Saletti MA, Impagnatiello A, D'Alessandro AM & Oratore A (1994) The binding of human serum transferrin to its specific receptor reconstituted into liposomes. *Cellular Signalling*, 6:83-90.

14. Hunt RC, Riegler R & Davis AA (1989) Changes in glycosylation alter the affinity of the human transferrin receptor for its ligand. *Journal of Biological Chemistry*, 264:9643-9648.
15. Petry CD, Wobken JD, McKay H, Eaton MA, Seybold VS, Johnson DE & Georgieff MK (1994) Placental transferrin receptor in diabetic pregnancies with increased fetal iron demand. *American Journal of Physiology*, 267:E507-E514.
16. Georgieff MK, Petry CD, Mills MM, McKay H & Wobken JD (1997) Increased N-glycosylation and reduced transferrin-binding capacity of transferrin receptor isolated from placentae of diabetic women. *Placenta*, 18:563-568.
17. Cerneus DP, Strous GJ & van der Ende A (1993) Bidirectional transcytosis determines the steady state distribution of the transferrin receptor at opposite plasma membrane domains of BeWo cells. *Journal of Cell Biology*, 122:1223-1230.
18. Aroeti B, Okhrimenko H, Reich V & Orzech E (1998) Polarized trafficking of plasma membrane proteins: emerging roles for coats, SNAREs, GTPases and their link to the cytoskeleton. *Biochimica et Biophysica Acta*, 1376:57-90.
19. Schaeffer E, Boissier F, Py MC, Cohen GN & Zakin MM (1989) Cell-type-specific expression of the human transferrin gene. Role of promoter, negative, and enhancer elements. *Journal of Biological Chemistry*, 264: 7153-7160.
20. Aldred AR, Dickson PW, Marley PD & Schreiber G (1987) Distribution of transferrin synthesis in brain and other tissues in the rat. *Journal of Biological Chemistry*, 262:5293-5297.
21. Yang F, Friedrichs WE, Buchanan JM, Herbert DC, Weaker FJ, Brock JH & Bowman BH (1990) Tissue specific expression of mouse transferrin during development and aging. *Mechanisms of Ageing and Development* 56:187-197.
22. Kasik JW & Rice EJ (1993) Transferrin gene expression in maternal liver, fetal liver and placenta during pregnancy in the mouse. *Placenta*, 14:365-371.
23. Boockfor FR, Harris SE, Barto JM & Bonner JM (1994) Placental cell release of transferrin: analysis by reverse haemolytic plaque assay. *Placenta*, 15:501-509.
24. Kaysen GA, Sun X, Jones H, Martin VI, Joles JA, Tsukamoto H, Couser WG & Al-Bander H (1995) Non-iron mediated alteration in hepatic transferrin gene expression in the nephrotic rat. *Kidney International*, 47:1068-1077.
25. Ekblom P & Thesleff J (1985) Control of kidney differentiation by soluble factors secreted by the embryonic liver and the yolk sac. *Developmental Biology*, 110:29-38.
26. De M, Hunt JS & Soares MJ (1988) Stimulation of rat placental cell DNA synthesis by transferrin. *Biology of Reproduction*, 38:1123-1128.

27. Hamlin GP & Soares MJ (1995) Regulation of deoxyribonucleic acid synthesis in proliferating and differentiating trophoblast cells: involvement of transferrin, transforming growth factor- β , and tyrosine kinases. *Endocrinology*, 136:322-331.
28. Qian ZM, Tang PL & Wang Q (1997) Iron crosses the endosomal membrane by a carrier-mediated process. *Progresses in Biophysics and Molecular Biology*, 67:1-15.
29. Watkins JA, Altazan JD, Elder P, Li CY, Nunez MT, Cui XX & Glass J (1992) Kinetic characterization of reductant dependent processes of iron mobilization from endocytic vesicles. *Biochemistry*, 31:5820-5830.
30. Breuer W, Epsztejn S & Cabantchik ZI (1995) Iron acquired from transferrin by K562 cells is delivered into a cytoplasmic pool of chelatable iron(II). *Journal of Biological Chemistry*, 270:24209-24215.
31. Bax BE & Bloxam DL (1997) Energy metabolism and glycolysis in human placental trophoblast cells during differentiation. *Biochimica et Biophysica Acta*, 1319:283-292.
32. Van Dijk JP, van Kreel BK & Heeren JWA (1985) Studies on the mechanisms involved in iron transfer across the isolated guinea pig placenta by means of bolus experiments. *Journal of Developmental Physiology*, 7:1-16.
33. Mc Ardle HJ (1992) The transport of iron and copper across the cell membrane: different mechanisms for different metals? *Proceedings of the Nutrition Society*, 51:199-209.
34. Li CY, Watkins JA, Hamazaki S, Altazan D & Glass J (1995) Iron binding, a new function for the reticulocyte endosome H^+ -ATPase. *Biochemistry*, 34:5130-5136.
35. Li CY, Watkins JA & Glass J (1994) The H^+ -ATPase from reticulocyte endosomes reconstituted into liposomes acts as an iron transporter. *Journal of Biological Chemistry*, 269:10242-10246.
36. Simon BJ, Kulanthaivel P, Burckhardt G, Ramamoorthy S, Leibach FH & Ganapathy V (1992) Characterization of an ATP-driven H^+ pump in human placental brush-border membrane vesicles. *Biochemical Journal*, 287:423-430.
37. Conrad ME, Umbreit JN, Moore EG, Uzel C & Berry MR (1994) Alternate iron transport pathway. Mobilferrin and integrin in K562 cells. *Journal of Biological Chemistry*, 269:7169-7173.
38. Conrad ME, Umbreit JN, Moore EG & Heiman D (1996) Mobilferrin is an intermediate in iron transport between transferrin and hemoglobin in K562 cells. *Journal of Clinical Investigation*, 98:1449-1454.
39. Umbreit JN, Conrad ME, Berry MA, Moore EG & Latour LF (1997) The alternate iron transport pathway: mobilferrin and integrin in reticulocytes. *British Journal of Haematology*, 96:521-529.



Summary

Samenvatting

Summary

Iron is an essential element for all living cells. It plays an important role in growth and development. During pregnancy, a large amount of iron is transferred across the placenta from mother to fetus. In this thesis, we describe some mechanisms involved in placental iron transfer.

Chapter 1 is a general introduction to our studies of placental iron transfer. It gives an overview of the regulation of cellular iron uptake mechanisms; the regulation of the intracellular iron pool; the human term placenta; general placental transport mechanisms; and placenta iron transport mechanisms as studied thus far.

Chapter 2 describes the materials and methods that have been used in this study.

In *Chapter 3*, the two in vitro models that have been used in this study are described. We describe the methods of isolation of microvillous and basal membrane vesicles and give a good characterization of our membrane preparations. Furthermore, we give a description of trophoblast cells in culture.

In *Chapter 4* we have studied the binding of transferrin to microvillous and basal membrane vesicles. We show that microvillous membrane vesicles contain a higher number of transferrin receptors than basal membrane vesicles, whereas the affinity of transferrin for the receptors on basal membranes is higher. We also show that the affinity of transferrin for its receptor slightly decreases as the complexity of transferrin increases.

In *Chapter 5* we show that transferrin receptors on microvillous and basal membranes of polarly cultured trophoblast cells are able to endocytose diferric transferrin. Iron is accumulated in the cells. We suppose that despite the accumulation of iron, cells are also able to transfer iron.

Chapter 6 shows that transferrin is synthesized in cultured trophoblast cells and that de novo synthesized transferrin can be released from the cells. The isoelectric focusing pattern of trophoblast transferrin is shifted to lower pH values compared to normal serum transferrin, serum transferrin from pregnant women and umbilical cord serum transferrin, suggesting higher complexity of trophoblast transferrin.

Chapter 7 describes the uptake of non-transferrin iron by trophoblast cells in culture. A NADH-dependent ferrireductase is characterized in isolated membrane vesicles. This reductase may be involved in transferrin-independent iron transport. Moreover, we suggested the involvement of the ferrireductase in iron transfer across the basal membrane.

In *Chapter 8* we discuss the experimental results described in this thesis. Moreover, we propose a descriptive model for iron transfer in human term placenta.

Samenvatting

IJzer is een essentieel element voor alle levende cellen. Het speelt een belangrijke rol in groei en ontwikkeling. Tijdens de zwangerschap wordt een grote hoeveelheid ijzer van moeder naar foetus over de placenta getransporteerd. In dit proefschrift worden enkele mechanismen beschreven die betrokken zijn bij het transport van ijzer over de placenta.

Hoofdstuk 1 is een algemene introductie op onze studies van het ijzertransport over de placenta. Het geeft een overzicht van mechanismen van cellulaire ijzeropname; de regulatie van de intracellulaire ijzer pool; de humane placenta aan het einde van de zwangerschap; algemene transport mechanismen in de placenta; en van wat tot nu toe bekend is over het placentair ijzertransport.

Hoofdstuk 2 beschrijft de materialen en methoden die gebruikt zijn in deze studie.

In *Hoofdstuk 3* worden de twee in vitro modellen beschreven die we gebruikt hebben in deze studie. We beschrijven de isolatie van microvillieuze en basale membraan vesicles en geven een goede karakterisering van onze vesicles. Verder beschrijven we de eigenschappen van gekweekte trofoblastcellen.

In *Hoofdstuk 4* hebben we de binding van transferrine aan microvillieuze en basale membraan vesicles bestudeerd. Microvillieuze membraan vesicles hebben een groter aantal transferrine receptoren dan basale membraan vesicles. De affiniteit van transferrine voor transferrine receptoren op de basale membranen is hoger dan voor die op de microvillieuze membranen. De affiniteit van transferrine voor de receptor wordt minder als het transferrine complexer wordt.

In *Hoofdstuk 5* laten we zien dat transferrine receptoren op microvillieuze en basale membranen van polair gekweekte trofoblast cellen in staat zijn om diferric transferrine te endocyteren. IJzer hoopt zich op in de cellen. We veronderstellen dat, ondanks dat de cellen ijzer stapelen, ze ook in staat zijn om ijzer te transporteren.

Hoofdstuk 6 laat zien dat gekweekte trofoblast cellen transferrine synthetiseren en dat dit nieuw gesynthetiseerde transferrine uit de cellen vrij kan komen. Het isoelectrisch focuserings patroon van trofoblast transferrine is verschoven naar lagere pH-waarden, in vergelijking tot normaal serum transferrine, serum transferrine van zwangere vrouwen en transferrine uit navelstreng serum. Dit suggereert een hogere complexiteit van trofoblast transferrine.

Hoofdstuk 7 beschrijft de opname van ijzer, niet gebonden aan transferrine, door gekweekte trofoblast cellen. Een NADH-afhankelijke ferrireductase is gekarakteriseerd in geïsoleerde membraan vesicles. Dit reductase is mogelijk betrokken bij het transferrine-onafhankelijke ijzer transport. Verder hebben we gesuggereerd dat de ferrireductase betrokken is bij het transport van ijzer over de basale membraan.

In *Hoofdstuk 8* bediscussiëren we de experimentele resultaten die in dit proefschrift beschreven zijn. Verder wordt er een beschrijvend model voor het ijzer transport over de humane placenta voorgesteld.

Publications

Abstracts

Van der Aa EM, Verrijt CEH, Copius Peereboom-Stegeman JHH and Russel FGM (1993) Uptake of cimetidine into syncytial microvillus membrane vesicles of human term placenta. *Placenta*, 14:A79.

Verrijt CEH, Kroos MJ, van Eijk HG and van Dijk JP (1995) Human trophoblast cells in culture produce transferrin. *Placenta*, 16:A73.

Verrijt CEH, Kroos MJ, van Noort WL, van Eijk HG and van Dijk JP (1995) Binding of transferrin isoforms to microvillous and basal membrane vesicles from human term placenta. *Placenta*, 16:A73.

Verrijt CEH, Cleton-Soeteman MI, Kroos MJ and van Dijk JP (1996) Receptor mediated endocytosis of Au-transferrin at microvillous and basal membrane of polar cultured cytotrophoblast cells. *Placenta*, 17:A34.

Verrijt CEH, Kroos MJ and van Dijk JP (1996) Reduction of ferric-NTA at microvillous and basal membrane vesicles from human term placenta. *Placenta*, 17:A34.

Verrijt CEH, Kroos MJ and van Dijk JP (1997) Transferrin production and secretion by differentiating cytotrophoblast cells. *Placenta*, 18:A57.

Verrijt CEH and van Dijk JP (1997) Reduction of Fe(III) by cultured human term cytotrophoblast. *Placenta*, 18:A57.

Publications

Starreveld JS, Kroos MJ, van Suijlen JD, Verrijt CEH, van Eijk HG and van Dijk JP (1995) Ferritin in cultured human cytotrophoblasts: synthesis and subunit distribution. *Placenta*, 16:383-395.

Van der Aa EM, Wouterse AC, Verrijt CEH, Copius Peereboom-Stegeman JHH and Russel FGM (1996) Uptake of cimetidine into syncytial microvillous membrane vesicles of human term placenta. *Journal of Pharmacology and Experimental Therapeutics*, 276:219-222.

Kroos MJ, Starreveld JS, Verrijt CEH, van Eijk HG and van Dijk JP (1996) Regulation of transferrin receptor synthesis by human cytotrophoblast cells in culture. *European Journal of Obstetrics, Gynecology & Reproductive Biology*, 65:231-234.

Verrijt CEH, Kroos MJ, van Noort WL, van Eijk HG and van Dijk JP (1997) Binding of human isotransferrin variants to microvillous and basal membrane vesicles from human term placenta. *Placenta*, 18:71-77.

Publications

Verrijt CEH, Kroos MJ, Verhoeven AJ, van Eijk HG and van Dijk JP (1997) Transferrin in cultured human term cytotrophoblast cells: synthesis and heterogeneity. *Molecular & Cellular Biochemistry*, 173:177-181.

Starreveld JS, van Denderen J, Verrijt CEH, Kroos MJ and van Dijk JP (1998) Morphological differentiation of cytotrophoblasts cultured in medium 199 and keratinocyte growth medium. *European Journal of Obstetrics & Gynecology and Reproductive Biology*, 79:205-210.

Verrijt CEH, Kroos MJ, Huijskes-Heins MIE, van Eijk HG & van Dijk JP (1998) Non-transferrin iron uptake by trophoblast cells in culture. Significance of a NADH-dependent ferrireductase. *Placenta* (in press).

Dankwoord

Een proefschrift schrijven kun je niet alleen. Velen hebben een steentje bijgedragen aan het tot stand komen van dit proefschrift. Een aantal personen wil ik hierbij speciaal bedanken.

Professor van Eijk wil ik bedanken voor de vrijheid die ik gekregen heb bij de uitvoering van dit onderzoek en voor de mogelijkheid om naast het onderzoek een gedeelte van de leraren opleiding te volgen.

Hans, jouw vele ideeën en suggesties hebben een belangrijke bijdrage geleverd aan dit proefschrift. Ik wil je bedanken voor de prettige samenwerking en alle tijd die je voor me had. Wanneer ik ook maar vragen had, ik kon altijd bij je terecht.

Martin, placenta's, placenta's, placenta's. Ik kan me voorstellen dat je af en toe wel eens gek van me werd. Toch stond je altijd weer voor me klaar, om een isolatie of een of ander proefje uit te voeren. Heel erg bedankt. Ik heb plezierig met je gewerkt.

Marja, ik mag me gelukkig prijzen dat jij me het laatste jaar kwam helpen. Het aantal data in de vesicle studies heb je in korte tijd erg opgekrikt. Ook bij het schrijven van het proefschrift zelf heb je me erg geholpen, met name bij het maken van de vele grafiekjes. Bedankt voor alles.

Maud, met jouw hulp zijn alle mooie EM-plaatjes tot stand gekomen. Dit kon natuurlijk niet zonder de gastvrijheid van de afdeling Pathologie, waar ik met name Peter van Run wil bedanken voor de vele, vele foto's die hij heeft afgedrukt.

Wim, bedankt voor de transferrines en de suiker- en aminozuur-analyses. Linda, Ben, Nel en Tiny, bedankt voor alle hulp en de gezelligheid in de afgelopen jaren. Peter en Warry, ex-collega-AIO's, jullie hebben me goed ingewerkt in het AIO-schap.

De afdeling Biochemie wil ik bedanken voor de hulp bij het moleculair biologische werk, voor de lipide- en vetzuur-bepalingen en voor de mogelijkheid om dit proefschrift bij jullie uit te printen..

De verpleegkundigen van de afdeling Gynaecologie and Obstetrie van het Sophia/Academisch Ziekenhuis Rotterdam wil ik hartelijk danken voor de vele placenta's, die toch wel noodzakelijk waren voor dit onderzoek.

Christel

Curriculum Vitae

Christel Verrijt werd geboren op 14 september 1970 te Someren. In 1989 behaalde zij het VWO diploma aan de Philips van Horne scholengemeenschap te Weert. In aansluiting hierop begon zij haar studie Scheikunde aan de Katholieke Universiteit te Nijmegen. Haar uitgebreide hoofdvakstage Toxicologie heeft zij gelopen bij de afdeling Farmacologie aan de Faculteit der Medische Wetenschappen van de Katholieke Universiteit te Nijmegen, onder leiding van Prof. Dr. J. Noordhoek. Zij heeft daar het transport van cimetidine over de humane placenta bestudeerd. Een hoofdvakstage Biochemie werd gedaan op het Urologisch Research Laboratorium van het Academisch Ziekenhuis te Nijmegen, waar zij een methode voor exon trapping heeft opgezet. Deze stage is uitgevoerd onder leiding van Prof. Dr. H.P. Bloemers. In 1994 behaalde zij het doctoraalexamen en kreeg zij een aanstelling als AIO op de afdeling Chemische Pathologie van de Erasmus Universiteit te Rotterdam. Onder leiding van Prof. Dr. H.G. van Eijk en Dr. J.P. van Dijk verrichtte zij onderzoek naar de regulatie van het ijzer transport over de humane placenta. De resultaten van dit onderzoek zijn beschreven in dit proefschrift.

